8-6-2021

Optimizing a biomass supply system: consideration of pellet quality and transportation under extreme events

Badr S. Aladwan
baladwan@hotmail.com

Optimizing a biomass supply system: consideration of pellet quality and transportation under extreme events

By

Badr S. Aladwan

Approved by:

Mohammad Marufuzzaman (Major Professor)
Nazanin Morshedlou
Raed Jaradat
Li Zhang
Linkan Bian (Graduate Coordinator)
Jason M. Keith (Dean, Bagley College of Engineering)

A Dissertation
Submitted to the Faculty of
Mississippi State University
in Partial Fulfillment of the Requirements
for the Degree of Doctor of Philosophy
in Industrial Engineering
in the Department of Industrial and Systems Engineering

Mississippi State, Mississippi

August 2021

Name: Badr S. Aladwan

Date of Degree: August 6, 2021

Institution: Mississippi State University

Major Field: Industrial Engineering

Major Professor: Mohammad Marufuzzaman

Title of Study: Optimizing a biomass supply system: consideration of pellet quality and transportation under extreme events

Pages of Study: 105

Candidate for Degree of Doctor of Philosophy

This dissertation studies a framework in support biomass wood pellet supply chain. The worldwide wood pellet market is growing at a phenomenal rate. However, the economic sustainment of this business depends on how well the producers manage the uncertainty associated with biomass yield and quality. In the first part of the dissertation, we propose a two-stage stochastic programming model that optimizes different critical decisions (e.g., harvesting, storage, transportation, quality inspection, and production decisions) of a biomass-to-pellet supply system under biomass yield and quality uncertainty to economically produce pellets while accounting for the different pellet standards set forward by the U.S. and European markets. The study develops a hybrid algorithm that combines Sample Average Approximation with an enhanced Progressive Hedging algorithm. We propose two parallelization schemes to efficiently speed up the convergence of the overall algorithm. We use Mississippi as a testing ground to visualize and validate the algorithms performance. Experimental results indicate that the biomass-to-pellet supply system is sensitive to the biomass quality parameters (e.g., ash and moisture contents).

In the second part of the dissertation, we propose a bi-level mixed-integer linear programming model that captures important features such as the hurricane's degree, quality of damaged timbers, price-related issues, optimizes different critical decisions (e.g., purchasing, storage, and transportation decisions) of a post-hurricane damaged timber management problem. Lack of efficient tools to manage the wood market interactions in the post-hurricane situation increases timber salvage loss drastically. The overall goal is to provide an efficient decision-making tool for planning and recovering damaged timber to maximize its monetary value and mitigate its negative ecological impacts. Due to the complexity associated with solving the proposed model, we developed two exact solution methods, namely, the enhanced Benders decomposition and the Benders-based branch-and-cut algorithms, to efficiently solve the model in a reasonable time-frame. We use 15 coastal counties in southeast Mississippi to visualize and validate the algorithms' performance. Key managerial insights are drawn on the sensitivity of a number of critical parameters, such as selling/purchasing prices offered by the landowners/mills, quality-level, and deterioration rate of the damaged timbers on their economic recovery following a natural catastrophe.

Key words: Biomass quality; pellet production; stochastic optimization; bi-level optimization; hurricane; timber quality; supply chain; wood industry

DEDICATION

To my parents for their endless prayers and my adorable daughters Aseel and Leyan.

ACKNOWLEDGEMENTS

I am so grateful to everyone who has helped me in my entire doctoral studies. I would like to thank Dr. Mohammad Marufuzzaman, my major professor, for his support and assistance to provide a distinguished great work. I am also extending my appreciation to the other committee members, Dr. Nazanin Morshedlou, Dr. Raed Jaradat, and Dr. Li Zhang, for their important and valuable comments, which undoubtedly helped improving this research.

I also thank my colleagues in the Department of Industrial and Systems Engineering for their help and support. Especially notable are Dr. Darweesh, Battawi, Abdul Quddus, Farjana, Amin, and Niamat. They helped me on my research and all related matters during my study.

Certainly, I cannot fail to thank the most important people in my life, my dear parents, Saleh Aladwan and Hussah Alhusain, brothers, sisters, and my wife for their unlimited support in overcoming all the difficulties that I faced in my study journey, which had the effect of providing the most that I could provide during my classes and research.

In conclusion, and most importantly, I thank God (ALLAH), the Almighty, for having bestowed upon me with his grace and generosity and has pleased me to obtain my PhD.

TABLE OF CONTENTS

LIST OF TABLES

LIST OF FIGURES

CHAPTER I

OPTIMIZING A PELLET SUPPLY SYSTEM: MARKET-SPECIFIC PELLET PRODUCTION WITH BIOMASS QUALITY CONSIDERATIONS

1.1 Introduction

1.1.1 Problem Motivation

The increasing commitment of government and private entities to reducing the carbon footprint have boosted the demand for wood pellet worldwide. The world pellet market is estimated to reach nearly 54 million tonnes by 2025, where approximately 70.4% of the total market demand is expected to be consumed in Europe alone [62]. This growing market trend is also expected in North America and Asia, pending ongoing legislative supports and the adoption of greenhouse gas (GHG) emission reduction policies [94]. Currently, wood pellets are one of the largest internationally traded solid biomass commodities [89]. These opportunities have leaned investors towards developing/improving the new/existing biomass-to-pellet supply chain, which can economically produce and transport pellets locally and for the overseas markets.

Unlike other supply chains, the optimization of a biomass-to-pellet supply chain is extremely challenging. A number of factors drive towards letting the system optimization complicated, including but not limited to biomass quality variability, seasonality, market-specific pellet production requirements, and many others. One of such complexities is provided in Table 1.1, which summarizes the pellet production standards for the U.S. and the European markets [91]. Clearly, the

two markets follow different pellet production standards which must be met to ensure customer satisfaction and long-term sustainment of this business. For instance, a pellet production facility in Mississippi needs to produce specific grades of the pellets for the local markets (e.g., PFI premium, PFI standard, PFI utility). The facility simultaneously needs to produce different grades of the pellets for the growing overseas markets (e.g., A1, A2, and B grades for the European markets). In addition to these market-specific pellet production requirements, challenges further lie in obtaining the quality and quantity of the feedstocks from the farmers, which essentially increases the complexity in producing the right pellet for the right market at the right time. For instance, the two markets have very different ash requirements for different grades of the pellets (see Table 1.1). Both markets also set an upper limit for the permittable moisture content. The European market set an additional restriction that mandates producing pellets from specified sources of the biomass (e.g., stemwood and chemically untreated wood residues can only be used to produce A1 grade pellet; see other pellet grade-specific biomass requirements in Table 1.1). Uncertainty exists in obtaining high quality biomass from the supply sources. Moreover, the yield of biomass is highly stochastic in nature and is not available throughout the year. All such random factors create challenges for pellet manufacturers to produce and market the correct grade of pellet. As such, rigorous decision tools are needed, which appropriately capture the stochasticity associated with biomass yield and quality and accounts for all the critical steps (e.g., harvesting, storage, transportation, quality inspection, and production decisions) that significantly impact the biomass-to-pellet supply chain

1.1.2 Literature Review

Biomass supply chain has a rich literature. Most of the past studies tend to focus on minimizing the overall biomass supply chain costs (e.g., feedstock collection, inventory, production, and facility

Table 1.1

Summary of pellet standards for the U.S. and European markets [91]

	U.S. Market			Europe Market		
Property	PFI Premium	PFI Standard	PFI Utility	A1	A2	B
Inorganic ash (%)	≤1.0	≤2.0	≤6.0	≤0.7	≤1.5	≤3.0
Moisture (%)	≤8.0	≤10.0	≤10.0	≤10.0	≤10.0	≤10.0
Biomass sources	n/a	n/a	n/a	sources[1]	sources[2]	sources[3]

[1]stemwood, chemically untreated wood residues
[2]whole trees (without roots), stemwood, logging residues, bark, chemically untreated wood residues
[3]forest plantation & other virgin wood, by-products & residues from wood processing industry, used woods

location decisions) under both deterministic (e.g., [28], [38], [108]) and stochastic (e.g., [39], [73], [74], [21], [11]) conditions. Given the biomass supply chain is highly stochastic in nature, a number of past studies adopted a stochastic programming approach to examine the impact of feedstock supply (e.g., [39], [73], [74]) and price (e.g., [100], [33], [104]), emission policy (e.g., [11]), and biofuel demand (e.g., [21], [33]) uncertainty on the design and management of a biofuel supply chain network. Researchers further attempted to optimize the biomass supply chain decisions under different possible situations, such as financial uncertainty (e.g., [29]), environmental restrictions (e.g., [51], [52], [11]), and even in managing risks under extreme weather situations, such as hurricanes and tornados (e.g., [53], [50], [75]).

Even though the biomass-to-biofuel supply chain received considerable attention in the research community, the promising biomass-to-pellet supply chain is vastly unexplored. Until recently, a number of studies performed a techno-economic analysis to find an economical pathway to produce pellets from various agricultural sources (e.g., unmerchantable forest residues, pole mill residues, straw, and switchgrass) [48, 6, 5, 95]. For instance, Mani et al. [48] estimate the capital and operating costs for different capacities of the biomass pellet production plants. Agar [6] perform an economic comparison between the torrefied pellets and the conventional wood pellets. Hoefnagels

et al. [5] perform an economic assessment to produce pellets from the underutilized wood resources available in the Southeast US. Based on the location and feedstock supply assumptions, the authors also estimate the optimal pellet plant size (55 to 315 Gg/year) for this region. Other than the economic assessment, a few studies perform cradle-to-gate life cycle assessment [2] and environmental impact assessment of exported wood pellets between two countries [45]. Note that none of these studies attempt to consider the uncertainty (biomass availability and quality) and market-driven pellet production requirements for the pellet supply chain network.

Consider biorefinery as a final destination, a number of researchers (e.g., [65, 81, 74, 11, 67]) consider depots as an intermediate biomass preprocessing layer within a four-layer supply chain network, where biomass, procured at the feedstock supply sites, transported to depots for converting into pellets which are then taken into biorefineries via intermodal facilities (i.e., rail or barge) for producing biofuels. It is important to note that even though these studies provide important managerial insights for the bioenergy communities, less attention is paid on modeling the key drivers (e.g., biomass seasonality and quality, market-driven pellet production requirements) of the biomass-to-pellet supply chain. Without such modeling efforts, the economic feasibility of the pellet production can not be obtained. Among the few available studies, Mobini et al. [59, 58] develop simulation-based models to simultaneously minimize both cost and carbon emissions for the regular and torrefied wood pellet-based supply chain. Boukherroub et al. [16] provide a comprehensive wood pellet-based supply chain modeling framework that explicitly accounts for a range of feedstock sources to ensure profitability by producing market-driven pellets under a deterministic setting. Quddus et al.[82] extended this study to develop a two-stage stochastic mixed-integer linear programming (MILP) model to optimally locate a set of multi-purpose pellet

processing depots for serving various markets (e.g., biorefinery, coal, animal feed, and paper industries) under biomass supply uncertainty. Note that none of the prior studies modeled the impact of biomass quality variability in identifying the economics behind market demand-specific pellet production (as can be seen in Table 1.1). A few recent studies (e.g., [1, 67]) accounted for the stochasticity associated with biomass quality in the modeling process and demonstrated how the depot locations can be changed with biomass quality variabilities. Different from the studies discussed above, our study, for the first time in the literature, aimed to focus on realistically modeling the key drivers into a biomass-to-pellet based supply system network. Specific attention is paid to optimizing how the different sources of the unused biomass resources can be utilized, transported, stored, pre-processed, and finally produced pellets to serve various consumers of the domestic and overseas markets under biomass seasonality and quality variability. A comprehensive review of different biomass-to-pellet supply chain cost drivers can be found in [105].

1.1.3 Summary of Major Contributions

In summary, the major contributions of this study to the existing literature are as follows:

- This paper is the first to develop a mathematical model which explicitly captures the impact of biomass quality (e.g., ash/moisture contents) on a biomass-to-pellet supply network. The proposed model captured several realistic features (e.g., different grades of the pellets, preprocessing requirements based on different ranges of ash/moisture contents, market requirements) that efficiently optimized in an attempt to minimize the overall pellet production cost under biomass yield and quality uncertainty.
- Due to the challenges associated with solving the proposed model in a realistic test setting, we propose to develop a highly customized solution approach, which combines Sample Average

Approximation with an enhanced Progressive Hedging algorithm. Our specific contribution is the development of two parallelization schemes to efficiently speed up the convergence of the overall algorithm.

- The final contribution of this paper is to develop a realistic case study by using Mississippi as a testing ground. Mississippi possesses a number of favorable factors (e.g., abundant biomass, cheap wood prices and wages, waterway transportation facilities) that are likely to attract stakeholders to invest in the pellet business in the future. The outcome of this study provides several managerial insights for the decision-makers, such as the optimal deployment of pelleting facilities, the amount of biomass stored, transported, and preprocessed under biomass yield and quality uncertainty.

The exposition of this paper is as follows. Section 1.2 and 1.3, respectively, introduces the proposed mathematical model and solution approaches. Section 1.4 describes the data used in the mathematical model, draws insights from real-life experiments, and compares the performance of the algorithms in solving the proposed mathematical model. Finally, Section 1.5 concludes this paper by introducing several future research avenues.

1.2 Problem Description and Model Formulation

This section presents a mathematical model that appropriately captures the stochasticity associated with the biomass yield and quality and accounts for all the critical steps (e.g., harvesting, storage, transportation, quality inspection, and production decisions) that significantly impact the biomass-to-pellet supply chain. We consider a two-layer supply chain network that consists of a set of existing feedstock supply sites, $\mathcal{I}$, and a set of candidate depot locations, $\mathcal{J}$, i.e., $\mathcal{N} = \mathcal{I} \bigcup \mathcal{J}$, where $\mathcal{N}$ to represent the set of nodes within the supply chain network. Locating a depot of size

$c \in C$ in a candidate site $j \in \mathcal{J}$ incurs a fixed investment cost of ψ_{cj}. Each feedstock supply site $i \in \mathcal{I}$ harvests a specific type of the biomass, denoted by set $b \in \mathcal{B}$, in time $t \in \mathcal{T}$. To capture the stochasticity associated with the system elements (e.g., biomass yield and quality), we introduce Ω to be the set of random events, where ρ_ω is the probability of a given realization, and $\sum_{\omega \in \Omega} \rho_\omega = 1$.

Before delving into the details, we first visualize the major decisions involved in a biomass-to-pellet supply chain in Figure 1.1. As can be seen in the figure, we set the boundary of our supply chain from harvesting the biomass until the pellets of different grades are produced in the depots to serve various markets. In practice, the biomass-to-pellet supply chain spans even further after producing the pellets; however, in this study, we are particularly interested in modeling the challenges involved in the earlier stages of this supply chain due to the stochasticity associated with the biomass yield and quality. Let $\overline{S}_{bit\omega}$ to be the availability of feedstock of type $b \in \mathcal{B}$ in supply site $i \in \mathcal{I}$ at time $t \in \mathcal{T}$ under scenario $\omega \in \Omega$. Biomass, once harvested, can be either stored in a feedstock site $i \in \mathcal{I}$, with a storage capacity of Π^1_{bi}, or can be transported to a nearby depot by incurring a unit transportation cost of $l_{bij\tau t\omega}$. Since the distances between the $(i, j) \in (\mathcal{I}, \mathcal{J})$ pairs are short, we consider trucks to be the only means to transport biomass between each source to destination pairs. Transportation cost, $l_{bij\tau t\omega}$, consists of two major components: (i) fixed cost, l^f_{bt} (e.g., loading and unloading costs) and (ii) variable cost, l^v_{bt} (e.g., fuel cost), and can be represented as follows: $l_{bij\tau t\omega} = l^f_{bt}(1+\varphi^f_{b\tau t\omega})+l^v_{bt}g_{ij}(1+\varphi^v_{b\tau t\omega}); \forall b \in \mathcal{B}, (i, j) \in (\mathcal{I}, \mathcal{J}), (\tau, t) \in \mathcal{T} | \tau \leq t, \omega \in \Omega$. Here, g_{ij} is the transportation distance between a feedstock site $i \in \mathcal{I}$ to a depot $j \in \mathcal{J}$, and $\varphi^f_{b\tau t\omega}$ and $\varphi^v_{b\tau t\omega}$ to denote the dry matter loss (in %) during loading/unloading and transporting biomass, respectively. Note that the longer the biomass is harvested before being transported, the higher the

dry matter loss (%), and consequently, the higher the transportation cost would be. As such, we assume that $l_{bij\tau_1 t\omega} \geq l_{bij\tau_2 t\omega}; \forall b \in \mathcal{B}, (i,j) \in (\mathcal{I},\mathcal{J}), (\tau_1,\tau_2,t) \in \mathcal{T}, 0 \leq \tau_1 \leq \tau_2 \leq t, \omega \in \Omega$.

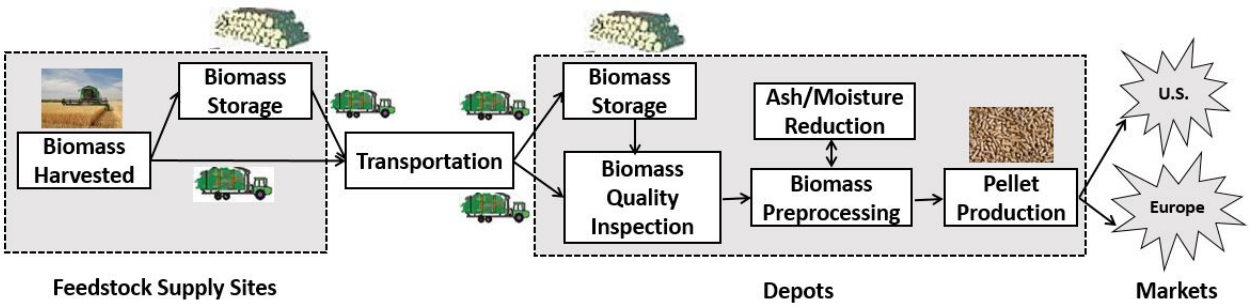

Figure 1.1

Summary of the decisions involved in a biomass-to-pellet supply chain

Biomass, if stored in a supply site $i \in \mathcal{I}$ upon harvesting, incurs a unit storage cost of $h^1_{bi\tau t}$. Let $\alpha_{b\tau t\omega}$ be the dry matter loss (%) due to storing feedstock $b \in \mathcal{B}$ between time $\tau \in \mathcal{T}$ to $t \in \mathcal{T}$ under scenario $\omega \in \Omega$, where $\tau \leq t$. Given the biomass post-harvest loss is quite intense, we assume that $\alpha_{b\tau_1 t\omega} \geq \alpha_{b\tau_2 t\omega}$ and $h^1_{bi\tau_1 t} \geq h^1_{bi\tau_2 t}; \forall b \in \mathcal{B}, i \in \mathcal{I}, (\tau,t) \in \mathcal{T}, 0 \leq \tau_1 \leq \tau_2 \leq t, \omega \in \Omega$. Upon receiving the unprocessed biomass from the feedstock sites, the depots either perform a quality inspection of the biomass or store them before this inspection (see Figure 1.1). For each depot $j \in \mathcal{J}$ with a storage capacity Π^2_{bcj}, let $h^2_{bj\tau t}$ to denote the unit storage cost for feedstock type $b \in \mathcal{B}$ between time τ to t, where $(\tau,t) \in \mathcal{T} | \tau \leq t$. Yet again, it can be assumed that $h^2_{bj\tau_1 t} \geq h^2_{bj\tau_2 t}; \forall b \in \mathcal{B}, j \in \mathcal{J}, (\tau,t) \in \mathcal{T}, 0 \leq \tau_1 \leq \tau_2 \leq t, \omega \in \Omega$. Given the different pellets must compromise the grade-specific biomass quality standards (see Table 1.1), the two essential quality metrics, namely, the *ash* and *moisture* contents, are checked in the collected biomass

samples. Let $\gamma_{bjt\omega}$ be the inspected ash content (%) in unprocessed biomass $b \in \mathcal{B}$ on depot $j \in \mathcal{J}$ at time $t \in \mathcal{T}$ under scenario $\omega \in \Omega$. Depending upon the observed ash level in the samples and the ash restrictions on different grades of the pellets, we introduce set $\mathcal{R}$ to define the range of ash contents for the pellets, i.e., $r \in \mathcal{R} \mid r_1 : 0 \leq \gamma_{bjt\omega} < 0.7; r_2 : 0.7 \leq \gamma_{bjt\omega} < 1.0; r_3 : 1.0 \leq \gamma_{bjt\omega} < 1.5, r_4 : 1.5 \leq \gamma_{bjt\omega} < 2.0; r_5 : 2.0 \leq \gamma_{bjt\omega} < 3.0; r_6 : 3.0 \leq \gamma_{bjt\omega} < 6.0; r_7 : \gamma_{bjt\omega} \geq 6$. We denote this inspection and segregation to range $r \in \mathcal{R}$ cost for biomass $b \in \mathcal{B}$ in depot $j \in \mathcal{J}$ at time $t \in \mathcal{T}$ to be ζ_{bjrt}.

Given the ash content in biomass can be divided into two major types, *authigenic* ash and *detrital* ash, we divide $\gamma_{bjt\omega}$ (%) into $\gamma^1_{bjt\omega}$ (%) and $\gamma^2_{bjt\omega}$ (%), respectively, to capture these two different ash levels, and $\gamma_{bjt\omega} = \gamma^1_{bjt\omega} + \gamma^2_{bjt\omega}$. Authigenic ash, $\gamma^1_{bjt\omega}$, is essentially the nutrient deposit inside the plant fibers, which is accumulated via water and soil uptake during growth. On the contrary, detrital ash, $\gamma^2_{bjt\omega}$, is the fine layer of soil and sand contaminants coated at the surface of the biomass (e.g., woody biomass), which is accumulated during collection, handling, transportation, and other subsequent processing of the biomass. Note that based on the value of the ash content level, $\gamma_{bjt\omega}$, we introduce an indicator $\mathbb{I}_{bjrt\omega} = (0, 1)$ to classify biomass $b \in \mathcal{B}$ to the appropriate ash range $r \in \mathcal{R}$. Once classified, it would be possible to reduce the ash contents of the sampled biomass in an attempt to produce pellets of the desired grade. Let $\theta_{bjrr't}$ be the unit ash content reduction cost of unprocessed biomass $b \in \mathcal{B}$ in depot $j \in \mathcal{J}$ from level r to r', where $(r, r')|r \in \mathcal{R}, r' \leq r$ at time $t \in \mathcal{T}$. Techniques, such as chemical leaching and water washing, can be used to reduce ash contents from the authigenic ash ($\gamma^1_{bjt\omega}$). On the other hand, in addition to

washing (e.g., chemical or water), procuring quality biomass[1] and better handling, processing, and transporting method can be utilized to minimize ash contents from the detrital ash ($\gamma^2_{bjt\omega}$) [76].

Unlike ash content, managing moisture content for producing different grades of the pellets is quite straightforward. First, the moisture content of the sampled biomass is checked. If the content exceeds 10% (except PFI Premium pellet of the U.S. market for which the requirement is less than 8% (see Table 1.1)), then preheating techniques are applied such that the resulting properties best suit the conversion process for different grades of the pellets. We introduce a binary indicator $\beta_{bjrt\omega} = (0, 1)$ to denote if the preheating for the sampled biomass $b \in \mathcal{B}$ at depot $j \in \mathcal{J}$ in time $t \in \mathcal{T}$ and under scenario $\omega \in \Omega$ is required to produce pellet in range $r \in \mathcal{R}_p$, i.e., $\beta_{bjrt\omega} = 1$; 0 otherwise. Given preheating is necessary only if the moisture content of the sampled biomass $b \in \mathcal{B}$ reaches over 8% for the PFI Premium pellet and 10% for all other pellets, we introduce parameter $\mu_{bjt\omega}$ to denote the excess moisture content in the sampled biomass under scenario $\omega \in \Omega$. For a specific biomass type $b \in \mathcal{B}$, sampled at depot $j \in \mathcal{J}$ in time $t \in \mathcal{T}$, if $\mu_{bjt\omega} > 0$ is observed, then we can set $\beta_{bjrt\omega} = 1$, depending on the expected production range of the pellet $r \in \mathcal{R}_p$. On the other hand, if $\mu_{bjt\omega} = 0$ (meaning the moisture content is below/at the required level for the pellet production), then no additional preheating would be necessary, i.e., $\beta_{bjrt\omega} = 0$. We then define κ_{bjrt} to be the unit moisture content reduction cost for unprocessed biomass $b \in \mathcal{B}$ to produce pellet in range $r \in \mathcal{R}_p$ in depot $j \in \mathcal{J}$ at time $t \in \mathcal{T}$. The overall unit moisture content management-related cost now becomes: $\kappa_{bjrt}\beta_{bjrt\omega}\mu_{bjt\omega}$. Clearly, the higher the moisture content,

[1]The ash content of woody biomass (e.g., poplar, sawdust) is typically in the low range of 2%, whereas the ash content of the herbaceous biomass is higher (e.g., rice husk contains an average of 22.6% ash content). Even for the same tree, the ash content is higher at the bark, branches, leaf, and needles over the stem or branch wood [76].

the more expensive the unit moisture reduction cost (due to increasing in preheating cost) would be.

The resultant quality-inspected, preprocessed biomass $b \in \mathcal{B}$ is now ready for the pellet production in order to serve both for the domestic (e.g., U.S.) and the overseas (e.g., Europe) markets. Let $\mathcal{P}_E$ and $\mathcal{P}_A$ to denote the set of pellets to produce for the Europe and the U.S. market, respectively, where $\mathcal{P} = P_E \bigcup P_A$. We further let d_{pt} to be the total demand for pellet $p \in \mathcal{P}$ at time $t \in \mathcal{T}$. The demand for pellet $p \in \mathcal{P}$ at time $t \in \mathcal{T}$, with an unit production cost η_{pjt} and capacity Γ_{cj}, can be satisfied either from the depots or via an external supplier(s) by incurring an additional penalty cost of π_{pt}. One can view this penalty cost (π_{pt}) as a threshold value beyond which producing pellets from the internal biomass-to-pellet supply chain is no longer considered economical. Below is a summary of the sets, parameters, and decision variables of the optimization model.

Sets:

- $\mathcal{I}$: set of feedstock suppliers, $i \in \mathcal{I}$
- $\mathcal{J}$: set of potential location for depots, $j \in \mathcal{J}$
- $\mathcal{B}$: set of biomass types, $b \in \mathcal{B}$
- $\mathcal{P}_E$: set of pellets to produce for the Europe market
- $\mathcal{P}_A$: set of pellets to produce for the U.S. market
- $\mathcal{P}$: set of all pellet types, $p \in \mathcal{P}$, where $\mathcal{P} = P_E \bigcup P_A$
- $\mathcal{B}_p$: set of possible feedstocks to produce pellet $p \in \mathcal{P}$, where $\mathcal{B}_p \subseteq \mathcal{B}$
- $\mathcal{C}$: set of depot capacities, $c \in \mathcal{C}$
- $\mathcal{T}$: set of time periods, $t \in \mathcal{T}$

- $\mathcal{R}$: range of ash contents for pellets $\{r \in \mathcal{R} \mid r_1 : 0 \leq \gamma_{bjt\omega} < 0.7; r_2 : 0.7 \leq \gamma_{bjt\omega} < 1.0; r_3 : 1.0 \leq \gamma_{bjt\omega} < 1.5, r_4 : 1.5 \leq \gamma_{bjt\omega} < 2.0; r_5 : 2.0 \leq \gamma_{bjt\omega} < 3.0; r_6 : 3.0 \leq \gamma_{bjt\omega} < 6.0; r_7 : \gamma_{bjt\omega} \geq 6\}$
- $\mathcal{P}_b$: set of pellets that can be produced using biomass $b \in \mathcal{B}$
- $\mathcal{R}_p$: subset of ranges associated with each pellet type $p \in \mathcal{P}$
- Ω: set of scenarios, $\omega \in \Omega$

Parameters:

- ψ_{cj}: investment cost to open a depot of size $c \in C$ at location $j \in \mathcal{J}$
- $l_{bij\tau t\omega}$: unit transportation cost of flowing feedstock $b \in \mathcal{B}$ from source $i \in \mathcal{I}$ to destination $j \in \mathcal{J}$ at time $t \in \mathcal{T}$ which are harvested in time $\tau \in \mathcal{T}$ $(\tau \leq t)$ under scenario $\omega \in \Omega$
- $h^1_{bi\tau t}$: unit storage cost for feedstock type $b \in \mathcal{B}$ at supply site $i \in \mathcal{I}$ between time τ and t, where $(\tau, t) \in \mathcal{T} | \tau \leq t$
- $h^2_{bj\tau t}$: unit storage cost for feedstock type $b \in \mathcal{B}$ at depot $j \in \mathcal{J}$ between time τ and t, where $(\tau, t) \in \mathcal{T} | \tau \leq t$
- σ_{bit}: unit cost of harvesting biomass of type $b \in \mathcal{B}$ in feedstock site $i \in \mathcal{I}$ at time $t \in \mathcal{T}$
- ζ_{bjrt} unit biomass of type $b \in \mathcal{B}$ inspection and segregation to range $r \in \mathcal{R}$ cost in depot $j \in \mathcal{J}$ at time $t \in \mathcal{T}$
- η_{pjt}: unit pellet production cost of type $p \in \mathcal{P}$ in depot $j \in \mathcal{J}$ at time $t \in \mathcal{T}$
- $\theta_{bjrr't}$: ash content reduction cost of unprocessed biomass $b \in \mathcal{B}$ in depot $j \in \mathcal{J}$ from level r to r', where $(r, r') | r \in \mathcal{R}, r' \leq r$ at time $t \in \mathcal{T}$
- π_{pt}: unit penalty cost for unsatisfied market demand of pellet $p \in \mathcal{P}$ at time $t \in \mathcal{T}$

- $\overline{S}_{bit\omega}$: availability of feedstock $b \in \mathcal{B}$ in supply site $i \in \mathcal{I}$ at time $t \in \mathcal{T}$ under scenario $\omega \in \Omega$
- $\alpha_{b\tau t\omega}$: dry matter loss (%) due to storing feedstock $b \in \mathcal{B}$ between time $\tau \in \mathcal{T}$ to $t \in \mathcal{T}$ under scenario $\omega \in \Omega$, where $\tau \leq t$
- ϕ_{brp}: conversion rate of unprocessed feedstock $b \in \mathcal{B}$ to pellet $p \in \mathcal{P}$ under ash range $r \in \mathcal{R}$
- Γ_{cj}: pellet production capacity of size $c \in \mathcal{C}$ at depot $j \in \mathcal{J}$
- Π^1_{bi}: storage capacity of feedstock $b \in \mathcal{B}$ in supply site $i \in \mathcal{I}$
- Π^2_{bcj}: storage capacity of size $c \in \mathbb{C}$ for unprocessed feedstock $b \in \mathcal{B}$ in depot $j \in \mathcal{J}$
- $\gamma_{bjt\omega}$: inspected ash content (%) in unprocessed biomass $b \in \mathcal{B}$ on depot $j \in \mathcal{J}$ at time $t \in \mathcal{T}$ under scenario $\omega \in \Omega$
- $\mathbb{I}_{bjrt\omega}$: an indicator to confirming the inspected ash content range, i.e., $\mathbb{I}_{bjtr\omega} = (0/1)$ to indicate if the ash content level of the inspected biomass of type $b \in \mathcal{B}$ in site $j \in \mathcal{J}$ at time $t \in \mathcal{T}$ falls in range $r \in \mathcal{R}$ under scenario $\omega \in \Omega$
- $\varphi^f_{b\tau t\omega}, \varphi^v_{b\tau t\omega}$: dry matter loss (in %) during loading/unloading and transporting biomass type $b \in \mathcal{B}$ under scenario $\omega \in \Omega$
- κ_{bjrt}: unit moisture content reduction cost for unprocessed biomass $b \in \mathcal{B}$ to produce pellet in range $r \in \mathcal{R}$ in depot $j \in \mathcal{J}$ at time $t \in \mathcal{T}$
- $\beta_{bjrt\omega}$: an indicator to denote if the preheating for the sampled biomass $b \in \mathcal{B}$ at depot $j \in \mathcal{J}$ in time $t \in \mathcal{T}$ and under scenario $\omega \in \Omega$ is required or not to produce pellet in range $r \in \mathcal{R}_p$, i.e., $\beta_{bjrt\omega} = 1$, if preheating is required; 0 otherwise
- $\mu_{bjt\omega}$: the excess moisture content (%) in the sampled biomass $b \in \mathcal{B}$ at depot $j \in \mathcal{J}$ in time $t \in \mathcal{T}$ under scenario $\omega \in \Omega$

- d_{pt}: demand for pellet $p \in \mathcal{P}$ at time $t \in \mathcal{T}$
- ρ_{ω}: probability of scenario $\omega \in \Omega$

Decision Variables:

- Y_{cj}: 1 if a depot of capacity $c \in C$ is opened in location $j \in \mathcal{J}$; 0 otherwise
- $S_{bit\omega}$: amount feedstock of type $b \in \mathcal{B}$ harvested in supply site $i \in \mathcal{I}$ at time $t \in \mathcal{T}$ under scenario $\omega \in \Omega$
- $X_{bij\tau t\omega}$: amount of biomass $b \in \mathcal{B}$ that were harvested in supply site $i \in \mathcal{I}$ at time τ and then transported to depot $j \in \mathcal{J}$ in time t under scenario $\omega \in \Omega$, where $(\tau, t) \in \mathcal{T} | \tau \leq t$
- $H^1_{bi\tau t\omega}$: amount of feedstock of type $b \in \mathcal{B}$ stored at supply site $i \in \mathcal{I}$ between time period τ to t under scenario $\omega \in \Omega$, where $(\tau, t) \in \mathcal{T} | \tau \leq t$
- $H^2_{bj\tau t\omega}$: amount of unprocessed biomass $b \in \mathcal{B}$ stored at depot $j \in \mathcal{J}$ between time period τ to t under scenario $\omega \in \Omega$, where $(\tau, t) \in \mathcal{T} | \tau \leq t$
- $P_{bj\tau t\omega}$: amount of unprocessed feedstock $b \in \mathcal{B}$ which are transported to depot $j \in \mathcal{J}$ at time $\tau \in \mathcal{T}$ and ready for quality inspection in time $t \in \mathcal{T}$ under scenario $\omega \in \Omega$, where $\tau \leq t$
- $Z_{bjt\omega}$: total availability of unprocessed biomass of type $b \in \mathcal{B}$ are ready for quality inspection at depot $j \in \mathcal{J}$ in time $t \in \mathcal{T}$ under scenario $\omega \in \Omega$
- $Q_{bjrt\omega}$: amount of inspected unprocessed biomass $b \in \mathcal{B}$ available at depot $j \in \mathcal{J}$ in time $t \in \mathcal{T}$ with an ash content level falling on range $r \in \mathcal{R}$ under scenario $\omega \in \Omega$
- $L_{brpjt\omega}$: amount of biomass $b \in \mathcal{B}$ with level $r \in \mathcal{R}$ used to produce pellet $p \in \mathcal{P}_b$ in depot $j \in \mathcal{J}$ at time $t \in \mathcal{T}$ under scenario $\omega \in \Omega$

- $R_{bjrr't\omega}$: amount of unprocessed biomass of type $b \in \mathcal{B}$ in depot $j \in \mathcal{J}$ at time $t \in \mathcal{T}$ needs to be converted from ash range $r \in \mathcal{R}$ to $r' \in \mathcal{R} | r' \leq r$ under scenario $\omega \in \Omega$
- $D_{pjrt\omega}$: amount of pellet of type $p \in \mathcal{P}$ produced at depot $j \in \mathcal{J}$ with an ash content level falling on range $r \in \mathcal{R}$ in time $t \in \mathcal{T}$ under scenario $\omega \in \Omega$
- $U_{pt\omega}$: shortage of pellet type $p \in \mathcal{P}$ at time $t \in \mathcal{T}$ under scenario $\omega \in \Omega$

Let us now introduce the decision variables for our proposed two-stage stochastic programming model formulation. The first-stage decision variable $\mathbf{Y} := \{Y_{cj} | \forall c \in C, j \in \mathcal{J}\}$ to denote the size and location to open a depot, i.e.,

$$Y_{cj} = \begin{cases} 1 & \text{if a depot of capacity } c \in C \text{ is opened in location } j \in \mathcal{J} \\ 0 & \text{otherwise;} \end{cases}$$

The second-stage decisions for this model include the amount of biomass stored, transported, inspected, preprocessed, converted to pellets, and demand shortage costs. More specifically, decision variables $\mathbf{S} := \{S_{bit\omega} | \forall b \in \mathcal{B}, i \in \mathcal{I}, t \in \mathcal{T}, \omega \in \Omega\}$ to denote the amount feedstock of type b harvested in supply site i at time t under scenario ω; $\mathbf{X} := \{X_{bij\tau t\omega} | \forall b \in \mathcal{B}, i \in \mathcal{I}, j \in \mathcal{J}, (\tau, t) \in \mathcal{T} | \tau \leq t, \omega \in \Omega\}$ to denote the amount of biomass b that were harvested in supply site i at time τ and then transported to depot j in time t under scenario ω; $\mathbf{H}^1 := \{H^1_{bi\tau t\omega} | \forall b \in \mathcal{B}, i \in \mathcal{I}, (\tau, t) \in \mathcal{T} | \tau \leq t, \omega \in \Omega\}$ to denote the amount of feedstock of type b stored at supply site i between time period τ to t under scenario ω; $\mathbf{H}^2 := \{H^2_{bj\tau t\omega} | \forall b \in \mathcal{B}, j \in \mathcal{J}, (\tau, t) \in \mathcal{T} | \tau \leq t, \omega \in \Omega\}$ to denote the amount of unprocessed biomass b stored at depot j between time period τ to t under scenario ω; $\mathbf{P} := \{P_{bj\tau t\omega} | \forall b \in \mathcal{B}, j \in \mathcal{J}, (\tau, t) \in \mathcal{T} | \tau \leq t, \omega \in \Omega\}$ to denote the amount of unprocessed

feedstock b which are transported to depot j at time τ and ready for quality inspection in time t under scenario ω; $\mathbf{Z} := \{Z_{bjt\omega} | \forall b \in \mathcal{B}, j \in \mathcal{J}, t \in \mathcal{T}, \omega \in \Omega\}$ to denote the total availability of unprocessed biomass of type b which are ready for quality inspection at depot j in time t under scenario ω; $\mathbf{Q} := \{Q_{bjrt\omega} | \forall b \in \mathcal{B}, j \in \mathcal{J}, r \in \mathcal{R}, t \in \mathcal{T}, \omega \in \Omega\}$ to denote the amount of inspected unprocessed biomass b available at depot j in time t with an ash content level falling on range r under scenario ω; $\mathbf{L} := \{L_{brpjt\omega} | \forall b \in \mathcal{B}, r \in \mathcal{R}, p \in \mathcal{P}_b, j \in \mathcal{J}, t \in \mathcal{T}, \omega \in \Omega\}$ to denote the amount of biomass b with level r used to produce pellet p in depot j at time t under scenario ω; $\mathbf{R} := \{R_{bjrr't\omega} | \forall b \in \mathcal{B}, j \in \mathcal{J}, (r, r') \in \mathcal{R} | r' \leq r, t \in \mathcal{T}, \omega \in \Omega\}$ to denote the amount of unprocessed biomass of type b in depot j at time t needs to be converted from ash range r to r' under scenario ω; $\mathbf{D} := \{D_{pjrt\omega} | \forall p \in \mathcal{P}, j \in \mathcal{J}, r \in \mathcal{R}, t \in \mathcal{T}, \omega \in \Omega\}$ to denote the amount of pellet of type p with ash range r produced at depot j in time t under scenario ω; and $\mathbf{U} := \{U_{pt\omega} | \forall p \in \mathcal{P}, t \in \mathcal{T}, \omega \in \Omega\}$ to denote the shortage of pellet type p at time t under scenario ω. For notation convenience, we group the storage sets as $\mathbf{H} := \mathbf{H}^1 \bigcup \mathbf{H}^2$. We formulate this problem as a two-stage stochastic mixed-integer linear programming model, referred to as **(BQP)**. We assume that the capacity and site selection decisions for the depots (Y_{cj}) will be made at the beginning of the planning horizon and prior to a realization of any stochastic event. We refer to this decision as a first-stage decision. However, after the uncertainty is revealed, a number of second-stage decisions will be made, which include the amount of biomass harvested, stored, transported, inspected, preprocessed, converted to pellets, and demand shortage.

The goal of **(BQP)** is to minimize the overall system cost, which includes minimizing the first-stage and the expected second-stage costs across all possible scenarios. Model **(BQP)** handles a number of uncertain parameters, such as the biomass supply availability ($\overline{S}_{bit\omega}$), the quality-related

parameters ($\gamma_{bjt\omega}$, $\mathbb{I}_{bjrt\omega}$, $\alpha_{b\tau t\omega}$, $\varphi^{f}_{b\tau t\omega}$, $\varphi^{v}_{b\tau t\omega}$, $\beta_{bjrt\omega}$, $\mu_{bjt\omega}$), and the associated costs ($l_{bijt\omega}$). We refer Θ to denote the vector of these parameters, i.e., $\Theta = (\overline{\mathbf{S}}, \boldsymbol{\gamma}, \mathbb{I}, \boldsymbol{\alpha}, \boldsymbol{\varphi}, \boldsymbol{\beta}, \boldsymbol{\mu}, \mathbf{l})$, where Θ_ω is a given realization of the uncertain parameters. With this, we are now ready to introduce formulation **(BQP)** below.

$$\textbf{(BQP)} \quad \underset{\mathbf{Y}}{Minimize} \sum_{c\in\mathcal{C}}\sum_{j\in\mathcal{J}} \psi_{cj}Y_{cj} + \sum_{\omega\in\Omega}\rho_\omega \mathbb{Q}(\mathbf{Y}, \Theta_\omega) \tag{1.1}$$

subject to

$$\sum_{c\in\mathcal{C}} Y_{cj} \leq 1 \qquad \forall j \in \mathcal{J} \tag{1.2}$$

$$Y_{cj} \in \{0,1\} \qquad \forall c \in \mathcal{C}, j \in \mathcal{J} \tag{1.3}$$

with $\mathbb{Q}(\mathbf{Y}, \Theta_\omega)$ being the solution of the following second-stage problem:

$$\begin{aligned}\mathbb{Q}(\mathbf{Y}, \Theta_\omega) = \underset{\mathbf{S,X,H,P,Z,Q,L,R,D,U}}{Minimize} \sum_{t\in\mathcal{T}}\Bigg\{ &\sum_{b\in\mathcal{B}}\Bigg(\sum_{i\in\mathcal{I}}\sigma_{bit}S_{bit\omega} + \sum_{i\in\mathcal{I}}\sum_{j\in\mathcal{J}}\sum_{\tau\leq t} l_{bij\tau t\omega}X_{bij\tau t\omega} \\ &\sum_{i\in\mathcal{I}}\sum_{\tau\leq t} h^1_{bi\tau t}H^1_{bi\tau t\omega} + \sum_{j\in\mathcal{J}}\sum_{\tau\leq t} h^2_{bj\tau t}H^2_{bj\tau t\omega} + \sum_{j\in\mathcal{J}}\sum_{r\in\mathcal{R}}\Bigg(\zeta_{bjrt}Q_{bjrt\omega} \\ &\sum_{r'\leq r}(\theta_{bjrr't} + \kappa_{bjr't}\beta_{bjr't\omega}\mu_{bjt\omega})R_{bjrr't\omega}\Bigg)\Bigg) \\ &+ \sum_{p\in\mathcal{P}}\Bigg(\sum_{j\in\mathcal{J}}\eta_{pjt}D_{pjt\omega} + \pi_{pt}U_{pt\omega}\Bigg)\Bigg\}\end{aligned} \tag{1.4}$$

subject to

$$S_{bit\omega} \leq \overline{S}_{bit\omega} \quad \forall b \in \mathcal{B}, i \in \mathcal{I}, t \in \mathcal{T}, \omega \in \Omega \tag{1.5}$$

$$S_{bit\omega} = H^1_{bitt\omega} + \sum_{j \in \mathcal{J}} X_{bijtt\omega} \quad \forall b \in \mathcal{B}, i \in \mathcal{I}, t \in \mathcal{T}, \omega \in \Omega \tag{1.6}$$

$$(1 - \alpha_{b\tau,t-1,\omega}) H^1_{bi\tau,t-1,\omega} = H^1_{bi\tau t\omega} + \sum_{j \in \mathcal{J}} X_{bij\tau t\omega} \quad \forall b \in \mathcal{B}, i \in \mathcal{I}, (\tau, t) \in \mathcal{T} | \tau \leq t-1, \omega \in \Omega \tag{1.7}$$

$$\sum_{i \in \mathcal{I}} X_{bijtt\omega} = H^2_{bjtt\omega} + P_{bjtt\omega} \quad \forall b \in \mathcal{B}, j \in \mathcal{J}, t \in \mathcal{T}, \omega \in \Omega \tag{1.8}$$

$$(1 - \alpha_{b\tau,t-1,\omega}) H^2_{bj\tau,t-1,\omega} + \sum_{i \in \mathcal{I}} X_{bij\tau t\omega} = H^2_{bj\tau t\omega} + P_{bj\tau t\omega} \quad \forall b \in \mathcal{B}, j \in \mathcal{J}, (t, \tau) \in \mathcal{T} | \tau \leq t-1, \omega \in \Omega \tag{1.9}$$

$$\sum_{\tau=1}^{t} H^1_{bi\tau t\omega} \leq \Pi^1_{bi} \quad \forall b \in \mathcal{B}, i \in \mathcal{I}, t \in \mathcal{T}, \omega \in \Omega \tag{1.10}$$

$$\sum_{\tau=1}^{t} H^2_{bj\tau t\omega} \leq \sum_{c \in C} \Pi^2_{bcj} Y_{cj} \quad \forall b \in \mathcal{B}, j \in \mathcal{J}, t \in \mathcal{T}, \omega \in \Omega \tag{1.11}$$

$$\sum_{\tau=1}^{t} P_{bj\tau t\omega} = Z_{bjt\omega} \quad \forall b \in \mathcal{B}, j \in \mathcal{J}, t \in \mathcal{T}, \omega \in \Omega \quad (1.12)$$

$$Z_{bjt\omega} = \sum_{r \in \mathcal{R}} \mathbb{I}_{bjrt\omega} Q_{bjrt\omega} \quad \forall b \in \mathcal{B}, j \in \mathcal{J}, t \in \mathcal{T}, \omega \in \Omega \quad (1.13)$$

$$\sum_{r \in \mathcal{R}} Q_{bjrt\omega} = Z_{bjt\omega} \quad \forall b \in \mathcal{B}, j \in \mathcal{J}, t \in \mathcal{T}, \omega \in \Omega \quad (1.14)$$

$$\sum_{r' \leq r} R_{bjrr't\omega} = Q_{bjrt\omega} \quad \forall b \in \mathcal{B}, j \in \mathcal{J}, r \in \mathcal{R}, t \in \mathcal{T}, \omega \in \Omega \quad (1.15)$$

$$\sum_{r' \leq r} R_{bjrr't\omega} = \sum_{p \in \mathcal{P}_b} L_{br'pjt\omega} \quad \forall b \in \mathcal{B}, j \in \mathcal{J}, r' \in \mathcal{R}, t \in \mathcal{T}, \omega \in \Omega \quad (1.16)$$

$$\sum_{b \in \mathcal{B}_p} \phi_{br'p} L_{br'pjt\omega} = D_{pjr't\omega} \quad \forall p \in \mathcal{P}, j \in \mathcal{J}, r' \in \mathcal{R}_p, t \in \mathcal{T}, \omega \in \Omega \quad (1.17)$$

$$\sum_{p \in \mathcal{P}} \sum_{r \in \mathcal{R}_p} D_{pjrt\omega} \leq \sum_{c \in C} \Gamma_{cj} Y_{cj} \quad \forall j \in \mathcal{J}, t \in \mathcal{T}, \omega \in \Omega \quad (1.18)$$

$$\sum_{j \in \mathcal{J}} \sum_{r \in \mathcal{R}_p} D_{pjrt\omega} + U_{pt\omega} = d_{pt} \quad \forall p \in \mathcal{P}, t \in \mathcal{T}, \omega \in \Omega \quad (1.19)$$

$$X_{bij\tau t\omega}, H^1_{bi\tau t\omega}, H^2_{bj\tau t\omega}, P_{bj\tau t\omega} \geq 0 \quad \forall b \in \mathcal{B}, i \in \mathcal{I}, j \in \mathcal{J}, (\tau, t) \in \mathcal{T} | \tau \leq t, \omega \in \Omega \quad (1.20)$$

$$S_{bit\omega}, Z_{bjt\omega}, Q_{bjrt\omega}, R_{bjrr't\omega}, D_{pjrt\omega}, U_{pt\omega} \geq 0 \quad \forall b \in \mathcal{B}, p \in \mathcal{P}, i \in \mathcal{I}, j \in \mathcal{J}, t \in \mathcal{T}, (r, r') \in \mathcal{R} | r' \leq r, \omega \in \Omega \quad (1.21)$$

The objective function (1.1) is the sum of the first-stage costs and the expected second-stage costs. The first-stage decisions minimize the depot opening costs. Constraints (1.2) ensure that

at most one depot of size $c \in C$ is opened in location $j \in \mathcal{J}$. Constraints (1.3) set the binary restrictions for the depot opening decisions. The objective function of the second-stage costs (1.4) consists of several parts, namely, the costs associated with biomass harvesting, transportation, storage at feedstock sites and depots, inspection, preprocessing, pellet production, and demand shortage decisions. Constraints (1.5) restrict the harvesting quantity of biomass of type $b \in \mathcal{B}$ at supply site $i \in \mathcal{I}$ in time $t \in \mathcal{T}$ and under scenario $\omega \in \Omega$ to it's availability $\overline{S}_{bit\omega}$. Constraints (1.6) and (1.7) are the flow balance constraints for biomass type $b \in \mathcal{B}$ at feedstock supply site $i \in \mathcal{I}$ in time $t \in \mathcal{T}$. Likewise, constraints (1.8) and (1.9) are the flow balance constraints for biomass type $b \in \mathcal{B}$ at depot $j \in \mathcal{J}$ in time $t \in \mathcal{T}$. Constraints (1.10) and (1.11) set the biomass storage capacity at feedstock supply site $i \in \mathcal{I}$ and depot $j \in \mathcal{J}$ to Π^1_{bi} and Π^2_{bcj}, respectively. Constraints (1.12) determine the total biomass availability for quality inspection at depot $j \in \mathcal{J}$ in time $t \in \mathcal{T}$. Constraints (1.13)-(1.16) classify the inspected biomass based on different ash level $r \in \mathcal{R}$ under scenario $\omega \in \Omega$. For each pellet type $p \in \mathcal{P}$, depot $j \in \mathcal{J}$, time $t \in \mathcal{T}$, and scenario $\omega \in \Omega$, constraints (1.17) ensure the conversion of raw biomass to pellets. Constraints (1.18) limit the pellet production capacity in a depot $j \in \mathcal{J}$ to Γ_{cj}. Constraints (1.19) ensure that the demand for pellet, $\{d_{pt}\}_{\forall p \in \mathcal{P}, t \in \mathcal{T}}$, must be satisfied either via the depots or from a third-party supplier. Finally, constraints (1.20) and (1.21) set the standard non-negativity restrictions.

1.3 Solution Approach

By setting $|\mathcal{B}| = |\mathcal{P}| = |\mathcal{B}| = |\mathcal{T}| = |\mathcal{R}| = |\Omega| = 1$, model **(BQP)** can be reduced to a *fixed charge network flow problem*, which is already known to be an $\mathcal{NP}$-hard problem [12, 42]. As such, our initial experiments reveal that the commercial solver, GUROBI, is unable to solve the large-scale instances of **(BQP)**. To overcome this challenge, this study proposes a hybrid

algorithm which combines the Sample Average Approximation (SAA) technique with an enhanced Progressive Hedging Algorithm (PHA) to solve **(BQP)** in a reasonable timeframe. Model **(BQP)** is a two-stage stochastic mixed-integer linear programming model. Evaluating **(BQP)** with a large scenario set, Ω, poses a serious computational challenge. To overcome this challenge, first, we adopt the SAA algorithm [86, 8], which reduces the size of **(BQP)** by decomposing into a set of smaller scenarios. Given SAA is a widely used sampling-based technique available in the literature (see applications of SAA in biomass supply chain [73, 81], port management [9, 8], logistics management [80, 79]), this study omits the detailed discussion of the SAA methodology. Instead, the steps involved to solve model (BQP) using the SAA algorithm is outlined in **Appendix A1**. The following subsections detail the hybrid algorithm.

1.3.1 Progressive Hedging Algorithm

Even though by applying the SAA algorithm the size of the original problem **(BQP)** is decreased significantly, the subroblems associated with replications of the SAA algorithm, referred to as **[BQP(SAA)]**, are still challenging from the solution standpoint. This is because **[BQP(SAA)]** is still a two-stage stochastic programming model of scenario size N, which is required to be solved repeatedly in different replications of the SAA algorithm. Further, if we consider the practice real-life sizes of $|\mathcal{B}|$, $|\mathcal{P}|$, $|\mathcal{T}|$, and $|\mathcal{R}|$, solving **[BQP(SAA)]** could still be considered challenging. To alleviate this challenge, we apply the PHA procedure, proposed by Rockafellar and Wets [84], to efficiently solve **[BQP(SAA)]**. This algorithm utilizes the augmented Lagrangian relaxation method, which decomposes a two-stage stochastic programming model by scenarios and attempts to solve the respective sub-problems in a much shorter time [106]. The PHA is widely applied in solving stochastic optimization problems in diversified areas, including applications in

financial planning [60], surgery planning [34], inland waterway port management [9, 10], and many others[7].

In **[BQP(SAA)]**, constraints (1.11) and (1.18) link the first-stage decision variables, $\{Y_{cj}\}$, with the second-stage decision variables. These constraints restrict **[BQP(SAA)]** to be separable by scenarios. To alleviate this problem, we introduce a new *copy* variable $\{Y_{cjn}\}_{c\in C, j\in\mathcal{J}, n\in\mathcal{N}} \in \{0,1\}$, which allows **[BQP(SAA)]** to be separable by scenarios. Introducing this new variable, we reformulate **[BQP(SAA)]** as follows:

$$\underset{\mathbf{Y,S,X,H,P,Z,Q,L,R,D,U}}{Minimize} \quad \frac{1}{N}\sum_{n=1}^{N}\left(\sum_{c\in C}\sum_{j\in\mathcal{J}}\psi_{cj}Y_{cjn} + \mathbb{Q}(\mathbf{Y},\Theta_n)\right) \tag{1.22}$$

subject to (1.5)-(1.10), (1.12)-(1.17), (1.19)-(1.21), and

$$\sum_{c\in C} Y_{cjn} \leq 1 \qquad \forall j\in\mathcal{J}, n\in\mathcal{N} \tag{1.23}$$

$$\sum_{\tau=1}^{t} H^2_{bj\tau tn} \leq \sum_{c\in C}\Pi^2_{bcj}Y_{cjn} \quad \forall b\in\mathcal{B}, j\in\mathcal{J}, t\in\mathcal{T}, n\in\mathcal{N} \tag{1.24}$$

$$\sum_{p\in\mathcal{P}}\sum_{r\in\mathcal{R}_p} D_{pjrtn} \leq \sum_{c\in C}\Gamma_{cj}Y_{cjn} \qquad \forall j\in\mathcal{J}, t\in\mathcal{T}, n\in\mathcal{N} \tag{1.25}$$

$$Y_{cjn} = Y_{cjn'} \qquad \forall c\in C, j\in\mathcal{J}, (n,n')\in\mathcal{N}, n\neq n' \tag{1.26}$$

$$Y_{cjn} \in \{0,1\} \qquad \forall c\in C, j\in\mathcal{J}, n\in\mathcal{N} \tag{1.27}$$

Constraints (1.26) are known as *nonanticipativity* constraints. Such constraints force all the scenario dependant first-stage variables to yield the same value for different scenarios. These constraints, however, restrict problem (1.22) separable by scenarios. To alleviate this issue, we

introduce $\{\bar{Y}_{cj}\}_{c\in C, j\in\mathcal{J}} \in \{0,1\}$, which is known as *overall design vectors*. With this, constraint (1.26) can now be replaced by the following set of constraints:

$$Y_{cjn} = \bar{Y}_{cj} \qquad \forall c \in C, j \in \mathcal{J}, n \in \mathcal{N} \tag{1.28}$$

$$\bar{Y}_{cj} \in \{0,1\} \qquad \forall c \in C, j \in \mathcal{J} \tag{1.29}$$

Now, problem (1.22) can be decomposable by scenarios. To do so, we utilize the *augmented Lagrangian strategy*, proposed by Rockafellar et al. [84], to obtain the following objective function:

$$\underset{\mathbf{Y,S,X,H,P,Z,Q,L,R,D,U}}{Minimize} \quad \frac{1}{N}\sum_{n=1}^{N}\left(\sum_{c\in C}\sum_{j\in\mathcal{J}}\psi_{cj}Y_{cjn} + \mathbb{Q}(\mathbf{Y},\Theta_n) + \sum_{c\in C}\sum_{j\in\mathcal{J}}\left(\zeta_{cjn}(Y_{cjn}-\bar{Y}_{cj}) + \frac{1}{2}\lambda(Y_{cjn}-\bar{Y}_{cj})^2\right)\right) \tag{1.30}$$

where $\{\zeta_{cjn}\}_{\forall c\in C, j\in\mathcal{J}, n\in\mathcal{N}}$ and λ are referred to as Lagrangian multiplier and penalty ratio, respectively. In (1.30), since both $\{Y_{cjn}\}_{c\in C, j\in\mathcal{J}, n\in\mathcal{N}} \in \{0,1\}$ and $\{\bar{Y}_{cj}\}_{c\in C, j\in\mathcal{J}} \in \{0,1\}$ are binary, we can reduce the quadratic term $\sum_{c\in C}\sum_{j\in\mathcal{J}}\lambda(Y_{cjn}-\bar{Y}_{cj})^2$ as follows:

$$\begin{aligned}\sum_{c\in C}\sum_{j\in\mathcal{J}}\lambda(Y_{cjn}-\bar{Y}_{cj})^2 &= \sum_{c\in C}\sum_{j\in\mathcal{J}}\left(\lambda(Y_{cjn})^2 - 2\lambda Y_{cjn}\bar{Y}_{cj} + \lambda(\bar{Y}_{cj})^2\right)\\ &\approx \sum_{c\in C}\sum_{j\in\mathcal{J}}\left(\lambda Y_{cjn} - 2\lambda Y_{cjn}\bar{Y}_{cj} + \lambda\bar{Y}_{cj}\right)\end{aligned}$$

With this simplification, the objective function (1.30) can be re-written as follow:

$$\underset{\mathbf{Y,S,X,H,P,Z,Q,L,R,D,U}}{Minimize} \quad \frac{1}{N}\sum_{n=1}^{N}\left(\sum_{c\in C}\sum_{j\in\mathcal{J}}(\psi_{cj}+\zeta_{cjn}+\frac{\lambda}{2}-\lambda\bar{Y}_{cj})Y_{cjn}+\mathbb{Q}(\mathbf{Y},\Theta_n)\right.$$
$$\left.\sum_{c\in C}\sum_{j\in\mathcal{J}}(-\zeta_{cjn}\bar{Y}_{cj}+\frac{1}{2}\lambda\bar{Y}_{cj})\right) \tag{1.31}$$

It is worth mentioning that when the value of $\{\bar{Y}_{cj}\}$ is fixed, the last term in (1.31) becomes a constant. As such, this term can be eliminated from (1.31). With this, the subproblems become separable by scenarios, as showing below.

$$\textbf{[BQP(PHA)]} \underset{\mathbf{Y,S,X,H,P,Z,Q,L,R,D,U}}{Minimize} \frac{1}{N}\sum_{n=1}^{N}\left(\sum_{c\in C}\sum_{j\in\mathcal{J}}(\psi_{cj}+\zeta_{cjn}+\frac{\lambda}{2}-\lambda\bar{Y}_{cj})Y_{cjn}\right.$$
$$\left.+\mathbb{Q}(\mathbf{Y},\Theta_n)\right) \tag{1.32}$$

subject to (1.5)-(1.10), (1.12)-(1.17), (1.19)-(1.21), (1.23)-(1.25), and (1.27). Let ζ^r_{cjn} and λ^r, respectively, represent the value of the lagrangian multipliers and the penalty parameters at iteration r of the PHA. In each iteration of the PHA procedure, N deterministic subproblems **[BQP(PHA)]** are solved, and the consensus value for the overall design vectors, $\{\bar{Y}_{cj}\}_{c\in C, j\in\mathcal{J}}$, is obtained. The algorithm pursues to find a better solution until some pre-specified conditions are satisfied (shown below). Otherwise, we update the values of $\{\zeta^r_{cj}\}$, and λ^r using the following equations:

$$\zeta^r_{cjn} \longleftarrow \zeta^{r-1}_{cjn}+\lambda^{r-1}(Y^r_{cj}-\bar{Y}^{r-1}_{cj})\ \forall c\in C, j\in\mathcal{J} \tag{1.33}$$

$$\lambda^r \longleftarrow \Delta\lambda^{r-1} \tag{1.34}$$

The values of parameter $\{\zeta_{cjn}^{r=0}\}_{\forall c\in C, j\in\mathcal{J}, n\in\mathcal{N}}$ and $\lambda^{r=0}$ are initially set to zero and a positive number, respectively. A pseudo-code of the basic PHA procedure is outlined in **Algorithm 1**.

Algorithm 1: Progressive Hedging Algorithm

Initialize, $r \leftarrow 1$, ϵ, $\{\zeta_{cjn}^{r}\}_{\forall c\in C, j\in\mathcal{J}} \leftarrow 0$, $\lambda^{r} \leftarrow \lambda^{0}$,
terminate $\leftarrow$ **false**
while (*terminate* = **false**) **do**
  for $n = 1$ to N
    Solve the respective **[BQP(PHA)]** and obtain $\{Y_{cjn}^{r}\}_{\forall c\in C, j\in\mathcal{J}}$
  end for
  Calculate the consensus parameter:
    $\bar{Y}_{cj}^{r} \leftarrow \frac{1}{N}\sum_{n=1}^{N} Y_{cjn}^{r}; \forall c \in C, j \in \mathcal{J}$
  if $(r > 1)$ **then**
    Update the largangian parameter:
      $\zeta_{cjn}^{r} \longleftarrow \zeta_{cjn}^{r-1} + \lambda^{r-1}(Y_{cjn}^{r} - \bar{Y}_{cj}^{r-1}); \forall c \in C, j \in \mathcal{J}, n \in \mathcal{N}$
    Update the penalty parameter:
      $\lambda^{r} \longleftarrow \Delta\lambda^{r-1}$ and $\Delta > 1$
  end if
  if $\frac{1}{N}\sum_{n\in N}\sum_{c\in C}\sum_{j\in\mathcal{J}}\left(\frac{|Y_{cjn}^{r} - \bar{Y}_{cj}^{r}|}{|C||\mathcal{J}|}\right) \leq \epsilon$ **then**
    terminate $\leftarrow$ **true**
  end if
  $r \leftarrow r + 1$
end while

Termination criteria: The PH algorithm terminates upon satisfying one of the following conditions:

- $\frac{1}{N}\sum_{n\in N}\sum_{c\in C}\sum_{j\in\mathcal{J}}\left(\frac{|Y_{cjn}^{r} - \bar{Y}_{cj}^{r}|}{|C||\mathcal{J}|}\right) \leq \epsilon$; where ϵ is a pre-specified tolerance gap.
- 10 consecutive non-improvement iterations.
- Maximum iteration limit is reached (e.g., $iter^{max} = 50$)
- Maximum time limit is reached (e.g., $t^{max} = 18,000$ CPU seconds)

To further improve the efficiency of the PHA on solving the **[BQP(SAA)]**, we adopt three different strategies, namely, penalty parameter updating [20], global and local heuristic strategies [24], and scenario boundling technique [3]. **Appendix A2** to **A4** detailed these enhancement techniques.

1.3.2 Implementing Parallel Processing Techniques:

In each iteration of the SAA algorithm, E number of replications is randomly generated and then solved sequentially. Even though different enhancement techniques (e.g., PHA and the enhanced PHA techniques) are developed to efficiently solve those replications, the overall algorithm may still find it difficult to solve realistic size problem instances of **(BQP)** (see the experimental results reported in Section 1.4.3). In this sub-section, we employ *two* different parallelization schemes, referred to as *Scheme 1* and *2*, to efficiently solve the SAA replications. Both the enhancements exploit the *multiprocessing* capabilities of the local computers to efficiently solve **(BQP)**. More specifically, we utilize the *master-slave* architecture in parallel computing to manage and assign loads of the processors. The aim is to reduce the computational time in solving each iteration of the SAA algorithm, which further speeds up the convergence. Note that the parallel execution does not impact the quality of the SAA solutions, and the basic convergence properties of the SAA retains.

The overall parallelized SAA algorithm is outlined as follows. The master is responsible for generating E independent samples of size N and N' ($N' \gg N$). Each pair of samples of size N and N' are then assigned to a slave (processor) by utilizing a load balancing rule, as illustrated below in *Schemes 1* and *2*. Then the slave proceeds to solve the SAA problem (A.1) of size N. Once the SAA problem (A.1) is solved, the optimal solution, $\hat{Y}_E^e$, and the corresponding optimal objective value, v_N^e, are stored in the slave. In the next step, fixing the value of the first-stage variables to the

optimal solution obtained in the slave $\hat{Y}_E^e$, the corresponding sample size of N' is used to estimate the true objective function value by the slave. At this point, the obtained objective value for the problem of the sample size N', i.e., $\tilde{g}_{N'}^e(\tilde{Y})$, as well as $\hat{Y}_E^e$ and v_N^e for each slave, are collected by the master node. Once all the subproblems are solved in the slaves, the master proceeds to calculate the lower and upper bound using the collected objective values from the slaves. The master estimates the lower-bond for the true problem in the current iteration, $\bar{v}_E^N$, as the average value of the collected objective values associated with samples of size N, i.e., $\bar{v}_E^N = \frac{1}{E}\sum_{e=1}^{E} v_N^e$. In addition, the master chooses the least objective value associated with samples of size N' as an estimate of the upper bound for the true problem, i.e., $\tilde{g}_{N'}(\tilde{Y}) = \min_{e \in E} \tilde{g}_{N'}^e(\tilde{Y})$. Finally, the gap between the estimated upper and lower-bounds is calculated in the master node. If the estimated gap falls below a threshold or other termination criteria (e.g., maximum running time or iteration limit) are satisfied, then the algorithm terminates; otherwise, the algorithm proceeds.

Below, we outline the two parallelization scheme.

Scheme 1:

This scheme first assigns scores to each replication, E, based on the observed supply scenarios $(\overline{S}_{bitn}; \forall b \in \mathcal{B}, i \in \mathcal{I}, t \in \mathcal{T}, n \in N)$ at the master node. The load and the assignment on the slaves (processors) are then made based on the scores. Let $r^E \geq 0$ be the total scores to be assigned for each replication. Let the observed feedstock supply $\overline{S}_{bitn}; \forall b \in \mathcal{B}, i \in \mathcal{I}, t \in \mathcal{T}, n \in N$ for each replication E can be categorized into three major categories: *high*, *medium*, and *low* feedstock supply scenarios with weights w_1, w_2, and w_3, respectively and $w_1 > w_2 > w_3$. Assume that each scenario set N in replication E contains N_1 number of high, N_2 number of medium, and N_3

number of low feedstock scenarios, and $N_1 + N_2 + N_3 = N$. The total score for each replication, r^E, can then be calculated as follows: $r^E = w_1 N_1 + w_2 N_2 + w_3 N_3$. The scores r^E are then sorted in descending order and assign the first p of them to p slaves (based on the available processors) in batches. Note that every time the master assigns a batch of p number of replications (based on the assigned scores) to p slaves and the process continues until all the replications are solved.

Scheme 2:

Unlike synchronous implementation, as can be seen in **Scheme 1**, this scheme *asynchronously* runs the SAA replications, E, to different available processors. The master is responsible for creating an initial pool for the SAA subproblems, where the subproblems are dynamically assigned to the available processors without following any specific order. The goal is to minimize the waiting time for the processors, which eventually speed up the computation time and convergence of the overall SAA algorithm. The master-slave architecture is used to perform this asynchronous implementation of the algorithm. The duties of the master and slave are summarized below.

Master:

- Create a pool of SAA subproblems
- Assigns each slave an equal number of SAA subproblems
- Check the load of slaves and adjusts the assignments
- Compute the estimate of the lower and upper bounds, optimality gap, and the corresponding variances of the SAA algorithm (as provided in Section A.1)

Slave:

- Solves the SAA subproblems of size N

- Store the optimal solution of the SAA subproblems of size N
- Solve the problem of size N' using the respective stored optimal solution

1.4 Computational Study and Managerial Insights

This section is organized as follows. First, we briefly describe the data used as an input in model **(BQP)**. Next, using Mississippi as a testing ground, a real-life case study is presented to visualize and validate the modeling results and to draw managerial insights. Finally, the computational performance of the proposed solution approaches is compared under varying test instances. All the algorithms are coded in Python 3.7 and executed on a desktop computer with Intel Core i7 3.60 GHz processor and 32.0 GB RAM. The optimization solver used is GUROBI 9.0.3.

1.4.1 Data Description

This sub-section describes the data utilized in this study. We considered nine feedstock types: corn-stover, hardwood lowland residues, hardwood upland residues, mixed wood residues, municipal solid waste, other forest residues, primary mill residues, softwood natural residues, and softwood planted residues. The county-wise availability of the feedstocks is obtained from the Billion-Ton study 2016 in the National Renewable Energy Laboratory (NREL) database [99]. Feedstocks are seasonal and are not available year-round. For instance, forest residues are available from March to November, while corn-stover is only available from September to November. Mississippi produces 2.09 million tons of forest residues and 0.48 million tons of corn-stover per year [99]. In total, 82 suppliers from Mississippi are considered, and their geographic distribution is shown in Figure 1.2. Finally, The average harvesting cost of forest residue is set to \$30/dry ton and \$35/dry ton for corn-stover. The total annual pellet demand for our test region is set at 1.54 million tons per year. It is assumed that 25% of the total produced pellet will be used to fulfill

the US market demand while the remaining 75% to satisfy Europe's market demand. It is further assumed that if the demand for pellets cannot be satisfied by our supply chain network, a third-party vendor shall satisfy the demand at a price (π_{pt}) that depends on the pellet type (see Table 1.2).

Table 1.2

Pellet prices (π_{pt}) for the US and Europe markets [103]

Pellet Type	Market	Value	Unit
Premium	US	161	$/ton
Standard	US	150	$/ton
Utility	US	143	$/ton
A1	Europe	178	$/ton
A2	Europe	166	$/ton
B	Europe	157	$/ton

In this study, we consider a total of 50 potential sites to open a pellet depot (see Figure 1.3). The fixed cost of locating a pelletizing depot of capacity 0.08 MTY costs $3,086,656, which is annualized to $327,458 using a project life of 30 years and a discount factor of 10% [44]. We consider 5 different pellet production capacities $C = \{0.020, 0.054, 0.073, 0.083,$ and $0.1\}$MTY. We consider trucks to be the only transportation mode to transport biomass from feedstock supply sites to depots. The unit transportation cost ($l_{bij\tau t\omega}$) can be computed as follows: $l_{bij\tau t\omega} = l^f_{bt}(1 + \Phi^f_{b\tau t\omega}) + l^v_{bt} g_{ij}(1 + \Phi^v_{b\tau t\omega})$, where l^f_{bt} is the fixed and l^v_{bt} is the variable cost components for unit biomass transportation, $\Phi^f_{b\tau t\omega}$ and $\Phi^v_{b\tau t\omega}$ to represent the post-harvest loss (%) due to loading/unloading biomass, and g_{ij} denotes the transportation distance between a harvesting site and a depot. Table 1.3 summarizes the key input parameters (e.g., production, storage costs, transportation, and quality related factors) utilized in this study. Finally, the factors related to the biomass quality are presented in Table 1.4.

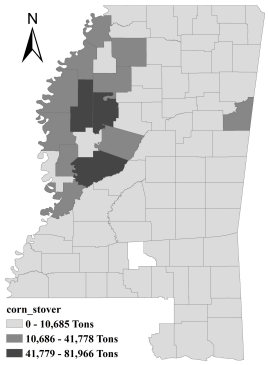

(a) Corn stover

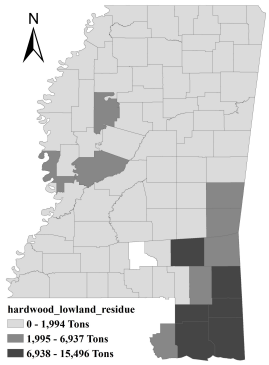

(b) Hardwood lowland residue

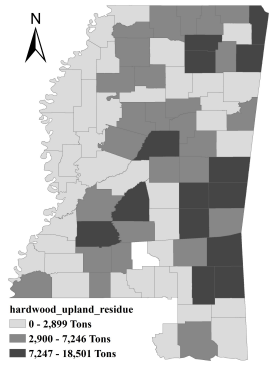

(c) Hardwood upland residue

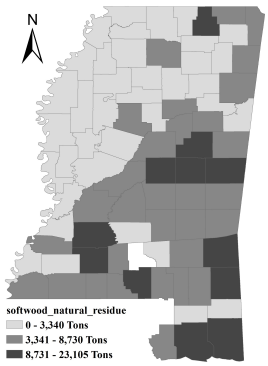

(d) Softwood natural residue

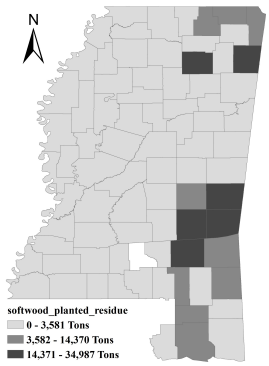

(e) Softwood planted residue

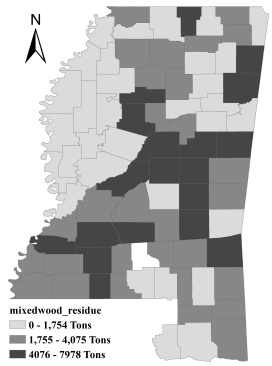

(f) Mixedwood residue

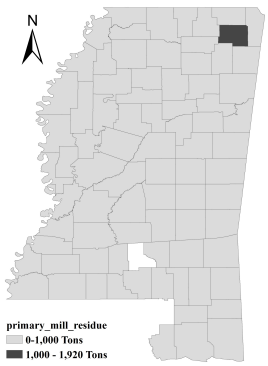

(g) Primary mill residue

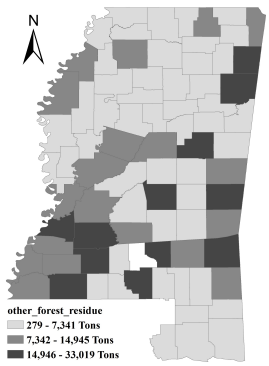

(h) Other mill residue

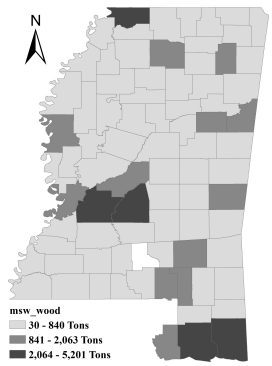

(i) MSW wood

Figure 1.2

Feedstock availability and distribution in Mississippi [99]

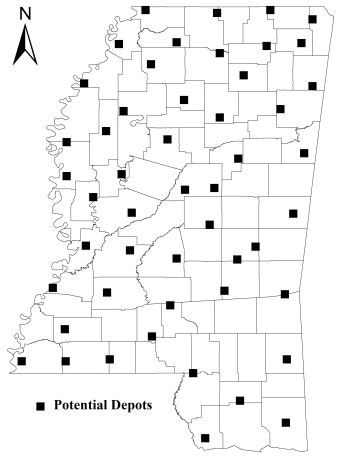

Figure 1.3

Illustration of the potential location to open the depots in Mississippi

Table 1.3

Summary of input parameters for model **(BQP)**

Parameters	Value	Unit	Reference
$h^1_{bi\tau t}$	4.9^1; 8.05^2	\$/ton	[27]
$h^1_{bj\tau t}$	8^1; 2^2	\$/ton	[107]
η_{pjt}	34.72	\$/ton	[44]
ϕ_{brp}	85.9^1; 89^2	%	Assumed
Π^2_{bcj}	0.51	MTY	Assumed
l^f_{bt}	5.55^1; 4.98^2	\$/ton	[87], [47]
l^v_{bt}	0.15^1; 0.111^2	\$/ton/mile	[87], [47]
$\Phi^f_{b\tau t\omega}$	12	%	[41]
$\Phi^v_{b\tau t\omega}$	0.4	%	[85]
κ_{bjrt}	10.30	\$/ton	[48]
$\theta_{bjrr't}$	0.95	\$/ton	[48]
ζ_{bjrt}	2.25	\$/ton	[18]

[1]corn-stover; [2]forest residues

Table 1.4

Summary of biomass quality parameters

Parameters	Feedstock	Value	Unit	Reference
$\mu_{bjt\omega}$	Corn-stover	15	%	[76]
	Forest residues	8.65	%	
$\gamma_{bjt\omega}$	Corn-stover	12	%	[67]
	Harddood residues	0.37	%	[55]
	Softwood residues	0.41	%	[92]
	MSW	2.4	%	[83]
	Mixedwood residues	0.4	%	[76]
	Other forest residues	3.3	%	
	Primary mill residues	2.24	%	
$\alpha_{b\tau t\omega}$	Corn-stover	10	%	[71]
	Forest residues	12	%	

1.4.2 Real-life Case Study

We now present a real-world case study to understand the impact of biomass quality variability (e.g., ash or moisture content) on pellet production and network design decisions. To serve this purpose, we create *five* different biomass quality scenarios, as illustrated in Table 1.5.

Table 1.5

Description of biomass quality scenarios

Quality Scenario	Description
Base	Assuming the base *ash* and *moisture* qualities, as described in Section 1.4.1
Low ash	Base *moisture* but *ash* quality dropped by 30% from the base case
Good ash	Base *moisture* but *ash* quality improved by 30% from the base case
Low moisture	Base *ash* but *moisture* quality dropped by 30% from the base case
Good moisture	Base *ash* but *moisture* quality improved by 30% from the base case

The key insights obtained from the experiments are summarized below.

- Results in Table 1.6 delineate that pellet depot location decisions ($|\mathcal{J}|$) are sensitive to the biomass quality parameters. We observe that the base quality case decides to open 34

pellet facilities within our test region. However, as the biomass quality improves, model **(BQP)** decides to open 36 and 35 depots under good ash and moisture quality scenarios, respectively. On the contrary, as the biomass quality drops in our test region, model **(BQP)** decides to open 31 and 33 depots under low ash and moisture quality scenarios, respectively. The distribution of the depots under different quality scenarios are illustrated in Figure 1.4. Overall, we observe that high-quality biomass promotes the growth of pelleting businesses; however, decision-makers should carefully consider the local biomass quality parameters to make appropriate site selection decisions.

Table 1.6

Number of depots selected under different biomass quality scenarios

	Ash Quality		Moisture Quality	
Base	Good	Low	Good	Low
34	36	31	35	33

- Figure 1.5 illustrates how different biomass quality parameters impact the biomass storage decisions (at the pelleting facilities). From the results, it appears that June to December is the peak biomass storage period, which is expected given this timeframe is also the peak biomass harvesting season for the Southeast USA. The results further reveal that storage is considered a favorable option when the biomass quality is high, while the converse is true when the quality of the biomass is low. For instance, it is observed that as the biomass base ash quality shifts to low- and high-quality scenarios, the overall biomass storage is changed by -19.8% and 20.1%, respectively, from the base case. A similar trend is observed for the moisture content for which the decisions are changed by -45.6% and 41.3%, respectively,

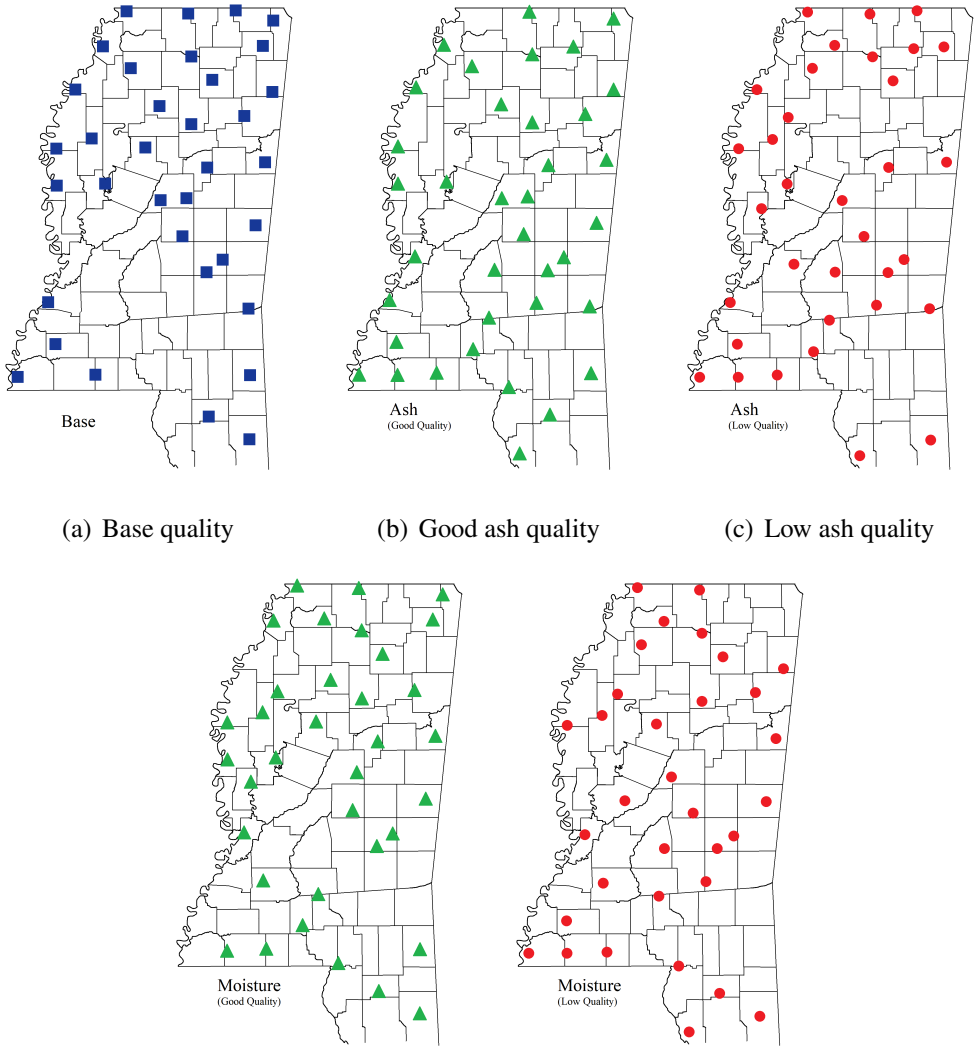

(a) Base quality (b) Good ash quality (c) Low ash quality

(d) Good moisture quality (e) Low moisture quality

Figure 1.4

Distribution of located depots under different ash and moisture quality scenarios

from the base moisture quality scenario. Finally, we observe that the storage decisions are more sensitive to the moisture content than the ash content.

- Next, we study the impact of biomass quality variability on feedstock transportation decisions. Recall that we consider the truck to be the only transportation mode to deliver biomass from

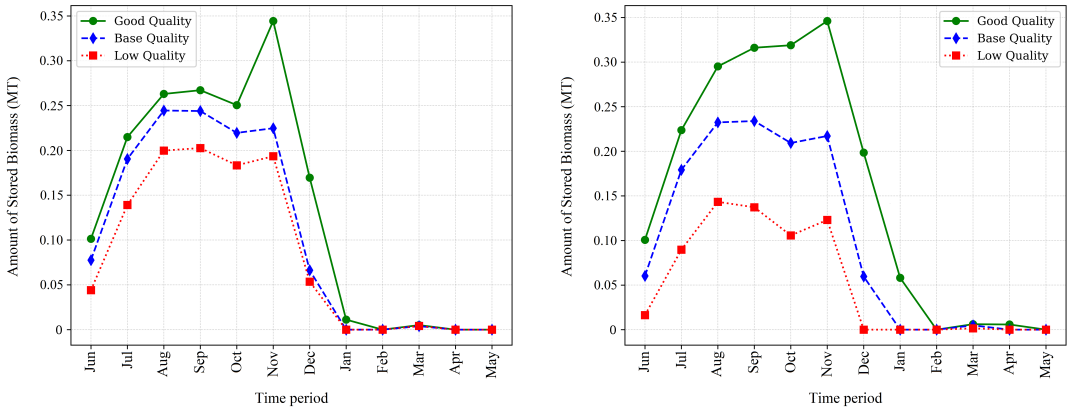

(a) Ash quality (b) Moisture quality

Figure 1.5

Biomass storage decisions under different quality levels

the feedstock supply sites to the pelleting facilities. Figure 1.6 indicates that varying quality-related factors such as ash content and moisture content has no significant impact on the transportation-related decisions in off-peak harvesting seasons of biomass (December to May). On the other hand, we observe that the biomass quality parameters mostly impact the peak harvesting seasons of biomass (June to November). For instance, compared to the base case scenario, the total biomass transportation changes by -10.9% and 20.2%, respectively, under the low and good ash quality scenarios. The numbers are -17.7% and 12.8%, respectively, under the same quality scenarios for the moisture content. Overall, we observe that biomass transportation is more sensitive to biomass quality during the peak harvesting seasons than the off-peak harvesting seasons. This reveals that once the feedstock quality is higher, the proposed model tends to deliver more feedstock from suppliers to the depots rather than performing the costly ash/moisture conversion processes to satisfy the corresponding demand in the following time periods. Finally, it can be seen that due to the

seasonal availability of the different feedstocks in the test region, the model primarily relies on stored feedstock to satisfy the pellet demand from December to February.

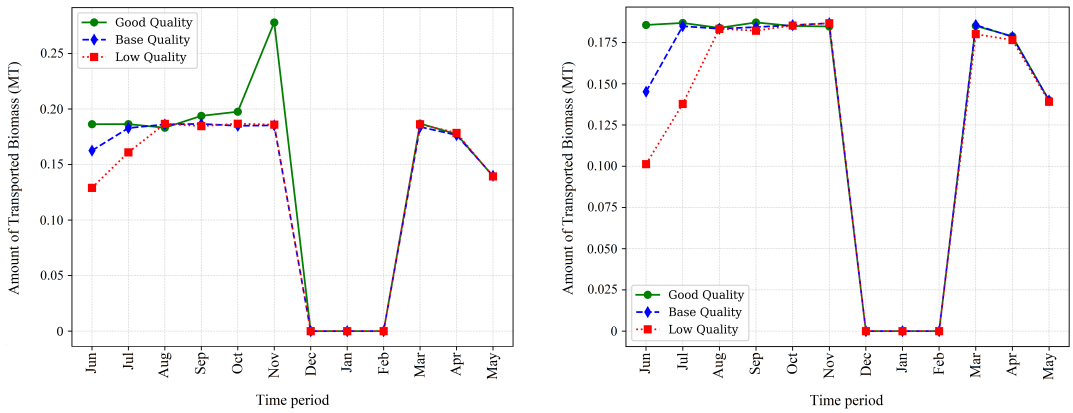

(a) Ash Quality (b) Moisture Quality

Figure 1.6

Feedstock transportation under different biomass quality levels

- In Figure 1.7, we evaluate the impact of biomass quality on pellet production. During the months when the feedstock availability is high, it can be seen that the proposed model finds it optimal to adopt ash/moisture conversion, purchase more or less feedstock, in an attempt to neutralize the impact of quality-related factors on biomass production. However, It is observed that as the biomass quality changes, the amount of pellets produced, especially during the months (November to February) when the feedstock availability is restricted, is impacted. For instance, as the ash quality level changes to low and high, on average, the amount of pellet production is changed by -13.6% and 48.4%, respectively, from the base case scenario. Even though following a similar trend, the change is roughly around -48.3%

and 84.2% for the moisture quality scenarios, signifying that moisture is more sensitive than ash for pellet production.

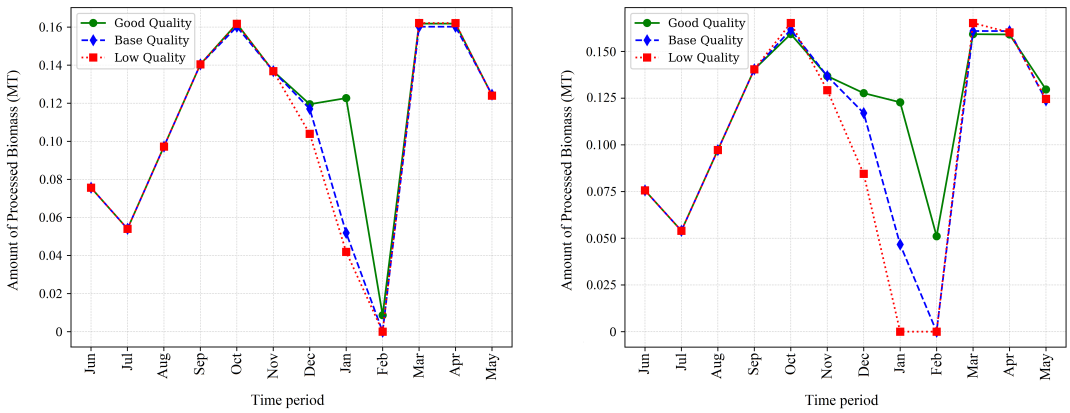

(a) Ash quality (b) Moisture quality

Figure 1.7

Pellet production under different biomass quality levels

1.4.3 Performance Evaluation of the Algorithms

This section presents the algorithms' (discussed in Section 1.3) computational performance in solving model **(BQP)**. In order to generate the test instances for performance evaluation of the algorithms, we vary sets $|\mathcal{I}|$, $|\mathcal{J}|$, and $|\mathcal{T}|$. By doing so, 9 test instances with varying sizes categorized into three groups, namely, *small*, *medium*, and *large*, are generated (see Table 1.7). To terminate the algorithms, the following termination criteria are used: (i) the optimality gap (i.e., $\epsilon = |UB - LB|/UB$) falls below a threshold value (e.g., $\epsilon = 1.0\%$); or (ii) the maximum time limit (t^{max}) is reached (e.g., $t^{max} = 18,000$ CPU seconds); or (iii) the maximum iteration limit (r^{max}) is reached (e.g., $q^{max} = 50$). To help the readers follow our solution approaches, the following notations are used to represent each particular variants of the proposed algorithms.

- **PHA**: Progressive Hedging Algorithm.
- **PHA+HR**: Enhanced Progressive Hedging Algorithm with application of Heuristics strategies discussed in Appendix A.3.
- **PHA+HR+SB**:Enhanced Progressive Hedging Algorithm with application of both Heuristics strategies and Scenario Bundling techniques discussed in Appendix A.3 and A.4.
- **SAA**: Sample Average Approximation Algorithm.
- **Hybrid**: Hybrid decomposition algorithm combining Sample Average Approximation and Enhanced Progressive Hedging Algorithm **(PHA+HR+SB)**.
- **Hybrid+PL1**: Parallelization scheme I is applied over hybrid algorithm **Hybrid**.
- **Hybrid+PL2**: Parallelization scheme II is applied over hybrid algorithm **Hybrid**.

Table 1.7

Problem size and test instances

	Instance	$\|I\|$	$\|J\|$	$\|T\|$	**Binary Variables**	**Continuous Variables**	**Total Variables**	**No. of Constraints**
Small	1	42	30	3	150	134,730	134,880	38,604
	2	42	30	6	150	379,782	379,932	83,010
	3	42	30	9	150	735,156	735,306	133,248
	4	42	30	12	150	1,200,852	1,201,002	189,318
Medium	5	62	40	3	200	223,320	223,520	52,114
	6	62	40	6	200	659,022	659,222	112,450
	7	62	40	9	200	1,307,106	1,307,306	181,048
	8	62	40	12	200	2,167,572	2,167,772	257,908
Large	9	82	50	3	250	333,510	333,760	65,624
	10	82	50	6	250	1,013,862	1,014,112	141,890
	11	82	50	9	250	2,041,056	2,041,306	228,848
	12	82	50	12	250	3,415,092	3,415,342	326,498

The first set of experiments evaluate the Gurobi solver's performance in solving model **(BQP)** over different variants of the **PHA** algorithm (see Table 1.8). It is worth mentioning that in Table 1.8 and the following tables used in this subsection, we highlight the algorithm that is able to solve the instances with the desired optimality gap within the prespecified time limit and in the shortest running time. However, if none of the algorithms could provide such desired quality solutions discussed in the mentioned termination criteria, we highlight the algorithm with the smallest optimality gap. The key observation associated with Table 1.8 are summarized below:

- Results in Table 1.8 indicate that GUROBI can solve 5 out of 12 problem instances (5/12) of **(BQP)** by obeying the prespecified termination criteria. However, 2/12 instances, Gurobi could not find an integer feasible solution (instance 8 and 10) and gets out of memory on the remaining 2/12 instances (instance 11 and 12). On the other hand, even though the solution quality is not improved significantly, the **PHA** algorithm could now provide a feasible solution in 11/12 problem instances.
- The results reported in Table 1.8 signifies that the computational performance of the basic **PHA** can be further improved by incorporating different accelerating techniques, such as penalty parameter updating, local and global heuristics, and scenario bundling techniques. For instance, it can be observed that **PHA+HR** drops down the average optimality gap to 5.23% from 10.23% as produced by the basic **PHA**. Most importantly, an improved solution is found in a number of problem instances over the basic **PHA**, such as instances 4, 6-8, 10, and 11. Finally, we observe an improved average optimality gap and running time when **(BQP)** is solved with the **PHA+HR+SB** algorithm. The average optimality gap obtained by **PHA+HR+SB** drops down to 1.34% from 5.23% and 10.23% as produced by

the **PHA+HR** and **PHA** algorithms, respectively, which signifies that the **PHA+HR+SB** algorithm outperforms both **PHA** and **PHA+HR** with respect to the running time and optimality gap in solving problem **(BQP)**.

Table 1.8

Experimental results with different variants of the **PHA** algorithm

Instance	Gurobi		**PHA**			**PHA+HR**			**PHA+HR+SB**		
	t(sec)	ϵ(%)	t(sec)	ϵ(%)	r	t(sec)	ϵ(%)	r	t(sec)	ϵ(%)	r
1	**394**	0.19	785	0.39	12	773	0.56	9	617	0.89	7
2	2,498	0.88	1,544	0.36	15	1,910	0.52	11	**1,121**	0.31	6
3	**7,328**	0.44	7,482	0.45	14	9,972	0.48	11	8,956	0.11	8
4	18,000	15.7	18,000	11.89	9	15,665	0.54	7	**12,707**	0.72	5
5	1,190	0.52	955	0.64	10	967	0.17	8	**935**	0.82	6
6	18,000	5.61	18,000	5.58	12	15,134	0.35	9	**12,697**	0.3	7
7	18,000	65.7	18,000	19.22	5	18,000	12.69	4	**14,387**	0.06	3
8	TL[1]	-	18,000	27.76	3	18,000	14.59	3	18,000	**6.92**	3
9	4,698	0.65	3,411	0.34	16	2,790	0.76	11	**1,581**	0.62	6
10	TL	-	18,000	8.6	7	**15,667**	0.15	5	16,032	0.25	4
11	OM [2]	-	18,000	37.32	3	18,000	26.77	3	18,000	**3.83**	3
12	OM	-	OM	-	-	OM	-	-	OM	-	-
Average	10,610	11.23	11,107	10.23	10	10,625	5.23	7	**9,548**	1.34	5

[1]TL: No feasible solution within time limit
[2]OM: Out of memory

Despite the encouraging performance demonstrated by the **PHA+HR+SB** algorithm over its counterparts, we observe that the algorithm still struggles to find quality solutions for a few large-scale problem instances, especially instances 8, 11, and 12 as observed in Table 1.8. To overcome this challenge, we explore two other algorithms, namely, **SAA** and **Hybrid**, which solve the **PHA+HR+SB** algorithm under an **SAA** framework. The results obtained for these algorithms are reported in Table 1.9, and the summary of the key observation corresponding to these results are as follows:

- Results in Table 1.9 indicate that the basic **SAA** algorithm fails to solve 6/12 problem instances by obeying the pre-specified termination criteria. However, comparing the average optimality gap corresponding to this algorithm (3.1%) over the Gurobi solver (11.23% as obtained from Table 1.8) and the number of instances for which they fail to provide a feasible solution (4 in Gurobi and 3 in **SAA**), we conclude that **SAA** demonstrates superiority in solving **(BQP)** over the Gurobi solver.
- Results in Table 1.9 further demonstrate that incorporating **PHA+HR+SB** under a **SAA** framework, i.e., the **Hybrid** algorithm, significantly reduces the average solution time for solving different instances of **(BQP)**. Both **PHA+HR+SB** and **Hybrid** algorithms provide similar quality solutions, but **Hybrid**, on average, saves approximately 19.4% time over algorithm **PHA+HR+SB** in providing the reported optimality gap shown in Table 1.9 .

Table 1.9

Experimental results comparison: **PHA+HR+SB**, **SAA**, and **Hybrid** algorithm

Instance	**PHA+HR+SB**			**SAA**			**Hybrid**		
	$t(sec)$	$\epsilon(\%)$	r	$t(sec)$	$\epsilon(\%)$	r	$t(sec)$	$\epsilon(\%)$	r
1	617	0.89	7	528	0.43	2	**401**	0.16	2
2	1,121	0.31	6	1,919	0.1	2	**1,048**	0.62	2
3	8,956	0.11	8	7,119	0.43	2	**1,525**	0.81	1
4	12,707	0.72	5	18,000	6.32	2	**8,304**	0.4	3
5	935	0.82	6	964	0.67	2	**366**	0.63	1
6	12,697	0.3	7	15,353	0.58	3	**5,418**	0.73	2
7	**14,387**	0.06	3	18,000	9.66	1	18,000	2.96	3
8	18,000	6.92	3	TL	-	-	18,000	**6.49**	1
9	**1,581**	0.62	6	2,748	0.63	3	2,252	0.31	4
10	16,032	0.25	4	18,000	9.06	2	**10,867**	0.3	3
11	18,000	**3.83**	3	TL	-	-	18,000	4.87	1
12	OM	-	-	TL	-	-	TL	-	
Average	9,548	1.34	5	9,181	3.1	2	**7,653**	1.66	2

As observed from Table 1.9 that although both **PHA+HR+SB** and **Hybrid** algorithms provide quality solutions for the majority of the test instances, none of the solution approaches are able to solve the largest instance of **(BQP)** (instance 12). As such, we introduce parallelization schemes **Hybrid+PL1** and **Hybrid+PL2** to further enhance the **Hybrid** algorithm's computational performance. The results are reported in Table 1.10. The key findings from these computational results are summarized below:

- As evidenced from the results in Table 1.10 that both the parallel schemes managed to solve all the test instances by obeying the prespecified termination criteria. It can be seen that utilizing the **Hybrid+PL1** to solve the **(BQP)**, the average optimality gap and running time drops by 67.4% and 19.7%, respectively, over the **Hybrid** algorithm. Additionally, we observe that **Hybrid+PL2** can drop down the average optimality gap and running time by 71.1% and 32.2%, respectively, over the **Hybrid** algorithm. In summary, it can be concluded that both the parallel schemes outperform the **Hybrid** algorithm in terms of the number of solved instances, average solution time, and optimality gap.
- Our final observation is made between algorithms **Hybrid+PL1** and **Hybrid+PL2**. Clearly, **Hybrid+PL2** outperforms **Hybrid+PL1** with respect to both running time and optimality gap in most of the test instances, except three instances (instance 1, 2, and 5). These results indicate that parallelizing the replications of the **SAA** algorithm using *scheme 2* saves approximately 15.6% solution time over algorithm **Hybrid+PL1**, while both provide competitive quality solutions.

Table 1.10

Experimental results with **Hybrid** algorithm under different parallelization schemes

Instance	**Hybrid**			**Hybrid+PL1**			**Hybrid+PL2**		
	$t(sec)$	$\epsilon(\%)$	r	$t(sec)$	$\epsilon(\%)$	r	$t(sec)$	$\epsilon(\%)$	r
1	401	0.16	2	**176**	0.9	2	251	0.65	3
2	1,048	0.62	2	**269**	0.27	1	512	0.33	2
3	1,525	0.81	1	1,996	0.94	3	**1,848**	0.33	3
4	8,304	0.4	3	2,689	0.36	2	**1,275**	0.51	1
5	366	0.63	1	**178**	0.09	1	332	0.71	2
6	5,418	0.73	2	4,367	0.67	3	**1,353**	0.47	1
7	18,000	2.96	3	10,487	0.09	4	**9,700**	0.29	4
8	18,000	6.49	1	17,149	0.29	2	**15,786**	0.76	2
9	2,252	0.31	4	815	0.89	3	**746**	0.5	3
10	10,867	0.3	3	6,054	0.46	3	**3,679**	0.24	2
11	18,000	4.87	1	13,483	0.63	2	**12,232**	0.77	2
12	TL	-		16,085	0.9	1	**14,521**	0.26	1
Average	7,653	1.66	2	6,146	0.54	2	**5,186**	0.48	2

1.5 Conclusions and Future Research Directions

This paper studies the impact of biomass quality and yield variability to the design and management of a biomass-to-pellet supply chain. A two-stage stochastic mixed-integer linear programming model is developed to determine the optimal pellet facility locations, and the amount of biomass stored, transported, and preprocessed decisions under biomass quality and yield uncertainty. The model captures several realistic features (e.g., different grades of the pellets, preprocessing requirements based on different ranges of ash/moisture contents, market requirements) to efficiently characterize and optimize the overall biomass-to-pellet supply chain. We then develop an innovative solution approach, enhanced by the parallel computing concepts, to efficiently solve the proposed optimization model. The extensive computational experiments denote that both parallelization schemes outperform the sequential Hybrid algorithm in terms of the number of solved instances, average solution time, and optimality gap. Furthermore, the scheme that asynchronously parallelizes the SAA algorithm's replications saves approximately 15.6% solution time over the

scheme with synchronous implementation. These parallel techniques can be easily generalized and applied to stochastic optimization problems which use Monte Carlo simulation as the underlying solution procedure. By using Mississippi as a testing ground, we conduct extensive computational experiments to test the performance of the algorithm and to draw important managerial insights. Results indicate that on average, biomass storage, transportation, and pellet production decisions are changed by -19.8%/20.1%, -10.9%/20.2%, and -13.6%/48.4%, respectively, under low/high ash quality scenarios. For the moisture content, the numbers would be -45.6%/41.3%, -17.7%/12.8%, and -48.3%/84.2%, respectively, indicating the sensitivity of the biomass-to-pellet supply chain decisions by the biomass quality variability.

This study can be extended in several directions. First, our work only considers the downstream of the biomass-to-pellet supply chain (i.e., feedstock sites and pelleting facilities). Future research can extend the boundary by incorporating the upstream of the biomass-to-pellet supply chain (e.g., intermodal facilities, markets) and investigate how the biomass quality and yield variability impact the overall system performance. Next, we assume that the system is reliable and will never fail. It might be interesting to investigate the sudden surge of woody biomass due to a natural catastrophe (e.g., hurricane) and its association with the pellet production decisions. In subsequent studies, using a multi-objective framework and developing rigorous techniques [49] (e.g., optimal condition decomposition [22]), we aim to enrich this existing study.

CHAPTER II

A BI-LEVEL MODEL FORMULATION FOR SOLVING A POST-HURRICANE DAMAGED TIMBER MANAGEMENT PROBLEM

2.1 Introduction

2.1.1 Problem Motivation

More than 150 hurricanes have struck the U.S. Atlantic and Gulf of Mexico coasts during the past century. These storms have caused significant ecological and economic damages totaling billions of dollars [13]. Less appreciated, perhaps, are the effects that catastrophic storms have on forests and the people who own them. The frequent occurrence of these extreme weather events increases the economic vulnerability of forest product manufacturers and forest-dependent coastal communities and results in undesired environmental impacts. For example, approximately 5 million acres of forest land were damaged by Hurricane Katrina [57, 101], and it has been estimated that 125 million tons of timber were lost, which was equivalent to five years of annual harvests. The value of damaged timber was estimated at $3 billion, which corresponded to a loss of 60,000 jobs, $2 billion in wages, and $4 billion in value-added [61]. Mitigation of hurricane damages is of particular importance to the Southeast U.S., such as Mississippi, because timber is it's second-leading agricultural crop [102] and the economic contribution of the forest sector to the state economy amounts to $10 billion [25].

Due to a lack of pre-disaster planning for recovery of damaged timber, only a small portion of the original timber was recovered in most of the past major hurricanes affecting the Southeast

U.S. (e.g., Hurricane Katrina in 2005, Hurricane Isaac in 2012, and Hurricane Sally in 2020) [30, 36]. Additionally, due to high temperature and humidity in affected region (e.g., Southeast U.S.), damaged timber is expected to have a very short salvage period before being affected by insects and molds and decay fungi. Therefore, it is critical to recover damaged timber quickly not only to recover its monetary value but also to mitigate negative ecological impacts such as wildfires, the proliferation of invasive plants (e.g., Cogon grass (Imperata cylindrical), Chinese tallow (Triadica sebifera)) and insect species, and diseases. The problem associated with efficient planning and recovery of damaged timber is challenging because of its association with many complex factors, including storm severity (wind speeds), prior rainfall activity (whose effect, in turn, is modified partially by soils), strength of the timber market, tree species affected, and timber decay rates [78].

Landowners and mills need answers to a number of pending research questions, such as the optimal harvesting time for different qualities of the damaged timber (e.g., uprooted hardwoods or pines, severely bent or broken tops), the portion of the damaged timber that is economically unattractive or operationally inaccessible (e.g., capacity restrictions at the mills), and the optimal prices to offer for the damaged timbers that benefit both the mills and the landowners under a non-cooperative environment. The purpose of this study is to develop a rigorous mathematical modeling framework that provides local government, landowners, forest industry, bio-refineries, and coastal communities with the tool needed to answer these questions and to expedite the recovery of damaged timber following hurricanes.

2.1.2 Literature Review

After a series of successive natural disasters in recent years and given the large amount of damaged timber, response to these extreme events makes it clear that there is not yet a consistent approach to allow the forest community (i.e., the forest owners; their customers, the forest industries; local, state and federal governments; and regulatory bodies) on how to economically collect the damaged timber (e.g., from the landowners) to bring economic benefit to all affected stakeholders. Most of the recent studies analyzed the impact of timber price dynamics (e.g., [19], [90]) and economic analyses of forest industries and coastal communities (e.g., [78], [32], [68]) following an extreme event (e.g., hurricanes). For instance, Syme and Saucier [97] study the effect of Hurricane Hugo on timber-processing mills and show how it caused a shutdown of the mills in the affected area as a shortterm impact of the disaster. Yin and Newman [109] study the timber price after Hurricane Hugo and indicate a trade correlation between the damaged area and the timber market, which causes the price variation. The authors conducted an intervention analysis to inspect different possibilities concerning the long-run effect of timber prices that have changed since Hugo's incidence. Kinnucan [43] utilized two simulation sets to investigate the elasticity of timber price with demand in a hurricane-damaged area. Butry et al. [17] performed regression analysis to understand the impact of timber prices after a wildfire. Likewise, several other researchers performed statistical analysis to understand how the timber prices changed under different situations in an extreme event situations, such as [109], [77], [66], and many others.

Despite remarkable findings on analyzing the price dynamics and economic analyses of timber salvage following natural catastrophes, researchers still need to find the best policies (acting between timber landowners and mills) to maximize the recovery of damaged timber under varying

conditions (e.g., hurricane intensity and timing, quality of the damaged timber). For instance, Bogle and van Kooten [15] developed a bilevel optimization model to understand how to manage a timber supply after a natural disaster. Paradis et al. [70] developed a bilevel optimization model to demonstrate how to mitigate the wood supply failure risk for the wood mills. Unlike adopting a bilevel optimization framework, several studies undertook a pre-disaster planning model to design the transportation network such that the biomass (e.g., forest residues, damaged timbers) could still be economically delivered to the demand sites after a natural catastrophe. Poudel et al. [75] developed a mixed-integer linear programming model to determine a set of transportation links to be strengthened such that the unit biomass delivery cost under a major hurricane could still be minimized. Along the same line of research, Marufuzzaman et al. [53] developed a mixed-integer linear programming model to optimize the biorefineries' location and the multi-modal facilities' utilization schedule in an attempt to deliver biomass economically and reliably following a natural catastrophe. This study later extended in [50] and [72], respectively, to consider supply chain dynamics and congestion in transportation caused by the sudden surge in biomass demand.

2.1.3 Summary of Major Contributions

In summary, most of the past studies either focus on analyzing timber price dynamics, economic analyses of lost timber value, or developing a pre-disaster planning model to strengthen the transportation infrastructure against a possible natural catastrophe. However, none of the prior studies modeled the complex interactions between the landowners of the damaged timbers and mills following a natural disaster. This problem is critical not only to recover the monetary value of the damaged timber but also to mitigate negative ecological impacts such as wildfires, the proliferation of invasive plant (e.g., Cogon grass (Imperata cylindrical), Chinese tallow (Triadica

sebifera)) and insect species and diseases, and mitigate price arbitrage, and mitigate price arbitrag. To fill this research gap, this study proposes a bilevel mixed-integer linear programming model to understand the complex interactions between the timber landowners and mills and to answer a number of pending research questions, such as the optimal harvesting time for different qualities of the damaged timber (e.g., uprooted hardwoods or pines, severely bent or broken tops), the portion of the damaged timber that is economically unattractive or operationally inaccessible (e.g., capacity restrictions at the mills), and the optimal prices to offer for the damaged timbers that benefit both the mills and the landowners under a non-cooperative environment.

Due to the complexity associated with solving the proposed mathematical model, we develop two highly customized solution approaches, namely, an enhanced Benders decomposition algorithm and a Benders-based branch-and-cut algorithm. The performance of both the algorithms is accelerated with multiple enhancement techniques, such as Pareto-optimal cut, warm-start strategies, and problem-specific valid inequalities and preprocessing techniques. The performance of the algorithms is tested under different simulated hurricane situations (e.g., Hurricanes Katrina, Camille, and Nate). Finally, a number of real-life experiments are conducted to draw managerial insights for the decision-makers on how economically damaged timber could be recovered following a natural catastrophe.

The exposition of this paper is as follows. Section 2.2 introduced the proposed mathematical formulation. Section 2.3 developed a customized solution approach to efficiently solve the proposed optimization model. Section 2.4 discussed the case study results and the performance of the customized solution approaches. Finally, Section 2.5 concludes this study with a few future research directions.

2.2 Problem Description and Model Formulation

This section develops a mathematical model for a post-hurricane damaged timber management problem in a non-cooperative two-echelon supply chain network. Let $\mathcal{I} := \{1, 2, ..., I\}$ and $\mathcal{J} := \{1, 2, ..., J\}$, respectively, be the set of timberland owners and mills which are geographically distributed over the hurricane-impacted region. Let $\mathcal{Q} := \{1, 2, \ldots, Q\}$ be the set of quality-levels of the remaining twisted, broken, and damaged timber, which is required to be salvaged over a set of time periods, denoted by $\mathcal{T} := \{1, 2, ..., T\}$.

Let $\hat{s}_{iq}$ be the total availability of post-hurricane damaged timber of quality $q \in \mathcal{Q}$ at the timberland owner's site $i \in \mathcal{I}$. At the beginning of each time period $t \in \mathcal{T}$, the timberland owner decides either to sell or keep the damaged timber. Let π_{iqt} be the unit timber price (\$/ton) of quality $q \in \mathcal{Q}$ offered by timberland owner $i \in \mathcal{I}$ at time $t \in \mathcal{T}$. We further let h_{iqt} to be the unit timber storage cost (\$/ton) of quality $q \in \mathcal{Q}$ at timberland owner's site $i \in \mathcal{I}$ in time $t \in \mathcal{T}$. Given the hurricane-damaged trees are the prime targets for a host of destructive insects and diseases, the quality of the timber deteriorates significantly over time. We define α_{qt} to be the deterioration rate (in %) of damaged timber of quality $q \in \mathcal{Q}$ at time $t \in \mathcal{T}$. At the same time, the mills determine the viable timber price (\$/ton), denoted by $\psi_{jqt}; \forall j \in \mathcal{J}, q \in \mathcal{Q}, t \in \mathcal{T}$, to purchase timber from the landowners. The mills cannot purchase more than $d_{jt}; \forall j \in \mathcal{J}, t \in \mathcal{T}$ timbers (tons) from the landowners, and it would cost $c_{ijqt}; \forall i \in \mathcal{I}, j \in \mathcal{J}, q \in \mathcal{Q}, t \in \mathcal{T}$ (\$/ton) for them to transport the timbers from the nearby landowners. Given long-haul trucks will be used to transport the timbers, we restrict mills from procuring timbers greater than a 50 miles transportation radius. Below is a summary of the sets, parameters, and decision variables of the optimization model.

Sets:

- $\mathcal{I}$: set of timberland owners, $i \in \mathcal{I}$
- $\mathcal{J}$: set of mills, $j \in \mathcal{J}$
- $\mathcal{Q}$: set of quality levels of the damaged timber, $q \in \mathcal{Q}$
- $\mathcal{T}$: set of time periods, $t \in \mathcal{T}$

Parameters:

- π_{iqt}: unit timber price of quality $q \in \mathcal{Q}$ offered by timberland owner $i \in \mathcal{I}$ at time $t \in \mathcal{T}$
- $\hat{s}_{iq}$: total availability of damaged timber of quality $q \in \mathcal{Q}$ at timberland owner $i \in \mathcal{I}$
- h_{iqt}: unit storage cost of quality $q \in \mathcal{Q}$ at timberland owner's site $i \in \mathcal{I}$ in time $t \in \mathcal{T}$
- c_{ijqt}: unit cost of transporting damaged timber of quality $q \in \mathcal{Q}$ between source $i \in \mathcal{I}$ to destination $j \in \mathcal{J}$ at time $t \in \mathcal{T}$
- α_{qt}: the deterioration rate of timber of quality $q \in \mathcal{Q}$ at time $t \in \mathcal{T}$
- d_{jt}: the demand of mill $j \in \mathcal{J}$ at time $t \in \mathcal{T}$
- ψ_{jqt}: viable price for mill $j \in \mathcal{J}$ for purchasing timber of quality $q \in \mathcal{Q}$ at time $t \in \mathcal{T}$

Decision Variables:

- $\hat{Z}_{ijqt}$: 1 if mill $j \in \mathcal{J}$ decides to purchase timber of quality $q \in \mathcal{Q}_t$ from timberland owner $i \in \mathcal{I}$ at time $t \in \mathcal{T}$; 0 otherwise
- Y_{iqt}: 1 if timberland owner $i \in \mathcal{I}$ decides to sell timber of quality $q \in \mathcal{Q}_t$ at time $t \in \mathcal{T}$; 0 otherwise

- H_{iqt}: amount of damaged timber of quality $q \in Q_t$ left on site $i \in \mathcal{I}$ at time $t \in \mathcal{T}$
- X_{ijqt}: amount of damaged timber of quality $q \in Q_t$ which are decided to be sold by landowner $i \in \mathcal{I}$ to mill $j \in \mathcal{J}$ at time $t \in \mathcal{T}$

We now introduce the decision variables for our proposed mathematical model. First, binary variables $\mathbf{Z} := \{\hat{Z}_{ijqt} | \forall i \in \mathcal{I}, j \in \mathcal{J}, q \in Q, t \in \mathcal{T}\}$ and $\mathbf{Y} := \{Y_{iqt} | \forall i \in \mathcal{I}, q \in Q, t \in \mathcal{T}\}$ to capture the purchasing/selling decisions of the mills and landowners, respectively. More specifically, $\hat{Z}_{ijqt}$ is equal to 1 if mill $j \in \mathcal{J}$ decides to purchase timber of quality $q \in Q_t$ from timberland owner $i \in \mathcal{I}$ at time $t \in \mathcal{T}$; 0 otherwise and Y_{iqt} is equal to 1 if timberland owner $i \in \mathcal{I}$ decides to sell timber of quality $q \in Q_t$ at time $t \in \mathcal{T}$; 0 otherwise. The two other continuous variables include $\mathbf{H} := \{H_{iqt} | \forall i \in \mathcal{I}, q \in Q, t \in \mathcal{T}\}$ to denote the amount of damaged timber of quality $q \in Q_t$ left on site $i \in \mathcal{I}$ at time $t \in \mathcal{T}$ and $\mathbf{X} := \{X_{ijqt} | \forall i \in \mathcal{I}, j \in \mathcal{J}, q \in Q, t \in \mathcal{T}\}$ to denote the amount of damaged timber of quality $q \in Q_t$ which are decided to be sold by landowner $i \in \mathcal{I}$ to mill $j \in \mathcal{J}$ at time $t \in \mathcal{T}$.

With these variables, we are now ready to introduce the following bilevel mixed-integer non-linear programming model, referred to as **(P1)**, to capture the interactions among the timber landowners and the mills.

$$\textbf{(P1)} \quad \underset{\mathbf{Z},\mathbf{Y},\mathbf{H},\mathbf{X}}{Maximize} \sum_{i \in \mathcal{I}} \sum_{q \in Q} \sum_{t \in \mathcal{T}} \left(\sum_{j \in \mathcal{J}} \pi_{iqt} \hat{Z}_{ijqt} X_{ijqt} - h_{iqt} H_{iqt} \right) \tag{2.1}$$

subject to

$$H_{iq,1} + \sum_{j \in \mathcal{J}} X_{ijq,1} = \hat{s}_{iq} \quad \forall i \in \mathcal{I}, q \in \mathcal{Q} \tag{2.2}$$

$$(1 - \alpha_{qt}) H_{iq,t-1} = H_{iqt} + \sum_{j \in \mathcal{J}} X_{ijqt} \quad \forall i \in \mathcal{I}, q \in \mathcal{Q}, t \in \mathcal{T} | t > 1 \tag{2.3}$$

$$X_{ijqt} \leq \hat{s}_{iq} Y_{iqt} \quad \forall i \in \mathcal{I}, j \in \mathcal{J}, q \in \mathcal{Q}, t \in \mathcal{T} \tag{2.4}$$

$$\sum_{q \in \mathcal{Q}} \sum_{i \in \mathcal{I}} X_{ijqt} \leq d_{jt} \quad \forall j \in \mathcal{J}, t \in \mathcal{T} \tag{2.5}$$

$$Y_{iqt} \in \{0, 1\} \quad \forall i \in \mathcal{I}, q \in \mathcal{Q}, t \in \mathcal{T} \tag{2.6}$$

$$H_{iqt} \geq 0 \quad \forall i \in \mathcal{I}, q \in \mathcal{Q}, t \in \mathcal{T} \tag{2.7}$$

$$X_{ijqt} \geq 0 \quad \forall i \in \mathcal{I}, j \in \mathcal{J}, q \in \mathcal{Q}, t \in \mathcal{T} \tag{2.8}$$

for each $j \in \mathcal{J}$ we have

$$Z := \underset{\mathbf{Z}}{argmax} \sum_{i \in \mathcal{I}} \sum_{q \in \mathcal{Q}} \sum_{t \in \mathcal{T}} (\psi_{jqt} - \pi_{iqt} - c_{ijqt}) \hat{Z}_{ijqt} \tag{2.9}$$

subject to

$$\hat{Z}_{ijqt} \leq Y_{iqt} \quad \forall i \in \mathcal{I}, q \in \mathcal{Q}, t \in \mathcal{T} \tag{2.10}$$

$$\hat{Z}_{ijqt} \in \{0, 1\} \quad \forall i \in \mathcal{I}, q \in \mathcal{Q}, t \in \mathcal{T} \tag{2.11}$$

The upper-level objective function (2.1) captures the landowners total profit, including the total revenue by selling the timber minus the cost of keeping the damaged timber. Constraints (2.2) impose damaged timber availability to landowner $i \in \mathcal{I}$ at the beginning of the planning horizon. Constraints (2.3) are the flow balance constraints. Constraints (2.4) restrict the transportation of the timbers to mills based on the selling decision made by the landowner $i \in \mathcal{I}$. Constraints (2.5) ensure that the transported quantity of the damaged timber cannot exceed the mill's demand d_{jt}. Constraints (2.6) define binary timber selling decisions of the landowners $i \in \mathcal{I}$. Constraints (2.7) and (2.8) are the nonnegative decision variables for the storage and the selling quantity decisions for the landowners. In the lower level, objective function (2.9) includes mill j's total profit, $(\psi_{jqt} - \pi_{iqt} - c_{ijqt})$, resulting from procuring the damaged timber from the landowner, including the viable procurement cost, ψ_{jqt}, for the mills, minus the price paid to the landowner, π_{iqt}, and the necessary timber hauling cost, c_{ijqt}. Constraints (2.10) set a logical restriction, indicating that if the landowner decides not to sell the timber, the mill will not contract with the respective landowner. Finally, constraints (2.11) set binary restrictions for the mills timber purchasing decisions from a landowner.

Single-level Model Formulation of **(P1)**:

Note that in **(P1)**, the viable price ψ_{jqt} must have to be greater than or equal to the summation of the price paid by the mill to the landowner, π_{iqt}, and the transportation cost, c_{ijqt}, i.e., $(\psi_{jqt} - \pi_{iqt} - c_{ijqt}) \geq 0$, for the mills to be profitable. Otherwise, the mill will not purchase the damaged timber from the respective landowner. Therefore, we can define a set of quality timber/timberland owner that are attractive to mill j at time t as: $\mathcal{A}_j = \{(i,q) | \psi_{jqt} - \pi_{iqt} - c_{ijqt} \geq 0\}$. With this

introduction, we can set $\hat{Z}_{ijqt} = 0$ if $(i,q) \neq \mathcal{A}_j$ at time $t \in \mathcal{T}$. As such, we replace variable $\hat{Z}_{ijqt}$ with $Z_{ijqt}; \forall (i,q) \in \mathcal{A}_j$, and revise **(P1)** as follows:

$$\textbf{(P2)} \quad \underset{\mathbf{Z},\mathbf{Y},\mathbf{H},\mathbf{X}}{Maximize} \sum_{j \in \mathcal{J}} \sum_{(i,q) \in \mathcal{A}_j} \sum_{t \in \mathcal{T}} \pi_{iqt} Z_{ijqt} X_{ijqt} - \sum_{i \in \mathcal{I}} \sum_{q \in Q} \sum_{t \in \mathcal{T}} h_{iqt} H_{iqt} \tag{2.12}$$

subject to (2.2)-(2.8), and for each $j \in \mathcal{J}$ and $t \in \mathcal{T}$, we have

$$Z := \underset{\mathbf{Z}}{argmax} \sum_{(i,q) \in \mathcal{A}_j} (\psi_{jqt} - \pi_{iqt} - c_{ijqt}) Z_{ijqt} \tag{2.13}$$

subject to

$$Z_{ijqt} \leq Y_{iqt} \qquad \forall (i,q) \in \mathcal{A}_j \tag{2.14}$$

$$Z_{ijqt} \in \{0,1\} \qquad \forall (i,q) \in \mathcal{A}_j \tag{2.15}$$

With these changes, we are now ready to introduce the single-level formulation for model **(P1)**. To do so, we follow the approach provided by Hansen et al. [35], which enforces the second-level optimality conditions via constraints. With this approach, the following order relationship is maintained for all mills $j \in \mathcal{J}$: $(i,q) \preceq (i',q')$ if and only if $\psi_{jqt} - \pi_{iqt} - c_{ijqt} \leq \psi_{jq't} - \pi_{i'q't} - c_{i'jq't}$ that sorts all quality timber/timberland owner pairs at time $t \in \mathcal{T}$. This order implies that $(\psi_{jq't} - \pi_{i'q't} - c_{i'jq't})$ is greater than $(\psi_{jqt} - \pi_{iqt} - c_{ijqt})$ if it provides a larger reward for mill $j \in \mathcal{J}$ at time $t \in \mathcal{T}$. We then introduce the following set of quality timber/timberland owners that are preferred to $(i,q) \in \mathcal{A}_j$ for mill $j \in \mathcal{J}$ at time $t \in \mathcal{T}$ by $\mathcal{B}_{ijqt} = \{(i',q') \in \mathcal{A}_j | (i,q) \preceq (i',q')\}$.

As pointed out by Hansen et al. [35], a decision vector **Z**, feasible for the lower-level problem (2.13)-(2.15), is optimal for **(P2)** if and only if the following set of constraints hold:

$$\sum_{(i',q')\in\mathcal{B}_{ijqt}} Z_{i'jq't} \geq Y_{iqt} \quad \forall j \in \mathcal{J}, (i,q) \in \mathcal{A}_j, t \in \mathcal{T} \tag{2.16}$$

An alternative of constraints (2.16) can be formulated as follows. To serve this purpose, let us introduce a new set to the quality of the damaged timbers that are not attractive to the $(i,q) \in \mathcal{A}_j$ for mill $j \in \mathcal{J}$, i.e., $C_{ijqt} = \{(i',q') \in \mathcal{A}_j | (i,q) \succ (i',q')\}$. Then, for all $j \in \mathcal{J}, (i,q) \in \mathcal{A}_j, t \in \mathcal{T}$, constraints (2.16) is equivalent to the following constraints.

$$\sum_{(i',q')\in\mathcal{B}_{ijqt}} Z_{i'jq't} + \sum_{(i',q')\in C_{ijqt}} Z_{i'jq't} \geq Y_{iqt} + \sum_{(i',q')\in C_{ijqt}} Z_{i'jq't} \tag{2.17}$$

Since $\mathcal{A}_j = \mathcal{B}_{ijqt} \bigcup C_{ijqt}$ and $\mathcal{B}_{ijqt} \bigcap C_{ijqt} = \emptyset$, constraints (2.17) is equivalent to the following constraints:

$$\sum_{(i',q')\in\mathcal{A}_j} Z_{i'jq't} \geq Y_{iqt} + \sum_{(i',q')\in C_{ijqt}} Z_{i'jq't} \tag{2.18}$$

This gives the following equivalent single-level mixed-integer nonlinear programming model formulation, referred to as **(P3)**.

$$\textbf{(P3)} \quad \underset{\mathbf{Z},\mathbf{Y},\mathbf{H},\mathbf{X}}{Maximize} \sum_{j\in\mathcal{J}} \sum_{(i,q)\in\mathcal{A}_j} \sum_{t\in\mathcal{T}} \pi_{iqt} Z_{ijqt} X_{ijqt} - \sum_{i\in\mathcal{I}} \sum_{q\in Q} \sum_{t\in\mathcal{T}} h_{iqt} H_{iqt} \tag{2.19}$$

subject to (2.2)-(2.8), and (2.14), (2.15), and (2.18). Notice that **(P3)** in nonlinear due to the presence of $\{Z_{ijqt}X_{ijqt}\}$ term in the objective function, each of which is the product of a binary variable and a continuous variable. Following the technique proposed by Sherali and Alameddine [88], we can linearize formulation **(P3)**. For each $j \in \mathcal{J}, (i,q) \in \mathcal{A}_j, t \in \mathcal{T}$, we replace $\{Z_{ijqt}X_{ijqt}\}$ with a new variable $\mathbf{R} := \{R_{ijqt} | \forall j \in \mathcal{J}, (i,q) \in \mathcal{A}_j, t \in \mathcal{T}\}$ and linearize formulation **(P3)** as follows, referred to as **(P4)**.

$$\textbf{(P4)} \quad \underset{\mathbf{Z},\mathbf{Y},\mathbf{H},\mathbf{X},\mathbf{R}}{Maximize} \sum_{j\in\mathcal{J}} \sum_{(i,q)\in\mathcal{A}_j} \sum_{t\in\mathcal{T}} \pi_{iqt} R_{ijqt} - \sum_{i\in\mathcal{I}} \sum_{q\in\mathcal{Q}} \sum_{t\in\mathcal{T}} h_{iqt} H_{iqt} \tag{2.20}$$

subject to (2.2)-(2.8), and (2.14), (2.15), (2.18), and

$$R_{ijqt} \leq \hat{s}_{iq} Z_{ijqt} \qquad \forall j \in \mathcal{J}, (i,q) \in \mathcal{A}_j, t \in \mathcal{T} \tag{2.21}$$

$$R_{ijqt} \leq X_{ijqt} \qquad \forall j \in \mathcal{J}, (i,q) \in \mathcal{A}_j, t \in \mathcal{T} \tag{2.22}$$

$$R_{ijqt} \geq X_{ijqt} - \hat{s}_{iq}(1 - Z_{ijqt}) \qquad \forall j \in \mathcal{J}, (i,q) \in \mathcal{A}_j, t \in \mathcal{T} \tag{2.23}$$

2.3 Solution Approach

The proposed model **(P4)** is a mixed-integer linear programming model that the commercial solvers (e.g., GUROBI/CPLEX) find it challenging to solve with an increase in the problem size. To alleviate this challenge, we use the Benders decomposition algorithm [14], a well-known partitioning method for solving mixed-integer linear programming models. Next, we introduce how the classicial Benders decomposition algorithm can be embedded in a Branch-and-cut framework, referred to as the Benders-based Branch-and-cut algorithm, to efficiently solve **(P4)**. Finally,

different enhancement strategies are introduced, such as the generation of Pareto-optimal cut, warm-start strategies, and problem-specific valid inequalities and preprocessing techniques, to enhance the performance of the classical Benders decomposition algorithm and the Benders-based Branch-and-cut algorithm.

2.3.1 Benders decomposition algorithm

Benders decomposition algorithm partitions the original problem into two major components: an integer *master problem* and a *linear subproblem*. For our problem, once the selling/purchasing decisions of the landowners and the mills are set, i.e., $\hat{\mathbf{Y}} := \{Y_{iqt} | \forall i \in \mathcal{I}, q \in \mathcal{Q}, t \in \mathcal{T}\}$ and $\hat{\mathbf{Z}} := \{Z_{ijqt} | \forall j \in \mathcal{J}, t \in \mathcal{T}, (i,q) \in \mathcal{A}_j\}$, the problem can be reduced to the following primal subproblem [**PS**], involving only the continuous decision variables $\{H_{iqt}\}_{\forall i \in \mathcal{I}, q \in \mathcal{Q}, t \in \mathcal{T}}$, and $\{X_{ijqt}\}_{\forall i \in \mathcal{I}, j \in \mathcal{J}, q \in \mathcal{Q}, t \in \mathcal{T}}$, and $\{R_{ijqt}\}_{\forall j \in \mathcal{J}, (i,q) \in \mathcal{A}_j, t \in \mathcal{T}}$.

$$[\mathbf{PS}] \quad \underset{\mathbf{X},\mathbf{R},\mathbf{H}}{Maximize} \sum_{j \in \mathcal{J}} \sum_{t \in \mathcal{T}} \sum_{(i,q) \in A_j} \pi_{iqt} R_{ijqt} - \sum_{i \in \mathcal{I}} \sum_{q \in \mathcal{Q}} \sum_{t \in \mathcal{T}} h_{iqt} H_{iqt} \tag{2.24}$$

subject to

$$H_{iq,1} + \sum_{j\in\mathcal{J}} X_{ijq,1} = \hat{s}_{iq} \quad \forall i \in \mathcal{I}, q \in \mathcal{Q} \tag{2.25}$$

$$(1-\alpha_{q,t-1})H_{iq,t-1} = H_{iqt} + \sum_{j\in\mathcal{J}} X_{ijqt} \quad \forall i \in \mathcal{I}, q \in \mathcal{Q}, t \in \mathcal{T}|t>1 \tag{2.26}$$

$$X_{ijqt} \leq \hat{s}_{iq}\hat{Y}_{iqt} \quad \forall i \in \mathcal{I}, j \in \mathcal{J}, q \in \mathcal{Q}, t \in \mathcal{T} \tag{2.27}$$

$$\sum_{q\in\mathcal{Q}}\sum_{i\in\mathcal{I}} X_{ijqt} \leq d_{jt} \quad \forall j \in \mathcal{J}, t \in \mathcal{T} \tag{2.28}$$

$$R_{ijqt} \leq \hat{s}_{iq}\hat{Z}_{ijqt} \quad \forall j \in \mathcal{J}, t \in \mathcal{T}, (i,q) \in \mathcal{A}_j \tag{2.29}$$

$$R_{ijqt} \leq X_{ijqt} \quad \forall j \in \mathcal{J}, t \in \mathcal{T}, (i,q) \in \mathcal{A}_j \tag{2.30}$$

$$R_{ijqt} \geq X_{ijqt} - \hat{s}_{iq}(1-\hat{Z}_{ijqt}) \quad \forall j \in \mathcal{J}, t \in \mathcal{T}, (i,q) \in \mathcal{A}_j \tag{2.31}$$

$$X_{ijqt}, R_{ijqt}, H_{iqt} \in \mathbb{R}^+ \tag{2.32}$$

Let $\lambda = \{\lambda_{iq}|\forall i \in \mathcal{I}, q \in \mathcal{Q}\}$, $\theta = \{\theta_{iqt}|\forall i \in \mathcal{I}, q \in \mathcal{Q}, t \in \mathcal{T}|t>1\}$, $\kappa = \{\kappa_{ijqt} \geq 0|\forall i \in \mathcal{I}, j \in \mathcal{J}, q \in \mathcal{Q}, t \in \mathcal{T}\}$, $\nu = \{\nu_{jt} \geq 0|\forall j \in \mathcal{J}, t \in \mathcal{T}\}$, $\gamma = \{\gamma_{ijqt} \geq 0|\forall j \in \mathcal{J}, t \in \mathcal{T}, (i,q) \in \mathcal{A}_j\}$, $\sigma = \{\sigma_{ijqt} \geq 0|\forall j \in \mathcal{J}, t \in \mathcal{T}, (i,q) \in \mathcal{A}_j\}$, and $\rho = \{\rho_{ijqt} \geq 0|\forall j \in \mathcal{J}, t \in \mathcal{T}, (i,q) \in \mathcal{A}_j\}$ be the vector of the dual variables associated with constraints (2.25)-(2.31), respectively. We present the dual of the primal subproblem, denoted as **[DPS]**, as follows:

$$\begin{aligned}\textbf{[DPS]} \quad \underset{\lambda,\theta,\kappa,\nu,\gamma,\sigma,\rho}{Minimize} \quad & \sum_{i\in\mathcal{I}}\sum_{q\in\mathcal{Q}} \hat{s}_{iq}\lambda_{iq} + \sum_{i\in\mathcal{I}}\sum_{j\in\mathcal{J}}\sum_{q\in\mathcal{Q}}\sum_{t\in\mathcal{T}} \hat{s}_{iq}\hat{Y}_{iqt}\kappa_{ijqt} + \sum_{j\in\mathcal{J}}\sum_{t\in\mathcal{T}} d_{jt}\nu_{jt} \\ & + \sum_{j\in\mathcal{J}}\sum_{t\in\mathcal{T}}\sum_{(i,q)\in\mathcal{A}_j} \hat{s}_{iq}\hat{Z}_{ijqt}\gamma_{ijqt} + \sum_{j\in\mathcal{J}}\sum_{t\in\mathcal{T}}\sum_{(i,q)\in\mathcal{A}_j} \hat{s}_{iq}(1-\hat{Z}_{ijqt})\rho_{ijqt}\end{aligned} \tag{2.33}$$

subject to

$$\lambda_{iq} + (1 - \alpha_{q,2})\theta_{iq,2} \geq -h_{iq,1} \quad \forall i \in \mathcal{I}, q \in \mathcal{Q} \tag{2.34}$$

$$\lambda_{iq} + \kappa_{ijqt} + \nu_{jt} - \sigma_{ijqt} + \rho_{ijqt} \geq 0 \quad \forall j \in \mathcal{J}, t \in \mathcal{T}, (i,q) \in A_j | t = 1 \tag{2.35}$$

$$\lambda_{iq} + \kappa_{ijqt} + \nu_{jt} \geq 0 \quad \forall j \in \mathcal{J}, t \in \mathcal{T}, (i,q) \notin A_j | t = 1 \tag{2.36}$$

$$(1 - \alpha_{q,t+1})\theta_{iq,t+1} - \theta_{iqt} \geq -h_{iqt} \quad \forall i \in \mathcal{I}, q \in \mathcal{Q}, t \in \mathcal{T} | t > 1 \tag{2.37}$$

$$-\theta_{iqt} + \kappa_{ijqt} + \nu_{jt} - \sigma_{ijqt} + \rho_{ijqt} \geq 0 \quad \forall j \in \mathcal{J}, t \in \mathcal{T}, (i,q) \in A_j | t > 1 \tag{2.38}$$

$$-\theta_{iqt} + \kappa_{ijqt} + \nu_{jt} \geq 0 \quad \forall j \in \mathcal{J}, t \in \mathcal{T}, (i,q) \notin A_j | t > 1 \tag{2.39}$$

$$\gamma_{ijqt} + \sigma_{ijqt} - \rho_{ijqt} \geq \pi_{iqt} \quad \forall j \in \mathcal{J}, t \in \mathcal{T}, (i,q) \in A_j | t > 1 \tag{2.40}$$

$$\lambda_{iq}, \theta_{iqt} \in \mathbb{R} \tag{2.41}$$

$$\kappa_{ijqt}, \nu_{jt}, \sigma_{ijqt}, \rho_{ijqt} \in \mathbb{R}^{+} \tag{2.42}$$

Now, we introduce an additional free variable Θ to the underlying Benders reformulation and define the following Benders *Master problem* [**MP**]:

$$[\mathbf{MP}] \quad \underset{\mathbf{Y},\mathbf{Z},\Theta}{Maximize} \quad \Theta \tag{2.43}$$

subject to:

$$\Theta \leq \sum_{i\in\mathcal{I}}\sum_{q\in\mathcal{Q}} \hat{s}_{iq}\lambda_{iq} + \sum_{i\in\mathcal{I}}\sum_{j\in\mathcal{J}}\sum_{q\in\mathcal{Q}}\sum_{t\in\mathcal{T}} \hat{s}_{iq}Y_{iqt}\kappa_{ijqt} + \sum_{j\in\mathcal{J}}\sum_{t\in\mathcal{T}} d_{jt}\nu_{jt}$$
$$+ \sum_{j\in\mathcal{J}}\sum_{t\in\mathcal{T}}\sum_{(i,q)\in\mathcal{A}_j} \hat{s}_{iq}Z_{ijqt}\gamma_{ijqt} + \sum_{j\in\mathcal{J}}\sum_{t\in\mathcal{T}}\sum_{(i,q)\in\mathcal{A}_j} \hat{s}_{iq}(1 - Z_{ijqt})\rho_{ijqt}$$
$$\forall(\lambda, \theta, \kappa, \nu, \sigma, \rho) \in \mathcal{P}_d \tag{2.44}$$

$$Z_{ijqt} \leq Y_{iqt} \quad \forall j \in \mathcal{J}, t \in \mathcal{T}, (i,q) \in \mathcal{A}_j \tag{2.45}$$

$$\sum_{(\acute{\imath},\acute{q})\in\mathcal{A}_j} Z_{\acute{\imath}j\acute{q}t} \geq Y_{iqt} + \sum_{(\acute{\imath},\acute{q})\in C_{ijqt}} Z_{\acute{\imath}j\acute{q}t} \quad \forall j \in \mathcal{J}, t \in \mathcal{T}, (i,q) \in \mathcal{A}_j \tag{2.46}$$

$$Y_{iqt} \in \{0,1\} \qquad \forall i \in \mathcal{I}, q \in \mathcal{Q}, t \in \mathcal{T} \tag{2.47}$$

$$Z_{ijqt} \in \{0,1\} \qquad \forall j \in \mathcal{J}, t \in \mathcal{T}, (i,q) \in \mathcal{A}_j \tag{2.48}$$

In [**MP**], constraints (2.44) are referred to as *optimality cut* constraints, where $\mathcal{P}_d$ is the set of extreme points in the feasible region of [**DPS**]. Note that for any feasible values of **Y** and **Z**, both the primal [**PS**] and the dual [**DPS**] subproblems are always feasible. Therefore, in our study, we do not add any *feasible cuts* to [**MP**]. Further, it can be noted that [**MP**] contains an exponential number of constraints, causing serious challenge from solution standpoint. To alleviate this problem, we employ a cutting-plane method and solve a restricted master problem [**RMP**] in which the set $\mathcal{P}_d$ is replaced with $\mathcal{P}_d^r$, i.e., $\mathcal{P}_d^r \subset \mathcal{P}_d$. The idea is to start [**RMP**] with an empty set $\mathcal{P}_d^r$, which grows by iteratively solving the restricted master and the dual subproblem [**DPS**]. The overall algorithm is outlined below:

Let UB^r and LB^r to represent an upper and lower bound estimate of the original problem **(P4)**, which is obtained in the rth iteration of the Benders decomposition algorithm. The algorithm starts

by solving the restricted master problem **[RMP]**. The solution of this problem, denoted by Z_{RMP}, provides a valid upper bound for the original problem **(P4)** and also yields $\{Y_{iqt}\}_{\forall i\in\mathcal{I},q\in\mathcal{Q},t\in\mathcal{T}}$ and $\{Z_{ijqt}\}_{\forall j\in\mathcal{J},t\in\mathcal{T},(i,q)\in\mathcal{A}_j}$, which are then utilized to solve the dual subproblem [**DPS**]. The solution of the dual subproblem [**DPS**], denoted by Z_{DPS}, provides a valid lower bound for the original problem **(P4)**. The algorithm terminates if the the obtained gap between the upper and lower bounds falls below a pre-specified threshold limit ϵ; otherwise, if violated, the optimality cut (2.44) is added to **[RMP]** and set $\mathcal{P}_d^r$ is updated. The pseudo-code of the classical Benders decomposition algorithm is provided in **Algorithm 1**.

Algorithm 1: The Benders decomposition algorithm

Initialization: $r \leftarrow 1, \epsilon, UB^r \leftarrow +\infty, LB^r \leftarrow -\infty, \mathcal{P}_d^r \leftarrow \emptyset$
$terminate \leftarrow false$

while $terminate = false$ **do**
  Solve [**RMP**] to obtain $\{Y_{iqt}\}_{\forall i\in\mathcal{I},q\in\mathcal{Q},t\in\mathcal{T}}$, and $\{Z_{ijqt}\}_{\forall j\in\mathcal{J},t\in\mathcal{T},(i,q)\in\mathcal{A}_j}$ and z^r_{MP}
  if $z^r_{RMP} \leq UB^r$ **then**
    $UB^r \leftarrow z^r_{RMP}$
  end
  For fixed $\{\hat{Y}^r_{iqt}\}_{\forall i\in\mathcal{I},q\in\mathcal{Q},t\in\mathcal{T}}$, and $\{\hat{Z}^r_{ijqt}\}_{\forall j\in\mathcal{J},t\in\mathcal{T},(i,q)\in\mathcal{A}_j}$ solve [**DPS**] to obtain $(\lambda,\theta,\kappa,\nu,\sigma,\rho) \in \mathcal{P}_d$ and z^r_{DSP}
  if $z^r_{DSP} > LB^r$ **then**
    $LB^r \leftarrow z^r_{DSP}$
  end
  if $\frac{UB^r - LB^r}{UB^r} \leq \epsilon$ **then**
    $terminate \leftarrow true$
  else
    $\mathcal{P}_D^{r+1} \leftarrow \mathcal{P}_D^r \cup \{(\lambda,\theta,\kappa,\nu,\sigma,\rho)\}$
  end
  $r \leftarrow r+1$
end

2.3.2 Benders-based Branch-and-Cut Algorithm

Given the Benders cuts generated from any solution of the master problem of the classical Benders decomposition algorithm are valid, such cuts could be utilized in the nodes of the branch-and-bound tree of the master problem [54]. With this, the classical Benders decomposition algorithm can be embedded in a branch-and-cut framework, where the Benders cuts, generated via solving the dual subproblems, could be added at any node of the branch-and-bound tree of the master problem. This study adopts a framework, referred to as the Benders-based Branch-and-Cut algorithm [63, 26], that only builds and maintains one branch-and-bound search tree of **[MP]** at the end of the solution process. In other words, **[MP]** is solved into optimality only once, and the majority of the efforts are paid on each node of the tree to solving the LP-relaxation of the **[MP]** problem, which is much easier and faster to solve compared to the MILP. Past successful implementation of the Benders-based Branch-and-cut technique involves generating Benders optimality cuts when an incumbent solution is found (e.g., [3]) or at any node of the branch-and-bound tree (e.g., [63, 37]).

Note that only a few constraints can only be utilized in the solution process in large scale optimization problems. In our method, as stronger cuts are introduced to the **[MP]**, many of the previously added cuts may become redundant or may not binding near the optimal solution. As such, those redundant/non-binding constraints can be ruled out from **[MP]** without prior information. One possible way to avoid such cuts is to set them as *lazy constraints* and put them into a pool in GURUBI. When a solution is generated, the solver will check if any lazy constraints are violated and, if so, adds them to the active set. Lazy constraints that were previously added but have not been binding for a while will be returned to the pool. Note that the mentioned lazy constraints are added

to the **[MP]** by a callback function, i.e., the effectiveness of the generated cuts are checked before adding to the **[MP]** when every time Gurobi branch-and-cut framework finds a candidate solution. The step-by-step implementation of the Benders-based Branch-and-cut technique is illustrated by **Algorithm 2**.

Algorithm 2: Benders-based branch-and-cut algorithm

Initialization: Add the original **[MP]** into tree L
Let S^* represents the final solution for $\{Y_{iqt}\}_{\forall i\in\mathcal{I},q\in\mathcal{Q},t\in\mathcal{T}}$, and $\{Z_{ijqt}\}_{\forall j\in\mathcal{J},t\in\mathcal{T},(i,q)\in\mathcal{A}_j}$, set $S^* = \emptyset$
Let Z^*_{MP} represent the repective value of the objective function for the final solution, set $Z^*_{MP} = -\infty$
while *L is not empty* **do**
  Select a node of **[MP]** from L
  Solve LP relaxation of the **[MP]** to obtain an optimal solution $\bar{S}$ with objective value of $\bar{Z}_{MP}$.
  if *LP is infeasible or* $\bar{Z}_{MP} \le Z^*_{MP}$ **then**
    Prune the node.
  else
    if *$\bar{S}$ is integer* **then**
      Solve **[DPS]** based on $\bar{S}$ and generate Benders cuts.
      Add the cuts to the LP relaxation
      Prune the node.
      if $\bar{Z}_{MP} \le Z^*_{MP}$ **then**
        Update $S^* = \bar{S}$ and $Z^*_{MP} = \bar{Z}_{MP}$
      end
    else
      Solve **[DPS]** based on $\bar{S}$ and generate Benders cuts.
      Search for cutting planes that are violated by $\bar{S}$.
      If any cutting planes or Benders cuts are found, add them to the LP relaxation.
      Choose one non-integral variable from $\bar{S}$ to branch, create two nodes and add them to L.
    end
  end
end
Output: Return final solution S^* and respective objective function value Z^*_{MP}

2.3.3 Acceleration Strategies

To improve the convergence of the classical Benders decomposition algorithm and the Benders-based Branch-and-cut algorithm, the following three acceleration strategies are introduced: Pareto-

optimal cuts, warm start strategy, and problem-specific valid inequalities. These enhancements aim to accelerate the solution process by introducing stronger Benders optimality cuts, generating high-quality initial solutions, and reducing the search space of the problem. The following subsections describe these enhancement techniques.

2.3.3.1 Pareto-optimal Cuts

Magnanti and wong [46] realized that when the primal subproblem is degenerate, i.e., the dual of the subproblem has multiple solutions, there are quite a few optimality cuts that could be generated and added to the Benders master problem. While all the cuts are valid, the authors proposed an efficient method to construct stronger, non-dominated cuts, commonly referred to as *pareto-optimal cuts*, where the strength of two cuts is compared according to the following definition.

Definition 1. *The cut corresponding to* $(\lambda^1, \theta^1, \kappa^1, \nu^1, \sigma^1, \rho^1) \in \mathcal{P}_d$ *dominates the the cut corresponding to* $(\lambda^2, \theta^2, \kappa^2, \nu^2, \sigma^2, \rho^2) \in \mathcal{P}_d$*, if:*

$$\begin{aligned}
&\sum_{i\in\mathcal{I}}\sum_{q\in\mathcal{Q}} \hat{s}_{iq}\lambda^1_{iq} + \sum_{i\in\mathcal{I}}\sum_{j\in\mathcal{J}}\sum_{q\in\mathcal{Q}}\sum_{t\in\mathcal{T}} \hat{s}_{iq}Y_{iqt}\kappa^1_{ijqt} + \sum_{j\in\mathcal{J}}\sum_{t\in\mathcal{T}} d_{jt}\nu^1_{jt} \\
&+ \sum_{j\in\mathcal{J}}\sum_{t\in\mathcal{T}}\sum_{(i,q)\in\mathcal{A}_j} \hat{s}_{iq}Z_{ijqt}\gamma^1_{ijqt} + \sum_{j\in\mathcal{J}}\sum_{t\in\mathcal{T}}\sum_{(i,q)\in\mathcal{A}_j} \hat{s}_{iq}(1-Z_{ijqt})\rho^1_{ijqt} \leq \sum_{i\in\mathcal{I}}\sum_{q\in\mathcal{Q}} \hat{s}_{iq}\lambda^2_{iq} \\
&+ \sum_{i\in\mathcal{I}}\sum_{j\in\mathcal{J}}\sum_{q\in\mathcal{Q}}\sum_{t\in\mathcal{T}} \hat{s}_{iq}Y_{iqt}\kappa^2_{ijqt} \sum_{j\in\mathcal{J}}\sum_{t\in\mathcal{T}} d_{jt}\nu^2_{jt} + \sum_{j\in\mathcal{J}}\sum_{t\in\mathcal{T}}\sum_{(i,q)\in\mathcal{A}_j} \hat{s}_{iq}Z_{ijqt}\gamma^2_{ijqt} \\
&+ \sum_{j\in\mathcal{J}}\sum_{t\in\mathcal{T}}\sum_{(i,q)\in\mathcal{A}_j} \hat{s}_{iq}(1-Z_{ijqt})\rho^2_{ijqt}
\end{aligned} \tag{2.49}$$

with strict inequality for at least one point $\{Y_{iqt}\}_{\forall i\in\mathcal{I}, q\in\mathcal{Q}, t\in\mathcal{T}} \in \mathbb{F}$, and $\{Z_{ijqt}\}_{\forall j\in\mathcal{J}, t\in\mathcal{T}, (i,q)\in\mathcal{A}_j} \in \mathbb{F}$, where the $\mathbb{F}$ represents the the polyhedron defined by (2.45)-(2.48).

Definition 2. *A cut is referred to as Pareto-optimal if the cut could not be dominated by any other cut and corresponding solution is called the Pareto-optimal solution.*

In this study, we have used the subproblem independent Patero-optimal cut proposed by Papadakos [69]. Let $\mathbb{F}^{LP}$ be the polyhedron defined by (2.45), (2.46), $0 \leq \{Y_{iqt}\}_{\forall i\in\mathcal{I},q\in\mathcal{Q},t\in\mathcal{T}} \leq 1$, and $0 \leq \{Z_{ijqt}\}_{\forall j\in\mathcal{J},t\in\mathcal{T},(i,q)\in\mathcal{A}_j} \leq 1$, and let $ri(\mathbb{F}^{LP})$ to represent the relative interior of the $\mathbb{F}^{LP}$. We can construct a Pareto-optimal cut by solving the following auxiliary problem, referred to as **[DPS[MW]]**, where $\{Y^0_{iqt}\}_{\forall i\in\mathcal{I},q\in\mathcal{Q},t\in\mathcal{T}} \in ri(\mathbb{F}^{LP})$ and $\{Z^0_{ijqt}\}_{\forall j\in\mathcal{J},t\in\mathcal{T},(i,q)\in\mathcal{A}_j} \in ri(\mathbb{F}^{LP})$.

$$\begin{aligned}\textbf{[DPS(MW)]}\quad \underset{\lambda,\theta,\kappa,\nu,\gamma,\sigma,\rho}{Minimize}\ & \sum_{i\in\mathcal{I}}\sum_{q\in\mathcal{Q}}\hat{s}_{iq}\lambda_{iq} + \sum_{i\in\mathcal{I}}\sum_{j\in\mathcal{J}}\sum_{q\in\mathcal{Q}}\sum_{t\in\mathcal{T}}\hat{s}_{iq}Y^0_{iqt}\kappa_{ijqt} + \sum_{j\in\mathcal{J}}\sum_{t\in\mathcal{T}} d_{jt}\nu_{jt} \\ & + \sum_{j\in\mathcal{J}}\sum_{t\in\mathcal{T}}\sum_{(i,q)\in\mathcal{A}_j}\hat{s}_{iq}Z^0_{ijqt}\gamma_{ijqt} + \sum_{j\in\mathcal{J}}\sum_{t\in\mathcal{T}}\sum_{(i,q)\in\mathcal{A}_j}\hat{s}_{iq}(1-Z^0_{ijqt})\rho_{ijqt} \qquad (2.50)\end{aligned}$$

subject to (2.34)-(2.42). In **[DPS[MW]]**, $\{Y^0_{iqt}\}_{\forall i\in\mathcal{I},q\in\mathcal{Q},t\in\mathcal{T}} \in ri(\mathbb{F}^{LP})$ and $\{Z^0_{ijqt}\}_{\forall j\in\mathcal{J},t\in\mathcal{T},(i,q)\in\mathcal{A}_j} \in ri(\mathbb{F}^{LP})$ are denoted as *core points* which could be updated using the following equations:

$$Y^0_{iqt} = \tau Y^0_{iqt} + (1-\tau)\hat{Y}_{iqt} \qquad \forall i\in\mathcal{I}, q\in\mathcal{Q}, t\in\mathcal{T} \qquad (2.51)$$

$$Z^0_{ijqt} = \tau Z^0_{ijqt} + (1-\tau)\hat{Z}_{ijqt} \qquad \forall j\in\mathcal{J}, t\in\mathcal{T}, (i,q)\in\mathcal{A}_j \qquad (2.52)$$

In the above equations, the values of $\hat{Y}_{iqt}$ and $\hat{Z}_{ijqt}$ parameters are obtained from the solution of the current master problem. Further, as suggested in[69], we set the τ value to $\tau = 0.5$. In the first iteration of the basic Benders decomposition algorithm and the root node of the Benders-based branch-and-cut algorithm, the values of $\{Y^0_{iqt}\}_{\forall i\in\mathcal{I},q\in\mathcal{Q},t\in\mathcal{T}}$ and $\{Z^0_{ijqt}\}_{\forall j\in\mathcal{J},t\in\mathcal{T},(i,q)\in\mathcal{A}_j}$ are obtained

by solving the Benders master problem **[MP]**. Although the generation of Pareto-optimal cuts require solving two subproblems sequentially, such efforts usually improves the convergence of the Benders decomposition algorithm.

2.3.3.2 Warm Start Strategy

Figure 2.1 represents the convex hull of the feasible region of a hypothetical mixed-integer linear programming (MILP) model and its respective linear programming (LP) relaxation solution. As can be observed, the convex hull corresponding to the MILP problem is always inside the respective LP relaxation, which provides the underlying basis for implementing a *two-phase method* represented in [23]. In the *first phase* of this method, all integer variables' integrality restrictions are relaxed, and the corresponding relaxed problem is solved using the basic Benders decomposition algorithm illustrated in **Algorithm 1**. Afterward, the integer variables' integrality restrictions are reintroduced (*second phase* of this method), and the algorithm continues. Note that all the generated optimality cuts obtained from the first phase of this method are also added to the second phase. **Algorithm 3** outlines the general implementation framework of this method. The rationale behind implementing this method is to obtain quality solutions from the Benders master problem from the very beginning, intending to enhance the computational performance of the Benders decomposition algorithm (**Algorithm 1** or **2**).

2.3.3.3 Valid inequalities and Pre-processing

To improve the computational performance of the proposed model and solution approaches, the following valid inequalities are introduced.

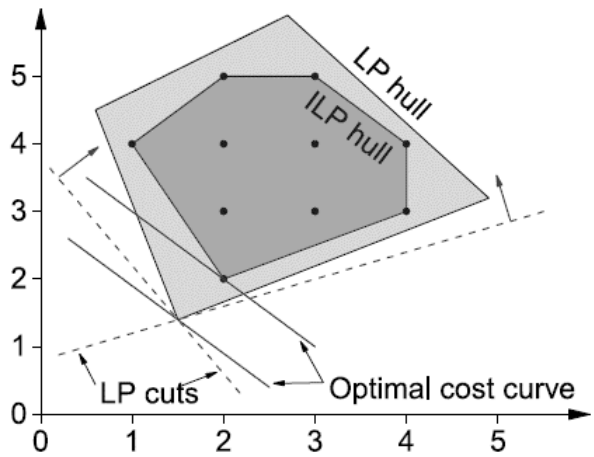

Figure 2.1

Illustration of mixed-integer linear programming hull versus the respective linear relaxation hull

Algorithm 3: Two-Phase method

Phase 1:
Relax the integrality restrictions on all integer variables
Solve the problem using **Algorithm 1** and keep all the generated cuts
Phase 2:
Reintroduce the integrality restrictions on the master problem variables. Add all cuts generated from **Phase 1** into **[MP]**, and solve the problem using **Algorithm 1** or **2**

- We assume the mill $j \in \mathcal{J}$ only covers timberland owner $i \in \mathcal{I}$ that are in a specific radius of the mill, d_{max}. For the mill $j \in \mathcal{J}$ at time $t \in \mathcal{T}$, let $\mathcal{N}_{jt} = |\{(i,q) \in \mathcal{A}_j | d_{ij} \leq d_{max}, s_{iq} > 0\}|$ to represent the maximum number of timberland owner and timber quality pairs available in the corresponding coverage range of the mill. With this, we add the following valid inequality to model **(P4)**:

$$\sum_{(i,q)\in\mathcal{A}_j} Z_{ijqt} \leq \mathcal{N}_{jt} \qquad \forall j \in \mathcal{J}, t \in \mathcal{T} \tag{2.53}$$

- Given the validity of inequality (2.53), it can also be concluded that the constraints (2.54) are valid for **(P4)**. See **Theorem 1** for details.

Theorem 1. *For mill $j \in \mathcal{J}$ at time $t \in \mathcal{T}$ and supply-quality pair $(i,q) \in \mathcal{A}_j$, constraints* (2.54) *are valid for **(P4)**.*

$$Y_{iqt} + \sum_{(i',q') \in C_{ijqt}} Z_{i'jq't} \leq \mathcal{N}_{jt} \qquad \forall j \in \mathcal{J}, t \in \mathcal{T}, (i,q) \in \mathcal{A}_j \tag{2.54}$$

Proof. This can be proved by constructing two cases.

Case 1: Assume that timberland owner $i \in \mathcal{I}$ decides to sell the timber of quality $q \in Q$ at time period $t \in \mathcal{T}$, i.e., $Y_{iqt} = 1$. This results in $\sum_{(i',q') \in C_{ijqt}} Z_{i'jq't} \leq \mathcal{N}_{jt} - 1$. Given that $\mathcal{A}_j = \mathcal{B}_{ijqt} \bigcup C_{ijqt}$, from (2.53) we can conclude that $\sum_{(i,q) \in C_{i'jq't}} Z_{ijqt} < \sum_{(i,q) \in \mathcal{A}_j} Z_{ijqt} \leq \mathcal{N}_{jt}$, i.e., $\sum_{(i',q') \in C_{ijqt}} Z_{i'jq't} \leq \mathcal{N}_{jt} - 1$.

Case 2: Let $Y_{iqt} = 0$, then constraints (2.54) reduce to constraints (2.53).

This proves that constraints (2.54) are valid for model **(P4)**.

To reduce the problem size, the following two easily checkable simplification processes are applied.

- If $|C_{ijqt}| = |\mathcal{A}_j| - 1$ ($|\mathcal{B}_{ijqt}| = 1$), then the pair (i,q) could be considered as a best option for mill $j \in \mathcal{J}$ at time $t \in \mathcal{T}$. With this assumption, from constraints (2.18), we infer that $Z_{ijqt} \geq Y_{iqt}$. Besides, constraints (2.14) denote that $Z_{ijqt} \leq Y_{iqt}$. Hence, once such condition holds in the model, both constraints are removed from the model and replaced by $Z_{ijqt} = Y_{iqt}$.

- If $|C_{ijqt}| = 0$ ($|\mathcal{B}_{ijqt}| = |\mathcal{A}_j|$), then the pair (i, q) could be considered as a worst choice for mill $j \in \mathcal{J}$. With this, constraints (2.54) may turn out to be $Y_{iqt} \leq \mathcal{N}_{jt}$; hence, the corresponding constraints could be removed from the formulation.

2.4 Computational Study and Managerial Insights

This section first discusses the data used in the model **(P4)**. Then, numerical experiments are performed to draw managerial insights by utilizing 15 coastal counties in Mississippi. Finally, by generating a set of problem-specific test instances, the performance of the customized solution approaches in solving model **(P4)** is evaluated. All the algorithms are coded in Python 3.7 and executed on a desktop computer with Intel Core i7 3.60 GHz processor and 32.0 GB RAM. The optimization solver used is GUROBI 9.0.3.

2.4.1 Data Description

This subsection discusses the input data used in the model **(P4)**. We consider 15 coastal counties in Mississippi as a testing ground to visualize and validate the modeling results. Figure 2.2 visualizes the distribution of pulpwood, sawtimebr, and available existing mill locations in our test region. In total, 15 mills are located in our test region (i.e., $|\mathcal{J}| = 15$). The county-wise availability of the aggregated timber data is obtained from Mississippi Forest Inventory (MFI) [56]. We then examine different hurricane categories, based on the Saffir-Simpson Hurricane Wind Scale (SSHWS) classifier [98], that landfall our test region since 1960 (see Table 2.1). Based on examining the past impact time, it is clear that the hurricanes favored August to October to landfall in Mississippi. Once such a hurricane makes landfall, they cause significant damages to the timbers. For instance, Hurricane Katrina, a category 3 hurricane, damaged approximately 40% of the forest cover in southeastern Mississippi [31]. In our study, we consider *three* representative hurricanes of

varying categories (based on the wind speed and central pressure) that landfall Mississippi in the past: (*i*) Hurricane Camille (category 5), (*ii*) Hurricane Katrina (category 3), and (*iii*) Hurricane Nate (category 1) (see Table 2.1 for details about the hurricanes). In our study, we classify the quality of the damaged timber (set Q in model **(P4)**) after a hurricane into *three* major types: *low* quality (snapped), *medium* quality (blown over), and *good* quality (leaning) timbers (see Figure 2.3[1]). An approximate distribution of different qualities of the damaged timbers under Hurricanes Camille, Katrina, and Nate are reported in Table 2.2[2]. We consider a total of 200 landowners in our test region (i.e., $|\mathcal{I}| = 200$). We randomly distribute the different post-hurricane damaged timbers (obtained from Table 2.2) among the landowners. Factors such as biomass availability and proximity of the county to the epicenter of the hurricane are considered to distribute the different qualities of the damaged timbers among the landowners.

Table 2.1

List of major hurricanes affected Mississippi State, U.S. [64]

Name	Category	Central Pressure[1] (mb)	Max Wind[2] (kt)	States Affected	Impact Time
Ethel	1	981	-	Mississippi	September, 1960
Camille	5	909	-	Mississippi, Louisiana	August, 1969
Frederic	3	946	-	Alabama, Mississippi	September, 1979
Elena	3	959	100	Alabama, Mississippi, Florida	September, 1985
Georges	2	964	90	Mississippi, Florida	September, 1998
Katrina	3	920	110	Alabama, Mississippi, Florida, Louisiana	August, 2005
Nate	1	983	65	Alabama, Mississippi, Florida, Louisiana	October, 2017
Zeta	1	970	110	Alabama, Mississippi, Florida	October, 2020

[1]Central Pressure: The observed or estimated central pressure of the hurricane at landfall.
[2]Maximum Winds: Estimated maximum sustained (1-min) surface (10 m) winds to occur along the U. S. coast.

Given the landowners are closely located with the mills, we consider trucks to be the only model of transportation to transport damaged timbers from landowner sites to mills. The unit

[1]The images are provided by the forest extension experts at Mississippi State University
[2]The numbers reported in Table 2.2 are obtained based on our discussion with the forest extension experts at Mississippi State University.

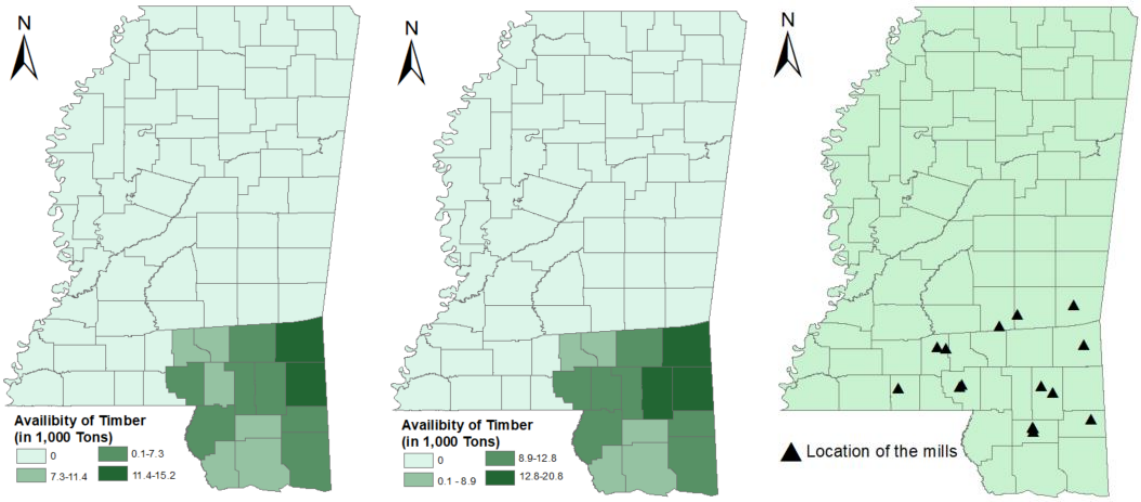

(a) Sawtimber availability (in 1,000 tons)

(b) Pulpwood availability (in 1,000 tons)

(c) Location of the mills in the experiments

Figure 2.2

Timber availability and existing mill locations in our test region

(a) Snapped Tree

(b) Blown over Tree

(c) Leaning Tree

Figure 2.3

Illustration of different types of damaged trees

Table 2.2

Distribution of damaged timber (in %) of varying qualities under different hurricane scenarios [93]

Hurricane	Damaged timbers (%)	Low quality timbers (%)	Medium quality timbers (%)	High quality timbers (%)
Camille	~U[65, 75]	~U[55, 65]	~U[25, 35]	~U[5, 15]
Katrina	~U[35, 50]	~U[30, 35]	~U[30, 35]	~U[30, 35]
Nate	~U[5, 15]	~U[5, 15]	~U[25, 35]	~U[55, 65]

transportation cost (c_{iqt}) can be computed as follows: $c_{iqt} = l^f_{qt}(1 + \Phi^f_{qt}) + l^v_{qt} g_{ij}(1 + \Phi^v_{qt})$, where l^f_{qt} is the fixed and l^v_{qt} is the variable cost components for unit timber transportation, Φ^f_{qt} and Φ^v_{qt}, respectively, denote the post-harvest loss (%) due to loading and unloading damaged timber, and g_{ij} denotes the transportation distance between a landowner site and a mill. Table 2.3 summarizes the key input parameters (e.g., production, storage, and transportation-related costs, and quality related factors) utilized in this study.

Table 2.3

Summary of input parameters for model **(P4)**

Parameters	Value	Unit	Reference
h^1_{iqt}	4.9^1; $5.05^{2,3}$	\$/ton	[27]
π_{qit}	$[1.7,4.6]^1_p$; $[2.5,6.8]^2_p$; $[3.4,9.1]^3_p$ $[3.4,9.11]^1_s$; $[10.1,26.9]^2_s$; $[11,29.5]^3_s$	\$/ton	[44, 96]
ψ_{jqt}	$[13.3,29.2]^1_p$; $[13.7,30.1]^2_p$; $[14.1,31.1]^3_p$ $[22.6,49.8]^1_s$; $[24.3,53.4]^2_s$; $[25.9,57.1]^3_s$	%	[44, 96]
l^f_{qt}	4.98^1; $5.55^{2,3}$	\$/ton	[87], [47]
l^v_{qt}	0.111^1; $0.15^{2,3}$	\$/ton/mile	[87], [47]
Φ^f_{qt}	12	%	[41]
Φ^v_{qt}	0.4	%	[85]

[1]low quality; [2]medium quality; [3]high quality
$_p$Pulpwood; $_s$Sawtimber

2.4.2 Real-life Case Study

This subsection provides managerial insights by solving model **(P4)** under different simulated hurricane scenarios. The first set of experiments, shown in Figure 2.4, illustrate how the storage and transportation decisions are impacted under the different quality of the damaged timbers (see Figure 2.3) and simulated hurricane scenarios (see Table 2.2). Note that due to the uncertainty associated with the availability of the damaged timber under different simulated hurricane scenarios, we run each experiment five times using the distribution provided in Table 2.2, and report the average values

in demonstrating the modeling results. The key findings obtained from this set of experiments are as follows:

- Figure 2.4 clearly reveals that hurricanes of different categories generate different qualities of the damaged trees (e.g., snapped, blown over, leaning), which eventually impact the storage and transportation decisions of the decision-makers (landowners and mills) in our test region. Figure 2.4(a) shows that, on average, under Hurricane Camille, respectively, the landowners stored 68.5% and 88.6% more lowquality pulpwood compared to Hurricane Katrina and Nate. The number is 66.2% and 87.4%, respectively, for the sawtimber case. This result is expected given Hurricane Camille produced more low-quality timbers over Hurricane Katrina and Nate. We then observe similar trends for the medium-quality timbers under different timber types and hurricane scenarios. As shown in Figure 2.4(b), on average, under Hurricane Camille, respectively, the landowners stored 41.1% and 56.2% more medium-quality pulpwood over Hurricane Katrina and Hurricane Nate, while the number is 68.6% and 88.7%, respectively, for the sawtimber case. On the other hand, we observe that undr Hurricane Nate and Katrina, the landowners stored more high-quality damaged timbers over Hurricane Camille (see Figure 2.4(c)). As such, the storage decisions for both hurricanes are significantly higher over Hurricane Camille (for both damaged pulpwood and sawtimber cases). Most importantly, we observe that, on average, the landowners kept storing the high-quality damaged timbers till March (assuming all the hurricanes strike in September) (see Figure 2.4(c)), which is only January for the low-quality damaged timbers (see Figure 2.4(a)). Due to the potential deterioration rates, This is understandable that the proposed model regards low-quality timbers over other quality timbers.

- Figure 2.4(d) shows how the transportation decisions are impacted under different damaged timber and simulated hurricane scenarios. For the pulpwood case, on average, mills transported 74.7% and 70.3% more damaged timbers (for all three qualities) during Hurricane Camille and Katrina compared to Hurricane Nate. The numbers are approximately 74.3% and 60.5%, respectively, for the damaged sawtimber case. Note that the mills continued to procure damaged timbers of any qualities from the landowners till April (almost eight months after the simulated hurricanes strike and assuming that all the hurricanes strike at the same time in September).

The next set of experiments examine the impact of damaged timber (pulpwood and sawtimber) deterioration rate (α_{qt}) on landowner's storage and mills transportation decisions (see Figure 2.5). To run the experiments, we consider only the base case instances with Hurricane Katrina. Our key findings from this set of experiments are summarized below.

- As can be seen in Figures 2.5(a) and (c), storage decisions are significantly impacted by the deterioration rate (α_{qt}) of the damaged timber (for both pulpwood and sawtimber cases). When the deterioration rate is high (i.e., 40% more than the base case), we observe that the landowners decide to sell the damaged timber as early as possible. For instance, the landowners sell all the damaged timbers[3] by February (within six months after the simulated hurricane strikes) under both the pulpwood and sawtimber cases. On the other hand, the landowners could store the damaged timbers for another two to four months if the deterioration of the damaged timber could have been better (e.g., 40% less than the base

[3]Note that not all damaged timbers could be profitable for the mills, i.e., this is the quantity for which the ($\psi_{jqt} - \pi_{iqt} - c_{ijqt}$) term is greater than or equal to zero)

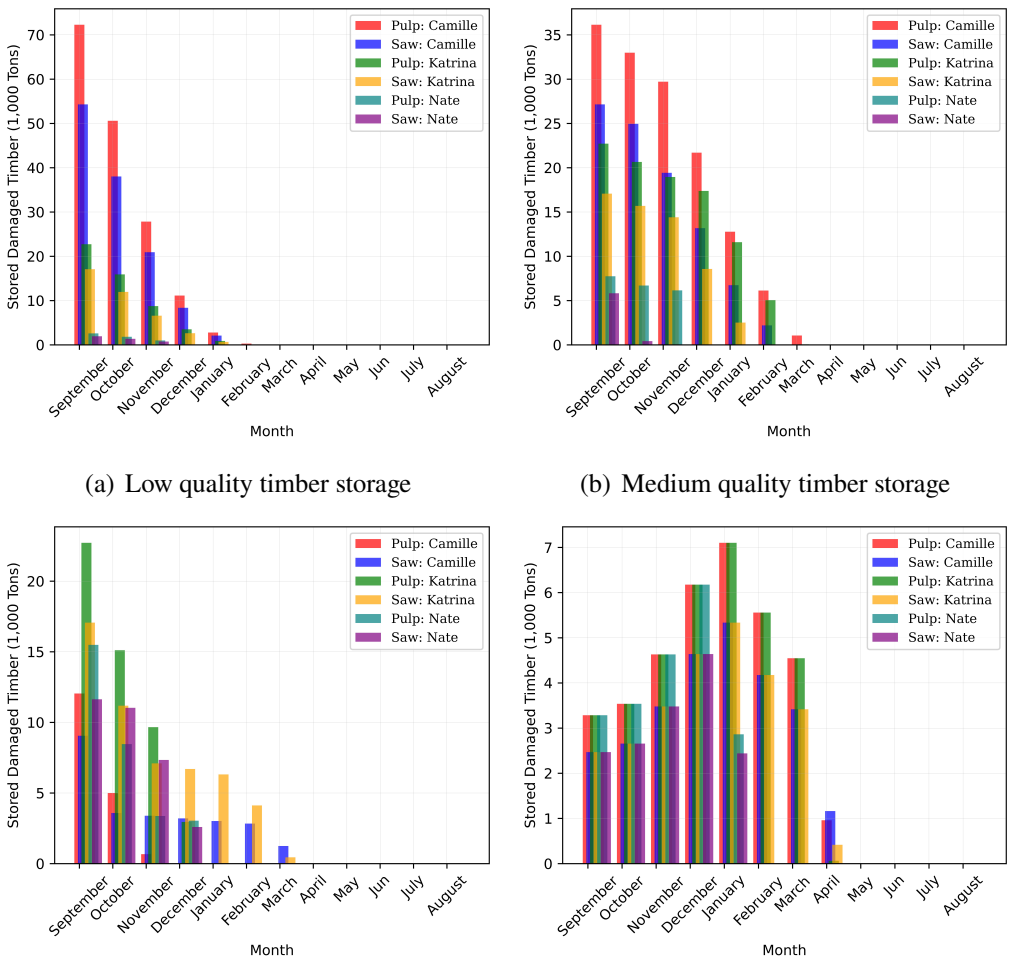

(a) Low quality timber storage

(b) Medium quality timber storage

(c) High quality timber storage

(d) Total transportation

Figure 2.4

Illustration of storage and transportation decisions under different quality of the damaged timbers and simulated hurricane scenarios

case). Subsequently, we observe in Figures 2.5(b) and (d) that the transportation decisions are also sensitive to deterioration rate.

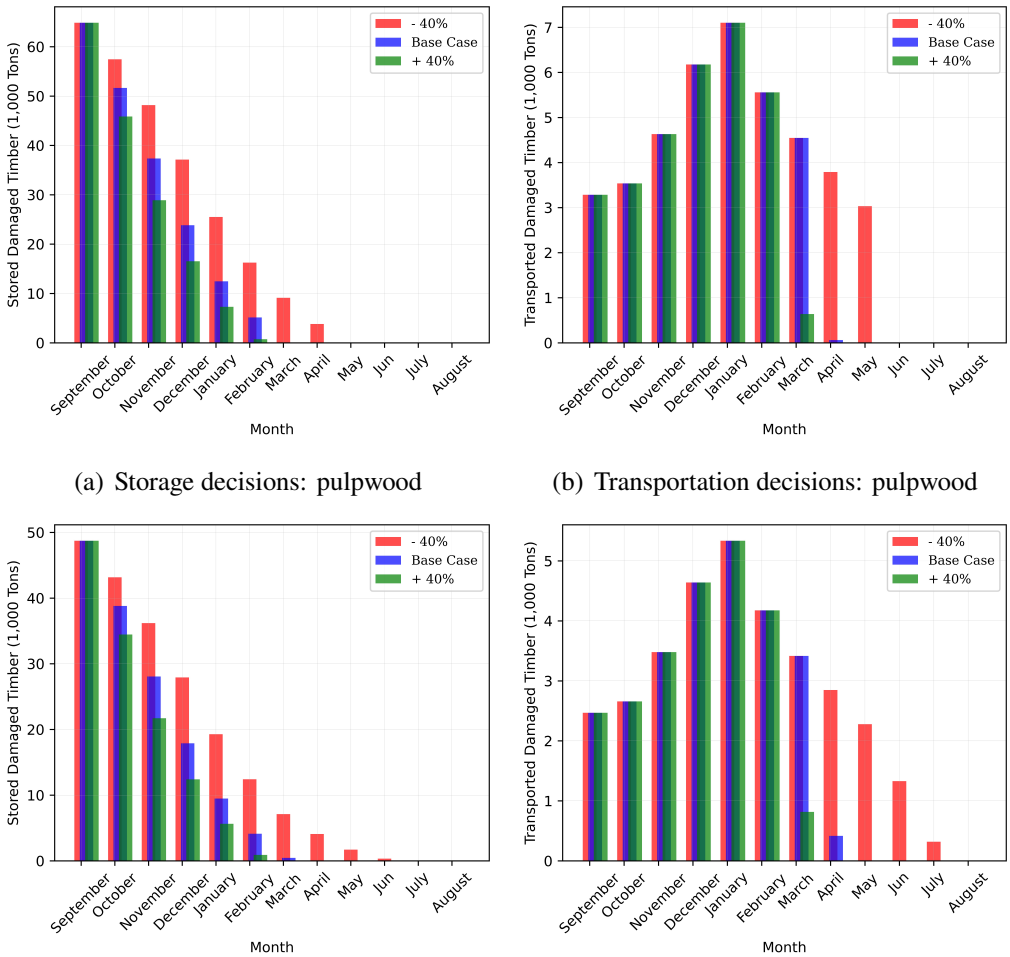

(a) Storage decisions: pulpwood

(b) Transportation decisions: pulpwood

(c) Storage decisions: sawtimber

(d) Transportation decisions: sawtimber

Figure 2.5

Impact of deterioration rate on damaged pulpwood and sawtimber

The last set of experiments examine the impact of landowner's damaged timber selling price (π_{iqt}) and mills viable purchasing price (ψ_{jqt}) over the transportation-related decisions (see Figure 2.6). Yet again, we only consider the base hurricane scenario (Hurricane Katrina) to run the

experiments shown in Figure 2.6. Our key findings from this set of experiments are summarized below.

- Results in Figure 2.6(a) and (c) clearly indicate that the transportation decisions are sensitive to the selling prices (π_{iqt}) offered by the landowners for both the damaged pulpwood and sawtimber. For instance, if the selling prices (π_{iqt}) offered by the landowners is increased by 40% from the base prices for both the damaged pulpwood and sawtimber, the average transportation is dropped by approximately 26% and 96%, respectively, for the months between September to April. On the other hand, the numbers could increase by up to 22% and 18% for damaged pulpwood and sawtimber, respectively, if the selling prices (π_{iqt}) offered by the landowners dropped by 40% from the base prices during months between September to November.

- We further observe interesting transportation decisions when the mills offered different prices (ψ_{jqt}) for the damaged pulpwood and sawtimber (see Figure 2.6(b) and (d)). For instance, when ψ_{jqt} is dropped by 40% from the base prices, the average transportation dropped significantly by approximately 91% and 143% for the damaged pulpwood and sawtimber cases, respectively. On the other hand, when ψ_{jqt} is increased by 40% from the base prices, the average transportation is increased by approximately 8% and 10% for the damaged pulpwood for sawtimber cases, respectively. The results clearly indicate the sensitivity of the purchasing prices ψ_{jqt} offered by the mills on the overall transportation decisions.

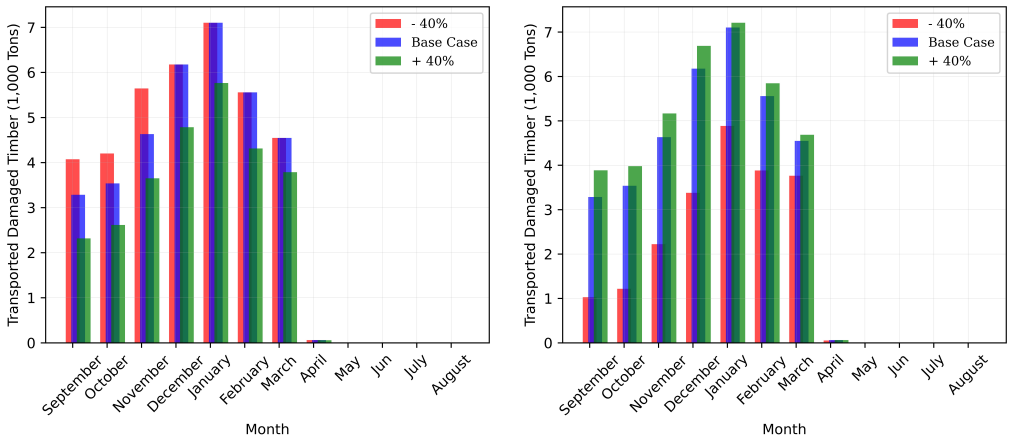

(a) Selling price (π_{iqt}): pulpwood

(b) Purchasing price (ψ_{jqt}): pulpwood

(c) Selling price (π_{iqt}): sawtimber

(d) Purchasing price (ψ_{jqt}): sawtimber

Figure 2.6

Impact of selling/purchasing prices on the transportation decisions of damaged pulpwood and sawtimber

2.4.3 Performance Evaluation of the Algorithms

This subsection demonstrates our computational experiences in solving model **(P4)** using the customized solution techniques discussed in Section 2.3. We vary sets $|\mathcal{I}|$ and $|\mathcal{T}|$ to generate 16 test instances (see Table 2.4). Note that in all the instances, the number of the mills $|\mathcal{J}|$ and quality of the damaged timbers $|Q|$ are set to 15 and 3, respectively. We use the following conditions to terminate the customized solution techniques: (i) the optimality gap (i.e., $\epsilon = |UB - LB|/UB$) falls below a threshold value (e.g., $\epsilon = 1.0\%$); or (ii) the maximum time limit (t^{max}) is reached (e.g., $t^{max} = 7,200$ CPU seconds); or the maximum iteration limit (r^{max}) is reached (e.g., $r^{max} = 1,000$). To help the readers follow our solution approaches, the following notations are used.

- `BD+VP`: Benders decomposition algorithm enhanced by the valid inequalities and preprocessing techniques discussed in Section 2.3.3.3.
- `BD+VP+PO`: Benders decomposition algorithm enhanced by the valid inequalities and preprocessing techniques discussed in Section 2.3.3.3 and the pareto-optimality cuts discussed in Section 2.3.3.1.
- `BD+VP+PO+WS`: Benders decomposition algorithm enhanced by the valid inequalities and preprocessing techniques discussed in Section 2.3.3.3, the pareto optimality cut discussed in Section 2.3.3.3, and the warm start strategy discussed in Section 2.3.3.2.
- `BCBD1+VP`: Benders-based Branch-and-cut algorithm enhanced by the valid inequalities and preprocessing techniques discussed in Section 2.3.3.3. This implementation utilizes incumbent solutions (integer) to generate the optimality cuts.

- `BCBD2+VP`: Benders-based Branch-and-cut algorithm enhanced by the valid inequalities and preprocessing techniques discussed in Section 2.3.3.3. This implementation utilizes any candidate solutions to generate the optimality cuts.
- `BCBD2+VP+WS`: Benders-based Branch-and-cut algorithm, utilizing any candidate solutions to generate the optimality cuts, enhanced by the valid inequalities and preprocessing techniques discussed in Section 2.3.3.3, and the warm start strategy discussed in Section 2.3.3.2.

Table 2.4

Test instances for model **(P4)**

Instances	$\|\mathcal{I}\|$	$\|\mathcal{T}\|$	Variables			Constraints
			Continous	Binary	Total	
S1	50	3	13,950	7,200	21,150	20,655
S2	50	6	27,900	14,400	42,300	41,310
S3	50	9	41,850	21,600	63,450	61,965
S4	50	12	55,800	28,800	84,600	82,620
S5	100	3	27,900	14,400	42,300	40,845
S6	100	6	55,800	28,800	84,600	81,690
S7	100	9	83,700	43,200	126,900	122,535
S8	100	12	111,600	57,600	169,200	163,380
S9	150	3	41,850	21,600	63,450	61,755
S10	150	6	83,700	43,200	126,900	123,510
S11	150	9	125,550	64,800	190,350	185,265
S12	150	12	167,400	86,400	253,800	247,020
S13	200	3	55,800	28,800	84,600	82,605
S14	200	6	111,600	57,600	169,200	169,200
S15	200	9	167,400	86,400	253,800	247,815
S16	200	12	223,200	115,200	338,400	330,420

Tables 2.5, 2.6, and 2.7 denote the performance of different variants of the Benders decomposition and Benders-based Branch-and-Cut algorithm. In these tables, the columns entitled with $\epsilon(\%)$ and $t(sec)$ indicate the optimality gap and solution time of the respective algorithms and

GUROBI. Besides, in all the aforementioned tables, we first highlight the algorithm that can solve the instances with the desired optimality gap in the shortest running time. However, if none of the algorithms could provide such desired quality solutions discussed in the mentioned termination criteria, we highlight the algorithm with the smallest optimality gap.

The first set of the experiments, reported in Table 2.5, compare the computational performance between different variants of the enhanced Benders decomposition algorithm with GUROBI. The experimental results indicate that GUROBI is capable of solving 9/16 problem instances by obeying the pre-specified termination criterion. Note that for instances 15 and 16 (i.e., S15 and S16), GUROBI could not find any integer feasible solution within the time limit. The average optimality gap of GUROBI is found to be 20.8%. Next, we use BD+VP algorithm to solve model **(P4)**. Clearly, algorithm BD+VP performs superior over GUROBI by dropping down the average optimality gap to 7.9% while maintaining a competitive running time. However, algorithm BD+VP still could not solve 6/16 problem instances by obeying the pre-specified termination criterion. Finally, we observe that the incorporation of the pareto-optimality cut inside the BD+VP algorithm, namely, the BD+VP+PO algorithm, further drops down the average optimality gap to 2.6% from 7.9% as provided by the BD+VP algorithm. However, it is important to note that the BD+VP+PO algorithm still could not provide a competitive optimality gap in solving a few larger instances of model **(P4)** (see instances S12, S14–S16).

The next set of experiments, reported in Table 2.6, compares the performance of different variants of the Benders-based Branch-and-Cut algorithm over the GUROBI solver. Clearly, both the two variants of the Benders-based branch-and-cut algorithm, namely, the BCBD1+VP and BCBD2+VP techniques, outperform GUROBI regarding both the running time and the solution quality. It can

Table 2.5

Computational performance of the classic Benders decomposition algorithm with enhancements

	GUROBI		BD+VP		BD+VP+PO	
Instance	$t(sec)$	$\epsilon(\%)$	$t(sec)$	$\epsilon(\%)$	$t(sec)$	$\epsilon(\%)$
S1	223.2	0.8	275.5	0.9	**204.1**	0.1
S2	453.6	0.3	493.1	0.2	**410.9**	0.3
S3	2,213.0	0.6	1,639.2	0.1	**1,463.6**	0.1
S4	4,767.9	0.8	3,017.6	0.5	**2,218.9**	0.9
S5	631.2	0.4	671.5	0.7	**395.8**	0.5
S6	2,372	0.2	2,496.9	0.2	**1,664.6**	0.8
S7	7,170.4	0.9	5,230.5	0.5	**3,874.4**	0.5
S8	7,200.0	5.3	6,796.9	0.9	**4,720.1**	0.5
S9	1,213.7	0.4	1,225.9	0.9	**1,021.6**	0.5
S10	7,200.0	8.1	7,200.0	3.1	**6,616.5**	0.2
S11	7,200.0	23.5	7,200.0	8.7	7,200.0	**1.9**
S12	7,200.0	54.7	7,200.0	17.4	7,200.0	**3.7**
S13	2,272.2	0.5	2,318.5	0.2	**2,070.1**	0.4
S14	7,200.0	35.6	7,200.0	11.5	7,200.0	**4.8**
S15	7,200.0	–[a]	7,200.0	29.9	7,200.0	**11.9**
S16	7,200.0	–	7,200.0	49.6	7,200.0	**14.7**
Average	4,482.3	20.8	4,210.4	7.9	**3,791.2**	2.6

[a] no integer feasible solution is obtained

be observed that algorithm BCBD1+VP drops down the average optimaility gap of GUROBI to 1.7% from 20.8%, which further drops down to 1.3% in algorithm BCBD2+VP. Similarly, we observe a decrease in the average running time of both the BCBD1+VP and BCBD2+VP algorithms over GUROBI. It shall be noted that even though both the two variants of the Benders-based branch-and-cut techniques demonstrates superior computational performance over GUROBI, the techniques still find it difficult to solve a few larger instances of model **(P4)** (see instances S12 and S14–S16 in Table 2.6).

The final set of experiments, reported in Table 2.7, investigates the impact of the warm start strategy, discussed in Section 2.3.3.2, in solving the model **(P4)**. Results in Tables 2.5 and 2.6 demonstrate that the algorithms BD+VP+PO and BCBD2+VP dominate their counterpart algorithms in their respective tables with respect to both running times and optimality gaps. With this, we then carry forward with the BD+VP+PO and BCBD2+VP algorithms and examine how the warm start strategy impacts the computational performance of the algorithms. Experimental results indicate that the BCBD2+VP+WS algorithm outperforms BD+VP+PO+WS algorithm with respect to both the running time and optimality gap. On average, the optimality gap reduces to 0.6% in the BCBD2+VP+WS algorithm from 1.6% as produced by the BD+VP+PO+WS algorithm. Further, such reduction in the optimality gap is achieved in a 7.6% reduction in the solution time. Most importantly, the BCBD2+VP+WS algorithm is now able to solve all the problem instances to less than 1% optimality gap. Clearly, the warm start strategy improves the convergence of both the Benders and the Benders-based branch-and-cut algorithms. Overall, the BCBD2+VP+WS algorithm provides competitive computational performance over other investigated algorithms in solving model **(P4)** within our experimental ranges.

Table 2.6

Computational performance of the classic Branch-and-Cut Benders decomposition method with enhancements

	GUROBI		BCBD1+VP		BCBD2+VP	
Instance	$t(sec)$	$\epsilon(\%)$	$t(sec)$	$\epsilon(\%)$	$t(sec)$	$\epsilon(\%)$
S1	223.2	0.8	239.3	0.4	**210.3**	0.9
S2	453.6	0.3	415.2	0.2	**347.6**	0.1
S3	2,213.0	0.6	1,442.9	0.4	**1,187.6**	0.2
S4	4,767.9	0.8	**1,901.4**	0.5	1,934.8	0.6
S5	631.2	0.4	413.7	0.5	**396.4**	0.8
S6	2,372.0	0.2	1,683.5	0.1	**1,562.3**	0.1
S7	7,170.4	0.9	4,610.2	0.8	**4,126.8**	0.9
S8	7,200.0	5.3	5,139.6	0.5	**5,046.2**	0.5
S9	1,213.7	0.4	1,149.7	0.2	**1,071.8**	0.8
S10	7,200.0	8.1	5,137.2	0.7	**4,627.7**	0.2
S11	7,200.0	23.5	7,107.7	0.2	**6,825.1**	0.6
S12	7,200.0	54.7	7,200.0	2.8	7,200.0	**1.6**
S13	2,272.9	0.5	2,192.6	0.4	**2,014.3**	0.9
S14	7,200.0	35.6	7,200.0	2.4	7,200.0	**2.1**
S15	7,200.0	–[a]	7,200.0	7.4	7,200.0	**4.1**
S16	7,200.0	-	7,200.0	9.3	7,200.0	**5.8**
Average	4,482.3	20.8	3,764.6	1.7	**3,634.4**	1.3

[a] no integer feasible solution is obtained

Table 2.7

Computational performance of BD+VP+PO and BCBD2+VP with the warm start strategy

	BD+VP+PO+WS		BCBD2+VP+WS	
Instance	$t(sec)$	$\epsilon(\%)$	$t(sec)$	$\epsilon(\%)$
S1	185.5	0.2	**193.0**	0.9
S2	342.4	0.6	**321.9**	0.3
S3	1,219.7	0.6	**1,109.9**	0.6
S4	1,849.1	0.7	**1,775.1**	0.6
S5	359.1	0.6	**344.7**	0.6
S6	1,513.3	0.4	**1,346.8**	0.4
S7	3,913.6	0.4	**3,717.9**	0.7
S8	4,767.8	0.1	**4,672.4**	0.3
S9	**945.9**	0.3	974.3	0.4
S10	5,513.8	0.9	**4,245.6**	0.5
S11	6,534.9	0.2	**5,698.3**	0.5
S12	**7,135.7**	0.9	7,161.3	0.9
S13	1,916.8	0.3	**1,782.6**	0.7
S14	7,200.0	2.4	**6,413.9**	0.1
S15	7,200.0	6.9	**6,814.9**	0.6
S16	7,200.0	9.4	**7,164.8**	0.9
Average	3,612.4	1.6	**3,358.5**	0.6

2.5 Conclusions and Future Research Directions

This paper provides a framework to efficiently manage the post-hurricane damaged timbers by considering the interaction between landowners and mills. To do so, we developed a bi-level mixed-integer programming model that characterizes and optimizes the landowner-related decisions (e.g., selling and storing timber) in the first level and the mills-related decisions (purchasing timber and transportation decisions) in the second level. We then define some problem-specific mathematical sets that enable us to combine the two-level formulation into a single-level formulation. We further developed two tailored, exact solution methods, namely, enhanced Benders decomposition, and enhanced Benders-based branch-and-cut, to optimally solve the real-world instances of the proposed model. The extensive computation experiments denote that the enhanced Bender-based branch-and-cut algorithm consistently provides quality solutions in less computational time over other solution approaches. Moreover, using 15 coastal counties in the southeast of Mississippi state as a testing ground under different hurricane scenarios, we design a real-life case study and conduct sensitivity analysis to test the algorithm's performance. These experiments provide important managerial insights for the landowners and mills. Results indicate that the damaged timber recovery decisions are highly sensitive to the selling and purchasing prices offered by the landowners and mills, respectively. Besides, it can be implied that the damaged timber recovery decisions are susceptible to the deterioration rate of the damaged timber, and the quality of the damaged timbers resulted from different hurricane categories.

This research can be extended in several research directions. This study assumes that the transportation network would remain functional to deliver damaged timbers from the landowner sites to mills following a natural catastrophe. However, depending upon the severity level of the

hurricanes, the transportation networks could also be impacted and may not remain functional. Next, due to many complex factors such as storm severity, prior rainfall, hurricanes within the same category could result in different damage levels in the forest cover and consequently in the related market. Hence, it would be interesting to model such uncertain behavior in the post-hurricane market under capable tools such as stochastic programming and inspect its impact on the system performance. These issues will be addressed in future studies.

REFERENCES

[1] Aboytes-Ojeda M., Castillo-Villar K.K., Eksioglu S.D., "Modeling and optimization of biomass quality variability for decision support systems in biomass supply chains," *Annals of Operations Research*, vol. in-press, 2019.

[2] Adams P.W.R., Shirley J.E.J., McManus M.C., "Comparative cradle-to-gate life cycle assessment of wood pellet production with torrefaction," *Applied Energy*, vol. 138, 2015, pp. 367–380.

[3] Y. Adulyasak, J.-F. Cordeau, and R. Jans, "Benders decomposition for production routing under demand uncertainty," *Operations Research*, vol. 63, no. 4, 2015, pp. 851–867.

[4] Adulyasak Y., Cordeau J.-F., Jans R., "Benders decomposition for production routing under demand uncertainty," *Operations Research*, vol. 63, 2015, pp. 851–867.

[5] Agar D.A., "The economic potential of wood pellet production from alternative, low-value wood sources in the southeast of the U.S.," *Biomass and Bioenergy*, vol. 71, 2014, pp. 443–454.

[6] Agar D.A., "A comparative economic analysis of torrefied pellet production based on state-of-the-art pellets.," *Biomass and Bioenergy*, vol. 97, 2017, pp. 155–161.

[7] Aghalari A., Aladwan B.S., Silva B., Tanger S., Marufuzzaman M., Gude V.G., "Pellet Production Optimization using a Parallelized Progressive Hedging Algorithm," *arXiv preprint arXiv:2104.13443*, 2021.

[8] Aghalari A., Nur F., Marufuzzaman M., "A Bender's based nested decomposition algorithm to solve a stochastic inland waterway port management problem considering perishable product," *International Journal of Production Economics*, vol. 229, 2020, p. 107863.

[9] Aghalari A., Nur F., Marufuzzaman M., "Solving a Stochastic Inland Waterway Port Management Problem using a Parallelized Hybrid Decomposition Algorithm," *Omega*, 2020, p. 102316.

[10] Aghalari A. Nur F., Marufuzzaman M., Puryear S.M., "Designing a Reliable Inland Waterway Transportation Network under Uncertainty," *arXiv preprint arXiv:2101.10120*, 2021.

[11] Alizadeh M., Ma J., Marufuzzaman M., Yu F. , "Sustainable olefin supply chain network design under seasonal feedstock supplies and uncertain carbon tax rate," *Journal of Cleaner Production*, vol. 222, 2019, pp. 280–299.

[12] Balinski M.L., "Fixed cost transportation problems," *Naval Research Logistics Quarterly*, vol. 8, 1961, pp. 41–54.

[13] Blake E.S., Landsea C.W., Gibney E.J., *The deadliest, costliest, and most intense United States tropical cyclones from 1851 to 2006 (and other frequently requested hurricane facts).*, Tech. Rep., NOAA Technical Memorandum NWS TPC-5. Available from: `http://www.nhc.noaa.gov/pdf/nws-nhc-6.pdf`, 2011.

[14] J. BnnoBRs, "Partitioning procedures for solving mixed-variables programming problems ‘," 1962.

[15] T. Bogle and G. C. van Kooten, "Protecting timber supply on public land in response to catastrophic natural disturbance: A Principal-Agent Problem," *Forest Science*, vol. 61, no. 1, 2015, pp. 83–92.

[16] Boukherroub T., LeBel L., Lemieux S., "An integrated wood pellet supply chain development: Selecting among feedstock sources and a range of operating scales," *Applied Energy*, vol. 198, 2017, pp. 385–400.

[17] D. T. Butry, E. Mercer, J. P. Prestemon, J. M. Pye, and T. P. Holmes, "What is the price of catastrophic wildfire?," *Journal of Forestry*, vol. 99, no. 11, 2001, pp. 9–17.

[18] K. K. Castillo-Villar, S. Eksioglu, and M. Taherkhorsandi, "Integrating biomass quality variability in stochastic supply chain modeling and optimization for large-scale biofuel production," *Journal of cleaner production*, vol. 149, 2017, pp. 904–918.

[19] S. Change, "The hurricane impact on southern pine sawtimber stumpage prices in Louisiana," *Louisiana Agriculture*, 2006, pp. 26–27.

[20] Chen C.-W., Fan Y., "Bioethanol supply chain system planning under supply and demand uncertainities.," *Transportation Research Part E*, vol. 48, 2012, pp. 150–164.

[21] Chen C.W., Fan Y., "Bioethanol supply chain system planning under supply and demand uncertainties," *Transportation Research Part E*, vol. 48, no. 1, 2012, pp. 150–164.

[22] A. J. Conejo, F. J. Nogales, and F. J. Prieto, "A decomposition procedure based on approximate Newton directions," *Mathematical programming*, vol. 93, no. 3, 2002, pp. 495–515.

[23] J.-F. Cordeau, G. Stojković, F. Soumis, and J. Desrosiers, "Benders decomposition for simultaneous aircraft routing and crew scheduling," *Transportation science*, vol. 35, no. 4, 2001, pp. 375–388.

[24] Crainic T.G., Fu X., Gendreau M., Rei W., Wallace S.W., "Progressive hedging-based metaheuristics for stochastic network design," *Networks*, vol. 58, 2011, pp. 114–124.

[25] Dahal R.P., Munn I.A., Henderson J.E., *Forestry in Mississippi: The impact of the industry on the Mississippi economy–an input-output analysis.*, Tech. Rep., Forest and Wildlife Research Center, Research Bulletin FO 438, Mississippi State University. 22 pp., 2013.

[26] R. S. De Camargo, G. de Miranda Jr, and R. P. Ferreira, "A hybrid outer-approximation/benders decomposition algorithm for the single allocation hub location problem under congestion," *Operations Research Letters*, vol. 39, no. 5, 2011, pp. 329–337.

[27] S. D. Ekşioğlu, A. Acharya, L. E. Leightley, and S. Arora, "Analyzing the design and management of biomass-to-biorefinery supply chain," *Computers & Industrial Engineering*, vol. 57, no. 4, 2009, pp. 1342–1352.

[28] Eksioglu S.D., Acharya A., Leightley L.E., Arora S., "Analyzind the design and management of biomass-to-biorefinery supply chain.," *Computers and Industrial Engineering*, vol. 57, 2009, pp. 1342–1352.

[29] Gebreslassie B.H., Yao Y., You F., "Design under uncertainty of hydrocarbon biorefinery supply chains: Multiobjective stochastic programming models, decomposition algorithm, and a comparison between CVaR and downside risk.," *AIChE Journal*, vol. 58, no. 7, 2012, pp. 2155–2179.

[30] Gillette B., *Post-Katrina timber? $1.1 billion in costs, lost dreams.*, Tech. Rep., Mississippi Business Journal. Available from: `http://msbusiness.com/2006/04/postkatrina-timber-11-billion-in-costs-lost-dreams/`, 2006.

[31] P. A. Glass and S. N. Oswalt, "Initial estimates of hurricane Katrina impacts of Mississippi gulf coast forest resources," *Mississippi Institute For Forest Inventory: 1-4*, 2007.

[32] Glass P.A. and Oswalt S.N., Tech. Rep., Mississippi Institute for Forest Inventory. Technical report, Available from: `http://www.mifi.ms.gov/documents/Katrin_Impacts_Gulf_Coast.pdf`, 2007.

[33] Gong J., Garcia D.J., You F., "Unraveling optimal biomass processing routes from bioconversion product and process networks under uncertainty: an adaptive robust optimization approach.," *ACS Sustainable Chemistry and Engineering*, vol. 4, no. 6, 2016, pp. 3160–3173.

[34] Gul S., Denton B.T., Fowler J., "A Multi-Stage Stochastic Integer Programming Model for Surgery Planning," *Michigan Engineering*, 2012.

[35] Hansen P., Kochetov Y., Mladenovi N., *Lower bounds for the uncapacitated facility location problem with user preferences*, Tech. Rep., Groupe d'etudes et de recherche en analyse des decisions, HEC Montreal, 2004.

[36] Hester M., *Hurricane Isaac just another hurdle to overcome.*, Tech. Rep., The Oregonian. Available from: http://www.oregonlive.com/opinion/index.ssf/2012/08/hurricane_isaac_just_another_h.html, 2012.

[37] S. Huang and V. Dinavahi, "A branch-and-cut benders decomposition algorithm for transmission expansion planning," *IEEE Systems Journal*, vol. 13, no. 1, 2017, pp. 659–669.

[38] Huang Y., Chen C.W., Fan Y., "Multistage optimization of the supply chains of bio-fuels.," *Transportation Research Part E*, vol. 46, no. 6, 2010, pp. 820–830.

[39] Huang Y., Fan Y., Chen C.W, "An integrated bio-fuel supply chain against feedstock seasonality and uncertainty.," *Transportation Science*, vol. 48, no. 4, 2014, pp. 540–554.

[40] Hvattum L.M., Lokketangen A., "Using scenario trees and progressive hedging for stochastic inventory routing problems," *Journal of Heuristics*, vol. 15, 2009, pp. 527–557.

[41] J. J. Jacobson, M. S. Roni, P. Lamers, and K. G. Cafferty, *Biomass feedstock and conversion supply system design and analysis*, Tech. Rep., Idaho National Lab.(INL), Idaho Falls, ID (United States), 2014.

[42] Kim D., Pardalos P.M., "A solution approach to the fixed charge network flow problem using a dynamic slope scaling procedure," *Operations Research Letters*, vol. 24, no. 4, 1999, pp. 195–203.

[43] H. W. Kinnucan, "Timber price dynamics after a natural disaster: Hurricane Hugo revisited," *Journal of Forest Economics*, vol. 25, 2016, pp. 115–129.

[44] Lamers, Patrick and Roni, Mohammad S and Tumuluru, Jaya S and Jacobson, Jacob J and Cafferty, Kara G and Hansen, Jason K and Kenney, Kevin and Teymouri, Farzaneh and Bals, Bryan, "Techno-economic analysis of decentralized biomass processing depots," *Bioresource technology*, vol. 194, 2015, pp. 205–213.

[45] Magelli F., Boucher K., Bi H.T., Melin S., Bonoli A., "An environmental impact assessment of exported wood pellets from Canada to Europe," *Biomass and Bioenergy*, vol. 33, 2009, pp. 434–441.

[46] T. L. Magnanti and R. T. Wong, "Accelerating Benders decomposition: Algorithmic enhancement and model selection criteria," *Operations research*, vol. 29, no. 3, 1981, pp. 464–484.

[47] H. Mahmudi and P. C. Flynn, "Rail vs truck transport of biomass," *Twenty-Seventh Symposium on Biotechnology for Fuels and Chemicals*. Springer, 2006, pp. 88–103.

[48] S. Mani, S. Sokhansanj, X. Bi, and A. Turhollow, "Economics of producing fuel pellets from biomass," *Applied Engineering in agriculture*, vol. 22, no. 3, 2006, pp. 421–426.

[49] Marufuzamman M., Aghalari A., Buchanan R.K., Rinaudo C.H., Houte K.M., and Ranta J.H., "Optimal Placement of Detectors to Minimize Casualties in an Intentional Attack," *IEEE Transactions on Engineering Management*, 2020.

[50] Marufuzzaman M., Eksioglu S.D., "Designing a reliable and dynamic multimodal transportation network for biofuel supply chains," *Transportation Science*, vol. 51, no. 2, 2017, pp. 494–517.

[51] Marufuzzaman M., Eksioglu S.D., Hernandez R. , "Environmentally friendly supply chain planning and design for biodiesel production via wastewater sludge," *Transportation Science*, vol. 48, no. 4, 2014, pp. 555–574.

[52] Marufuzzaman M., Eksioglu S.D., Huang Y., "Two-stage stochastic programming supply chain model for biodiesel production via wastewater treatment," *Computers and Operations Research*, vol. 49, 2014, pp. 1–17.

[53] Marufuzzaman M., Eksioglu S.D., Li X., Wang J, "Analyzing the impact of intermodal-related risk to the design and management of biofuel supply chain," *Transportation Research Part E*, vol. 69, 2014, pp. 122–145.

[54] D. McDaniel and M. Devine, "A modified Benders' partitioning algorithm for mixed integer programming," *Management Science*, vol. 24, no. 3, 1977, pp. 312–319.

[55] C. W. McMillin, "Ash content of loblolly pine wood as related to specific gravity, growth rate, and distance from pith," *Wood Science, Vol. 2 (1): 26-30*, 1968.

[56] Mississippi Forest Inventory (MFI) program, *Southeast Mississippi Forest Inventory 2013-2014*, Tech. Rep., Available from: `https://fires.mfc.ms.gov/sites/default/files/MIFI_SE_final.pdf`, 2014.

[57] Mississippi Institute for Forest Inventory (MIFI), *Study: Katrina caused major harm to South Mississippi forests.*, Tech. Rep., Available from: `http://www.mifi.ms.gov/story.asp?id=2`, 2007.

[58] Mobini M., Meyer J.C., Trippe F., Sowlati T., Frohling M., Schultmann F., "Assessing the integration of torrefaction into wood pellet production," *Journal of Cleaner Production*, vol. 78, 2014, pp. 216–225.

[59] Mobini M., Sowlati T., Sokhansanj S., "A simulation model for the design and analysis of wood pellet supply chains," *Applied Energy*, vol. 111, 2013, pp. 1239–1249.

[60] Mulvey J.M., Vladimirou H., "Applying the progressive hedging algorithm to stochastic generalized networks," *Annals of Operations Research*, vol. 31, 1991, pp. 399–424.

[61] Munn I.A., Tilley B.K., *Forestry in Mississippi – The impact of forest products industry on the Mississippi Economy: An input-output analysis.*, Tech. Rep., Forest and Wildlife Research Center, Bulletin FO 301, Mississippi State University. 27 pp., 2005.

[62] Murray G., "Status update: Canadian wood pellet industry.," Wood Pellet Association of Canada. Available from: http://www.pellet.org/, 2014.

[63] J. Naoum-Sawaya and S. Elhedhli, "An interior-point Benders based branch-and-cut algorithm for mixed integer programs," *Annals of Operations Research*, vol. 210, no. 1, 2013, pp. 33–55.

[64] National Oceanic and Atmospheric Administration, *Continental United States Hurricane Impacts/Landfalls 1851-2019*, Tech. Rep., Available from: https://www.aoml.noaa.gov/hrd/hurdat/All_U.S._Hurricanes.html, 2020.

[65] Ng R.T.L., Maravelias C.T., "Design of biofuel supply chains with variable regional depot and biorefinery locations," *Renewable Energy*, vol. 100, 2017, pp. 90–102.

[66] M. Nieuwenhuis and E. O'connor, "Financial impact evaluation of catastrophic storm damage in Irish forestry: a case study. I. Stumpage losses," *Forestry*, vol. 74, no. 4, 2001, pp. 369–381.

[67] Nur F., Aboytes M., Castillo-Villar K.K., Marufuzzaman M., "A two-stage stochastic programming model for biofuel supply chain network design with biomass quality implications," *IISE Transactions*, vol. in-press, 2020.

[68] S. N. Oswalt, C. Oswalt, and J. Turner, "Hurricane Katrina impacts on Mississippi forests," *Southern Journal of Applied Forestry*, vol. 32, no. 3, 2008, pp. 139–141.

[69] N. Papadakos, "Practical enhancements to the Magnanti–Wong method," *Operations Research Letters*, vol. 36, no. 4, 2008, pp. 444–449.

[70] G. Paradis, M. Bouchard, L. LeBel, and S. D'Amours, "A bi-level model formulation for the distributed wood supply planning problem," *Canadian Journal of Forest Research*, vol. 48, no. 2, 2018, pp. 160–171.

[71] N. Parker, P. Tittmann, Q. Hart, M. Lay, J. Cunningham, B. Jenkins, R. Nelson, K. Skog, A. Milbrandt, E. Gray, et al., "Strategic Assessment of Bioenergy Development in the West Spatial Analysis and Supply Curve Development Final Report," *Parker, Nathan; Tittman, Peter; Hart, Quinn, et al. 2008. Strategic assessment of Bioenergy in the West: spatial analysis and supply curve development. Final report. Davis, CA: University of California, Davis*, 2008.

[72] S. Poudel, M. Marufuzzaman, M. A. Quddus, S. Chowdhury, L. Bian, and B. Smith, "Designing a reliable and congested multi-modal facility location problem for biofuel supply chain network," *Energies*, vol. 11, no. 7, 2018, p. 1682.

[73] Poudel S., Marufuzzaman M., Bian L., "A hybrid decomposition algorithm for designing a multi-modal transportation network under biomass supply uncertainty," *Transportation Research Part E*, vol. 94, 2016, pp. 1–25.

[74] Poudel S., Quddus M.A., Marufuzzaman M., Bian L., Burch R., "Managing congestion in a multi-modal transportation network under biomass supply uncertainty," *Annals of Operations Research*, vol. 273, 2019, pp. 739–781.

[75] Poudel S.R., Marufuzzaman M., Bian L, "Designing a reliable bio-fuel supply chain network considering link failure probabilities," *Computers and Industrial Engineering*, vol. 91, 2016, pp. 85–99.

[76] Pradhan U., *Physical treatments for reducing biomass ash and effect of ash content on pyrolysis products.*, Masters dissertation, Auburn University, 2015.

[77] J. P. Prestemon and T. P. Holmes, "Timber price dynamics following a natural catastrophe," *American Journal of Agricultural Economics*, vol. 82, no. 1, 2000, pp. 145–160.

[78] Prestemon J.P., Holmes T.P., *Economic impacts of hurricanes on forest owners.*, Tech. Rep., General Technical Report. PNW-GTR-802. Portland, OR: U.S. Department of Agriculture, Forest Service, Pacific Northwest and Southern Research Stations: 207-221., 2010.

[79] M. A. Quddus, M. Kabli, and M. Marufuzzaman, "Modeling electric vehicle charging station expansion with an integration of renewable energy and Vehicle-to-Grid sources," *Transportation Research Part E: Logistics and Transportation Review*, vol. 128, 2019, pp. 251–279.

[80] M. A. Quddus, O. Shahvari, M. Marufuzzaman, J. M. Usher, and R. Jaradat, "A collaborative energy sharing optimization model among electric vehicle charging stations, commercial buildings, and power grid," *Applied Energy*, vol. 229, 2018, pp. 841–857.

[81] Quddus M.A., Chowdhury S., Marufuzzaman M., Yu F., Bian L., "A two-stage chance-constrained stochastic programming model for a bio-fuel supply chain network," *International Journal of Production Economics*, vol. 195, 2018, pp. 27–44.

[82] Quddus M.A., Hossain N.U.I., Marufuzzaman M., Jaradat R., Roni M.S., "Sustainable network design for multi-purpose pellet processing depots under biomass supply uncertainty," *Computers and Industrial Engineering*, vol. 110, 2017, pp. 462–483.

[83] J. Reina, E. Velo, and L. Puigjaner, "Kinetic study of the pyrolysis of waste wood," *Industrial & engineering chemistry research*, vol. 37, no. 11, 1998, pp. 4290–4295.

[84] Rockafellar R.T., Wets R.J.-B., "Scenarios and policy aggregation in optimization under uncertainty," *Mathematics of operations research*, vol. 16, 1991, pp. 119–147.

[85] M. A. Sanderson, R. P. Egg, and A. E. Wiselogel, "Biomass losses during harvest and storage of switchgrass," *Biomass and Bioenergy*, vol. 12, no. 2, 1997, pp. 107–114.

[86] Santoso T., Ahmed S., Goetschalckx M., Shapiro A., "A stochastic programming approach for supply chain network design under uncertainty.," *European Journal of Operational Research*, vol. 167, 2005, pp. 96–115.

[87] E. Searcy, P. Flynn, E. Ghafoori, and A. Kumar, "The relative cost of biomass energy transport," *Applied biochemistry and biotechnology*, vol. 137, no. 1-12, 2007, pp. 639–652.

[88] Sherali H.D., Alameddine A., "A new reformulation-linearization technique for bilinear programming problems," *Journal of Global Optimization*, vol. 2, no. 4, 1992, pp. 379–410.

[89] Sikkema R., Steiner M., Junginger M., Hiegl W., Hansen M.T., Faaij A., "The European wood pellet markets: current status and prospects for 2020.," *Biofuels Bioproducts and Biorefining*, vol. 5, 2011, pp. 250–278.

[90] A. T. Sikora and J. Ukalska, "Timber prices after natural disasters in the Forest District of Węgierska Górka," *Forest Research Papers*, vol. 75, no. 2, 2014, pp. 201–212.

[91] Sjoding D., Kanoa E., Jensen P., "Developing a wood pellet/densified biomass industry in Washington State: Opportunities and challenges.," Available from: `http://www.energy.wsu.edu/Documents/Densified%20Biomass%20Report.pdf`, 2013.

[92] D. Slocum, E. McGinnes Jr, D. McKown, et al., "Elemental analysis of oak and hickory charcoal using neutron activation analysis," *Wood and Fiber Science*, vol. 10, no. 3, 2007, pp. 200–209.

[93] J. A. Stanturf, S. L. Goodrick, and K. W. Outcalt, "Disturbance and coastal forests: a strategic approach to forest management in hurricane impact zones," *Forest Ecology and Management*, vol. 250, no. 1-2, 2007, pp. 119–135.

[94] Stelte W., Sanadi A.R., Shang L., Holm J.K., Ahrenfeldt J., Henriksen U.B. , "Recent developments in biomass pelletization – a review.," *Bioresources*, vol. 7, no. 3, 2012, pp. 4451–4490.

[95] Sultana A., Kumar A., Harfield D., "Development of agri-pellet production cost and optimum size.," *Bioresource Technology*, vol. 101, 2010, pp. 5609–5621.

[96] C. Sun, "Timber market recovery after a hurricane," *Forest Science*, vol. 62, no. 6, 2016, pp. 600–612.

[97] J. H. Syme, *Impacts of Hugo timber damage on primary wood manufacturers in South Carolina*, vol. 80, US Department of Agriculture, Forest Service, Southeastern Forest Experiment . . . , 1992.

[98] H. T. Taylor, B. Ward, M. Willis, and W. Zaleski, "The Saffir-Simpson hurricane wind scale," *Atmospheric Administration: Washington, DC, USA*, 2010.

[99] The National Renewable Energy Laboratory, "The Biofuels Atlas.," Available from: `https://maps.nrel.gov/biomass`, 2020.

[100] Tong K., Gong J., Yue D., You F., "Stochastic programming approach to optimal design and operations of integrated hydrocarbon biofuel and petroleum supply chains.," *ACS Sustainable Chemistry and Engineering*, vol. 2, no. 1, 2014, pp. 49–61.

[101] United States Department of Agriculture Forest Service, *Potential timber damage due to Hurricane Katrina in Mississippi, Alabama and Louisiana.*, Tech. Rep., Available from: `http://www.srs.fs.usda.gov/katrina/katrina_brief_2005-09-22.pdf`, 2005.

[102] United States Department of Agriculture Forest Service, *Mississippi Agriculture at a Glance.*, Tech. Rep., Available from: `http://www.mdac.state.ms.us/`, 2006.

[103] U.S. Energy Information Administration, "Densified Biomass Fuel Report.," Available from: `https://www.eia.gov/biofuels/biomass`, 2020.

[104] Uster H., Memisoglu, G., "Biomass logistics network design under price-based supply and yield uncertainty.," *Transportation Science*, vol. 52, no. 2, 2018, pp. 474–492.

[105] Visser L., Hoefnagels R., Junginger M., "Wood pellet supply chain costs – A review and cost optimization analysis," *Renewable and Sustainable Energy Reviews*, vol. 118, 2020, p. 109506.

[106] Watson J.P., Woodruff D.L., "Progressive hedging innovations for a class of stochastic mixed-integer resource allocation problems," *Computational Management Science*, vol. 8, 2011, pp. 355–370.

[107] F. Xie, Y. Huang, and S. Eksioglu, "Integrating multimodal transport into cellulosic biofuel supply chain design under feedstock seasonality with a case study based on California," *Bioresource technology*, vol. 152, 2014, pp. 15–23.

[108] Xie F., Huang Y., Eksioglu, S.D., "Integrating multimodal transport into cellulosic bio-fuel supply chain design under feedstock seasonality with a case study based on California.," *Bioresource Technology*, vol. 152, 2014, pp. 15–23.

[109] R. Yin and D. H. Newman, "An intervention analysis of Hurricane Hugo's effect on South Carolina's stumpage prices," *Canadian journal of forest research*, vol. 29, no. 6, 1999, pp. 779–787.

APPENDIX A

SAA METHODOLOGY

A.1 Sample Average Approximation

The steps involved in implementing the SAA algorithm in solving **(BQP)** are outlined below.

1. First, we generate E random samples of size N and solve the corresponding SAA problem. We refer to this SAA problem as **[BQP(SAA)]**.

$$\textbf{[BQP(SAA)]}\ \underset{Y\in\mathbf{Y}}{Minimize}\left\{\hat{\mathbf{g}}(Y) := \sum_{c\in\mathcal{C}}\sum_{j\in\mathcal{J}}\psi_{cj}Y_{cj} + \frac{1}{N}\sum_{n=1}^{N}\mathbb{Q}(\mathbf{Y},\Theta_n)\right\} \tag{A.1}$$

   Problem (A.1) is solved for each replication $e = 1, 2, ..., E$. Let v_N^e and $\hat{Y_N^e}$ to represent the objective function value and optimal solution of the problem (A.1), respectively.

2. In this step, we compute the average value of the objective functions associated with E replications, denoted by $\bar{v}_E^N$. Further, we let $\sigma^2_{\bar{v}_E^N}$ to represent the variance associated with E replications. We calculate $\bar{v}_E^N$ and $\sigma^2_{\bar{v}_E^N}$ as follows:

$$\bar{v}_E^N = \frac{1}{E}\sum_{e=1}^{E} v_N^e$$

$$\sigma^2_{\bar{v}_E^N} = \frac{1}{(E-1)E}\sum_{e=1}^{E}(v_N^e - \bar{v}_E^N)^2$$

   The estimator $\bar{v}_E^N$ is an unbiased estimator of the objective function value of the original problem **(BQP)**, referred to as v^*, and satisfies $\mathbb{E}(\bar{v}_E^N) \leq v^*$. Thus, $\bar{v}_E^N$ provides a valid lower bound for the optimal objective function value of v^* [86]. Further, the calculated variance, $\sigma^2_{\bar{v}_E^N}$, is the estimate of the variance of the achieved lower bound.

3. In this step, using the optimal solution of the SAA problems for each replication, $\tilde{Y}_N^e \in \mathbf{Y}$, generate a new reference sample size N' ($N' \gg N$) and estimate the objective function value of the original problem **(BQP)** as follows:

$$\tilde{g}_{N'}^e(\tilde{Y}) := \sum_{c\in C}\sum_{j\in J} \psi_{cj}\tilde{Y}_{cj} + \frac{1}{N'}\sum_{n=1}^{N'} \mathbb{Q}(\mathbf{Y}, \Theta_n)$$

The estimator $\tilde{g}_{N'}(\tilde{Y}) = \min_{e\in E} \ \tilde{g}_{N'}^e(\tilde{Y})$ provides a valid upper bound for **(BQP)**. The variance of this estimator could be calculated as follow:

$$\sigma_{N'}^2(\tilde{Y}) = \frac{1}{(N'-1)N'}\sum_{n=1}^{N'}\left\{\sum_{c\in C}\sum_{j\in J}\psi_{cj}\tilde{Y}_{cj} + \mathbb{Q}(\mathbf{Y}, \Theta_n) - \tilde{g}_{N'}(\tilde{Y})\right\}^2$$

4. Using the estimators obtained via **Steps 2** and **3**, the optimality gap of the SAA algorithm and its variance after each iteration can be calculated as follows:

$$gap_{N,E,N'}(\tilde{Y}) = \tilde{g}_{N'}(\tilde{Y}) - \bar{v}_E^N$$

$$\sigma_{gap}^2 = \sigma_{N'}^2(\tilde{Y}) + \sigma_{\bar{v}_E^N}^2$$

The confidence interval of the optimality gap, $gap_{N,E,N'}(\tilde{Y})$, is obtained as follows:

$$\tilde{g}_{N'}(\tilde{Y}) - \bar{v}_E^N + z_\alpha\left\{\sigma_{N'}^2(\tilde{Y}) + \sigma_{\bar{v}_E^N}^2\right\}^{1/2}$$

where $z_\alpha = \Phi^{-1}(1-\alpha)$ and $\Phi(z)$ is the cumulative distribution function of the standard normal distribution.

A.2 Penalty Parameter Updating

Prior studies [20, 39] reveal that the performance of the basic PHA is sensitive to the values set for the penalty parameter. A conservative λ value may lead to a near-optimal solution, but with an expense of high computational time. On the contrary, setting a large λ value could accelerate PHA's solution time but lead to a sub-optimal solution. To remedy this problem, we utilize the *dynamic penalty parameter adjustment approach*, proposed by Hvattum and Lokketangen [40], which dynamically updates the value of the penalty parameter, λ, given the consensus value of the overall design vectors obtained in prior iterations. Let Δ_1^r and Δ_2^r be the indicators of the convergence rates in the *dual* and *primal* space, respectively. Using the following equations, we will dynamically update the value of the penalty parameter λ:

$$\begin{aligned}\Delta_1^r &= \sum_{c\in C}\sum_{j\in\mathcal{J}}\sum_{n\in\mathcal{N}}(Y_{cjn}^r - \bar{Y}_{cj}^r)^2\\ \Delta_2^r &= \sum_{c\in C}\sum_{j\in\mathcal{J}}(\bar{Y}_{cj}^r - \bar{Y}_{cj}^{r-1})^2\end{aligned}$$

$$\vartheta^r = \begin{cases}\Gamma\lambda^{r-1} & \textit{if } \Delta_1^r - \Delta_1^{r-1} > 0\\ \frac{1}{\Gamma}\lambda^{r-1} & \textit{else if } \Delta_2^r - \Delta_2^{r-1} > 0\\ \lambda^{r-1} & \textit{Otherwise}\end{cases}$$

where Γ is a positive constant and its value is set to grater than 1, i.e., $\Gamma > 1$.

A.3 Global and Local Heuristic Strategies

The first term in the objective function of problem (A.2), i.e., $(\psi_{cj} + \zeta_{cjn} + \frac{\lambda}{2} - \lambda \bar{Y}_{cj})$, represents the adjusted investment cost associated with different scenarios. Let $\{\psi_{cjn}\}_{\forall c \in \mathcal{C}, j \in \mathcal{J}, n \in \mathcal{N}}$ indicates the investment cost to open a depot of size $c \in \mathcal{C}$ at loaction $j \in \mathcal{J}$ under scenario $n \in \mathcal{N}$. In the basic PHA, to adjust the value of scenario-dependant investment costs, $\{\psi_{cjn}\}_{\forall c \in \mathcal{C}, j \in \mathcal{J}, n \in \mathcal{N}}$, we first update the values of lagrangian multipliers and penalty parameters using equations (1.33) and (1.34). Then, using the updated parameters, the adjusted $\{\psi_{cjn}\}_{\forall c \in \mathcal{C}, j \in \mathcal{J}, n \in \mathcal{N}}$ is calculated for the following iteration. Instead of using this procedure, in this sub-section, we adopt the two heuristic strategies, namely, the *local and global heuristics* as proposed by [24], to calculate the value of adjusted investment cost for the following iterations.

Upon completion of a PHA iteration, the consensus value of the first-stage decision variables, $\{\bar{Y}^r_{cj}\}_{\forall c \in \mathcal{C}, j \in \mathcal{J}, n \in \mathcal{N}}$, is obtained. A higher value of $\bar{Y}^r_{cj}$ signifies that a depot of size c and location j was favorable to be opened many times in the previous iterations. On the contrary, a lower value of the consensus parameter indicates that selecting the respective depot was not favorable in the previous iterations. Let $\bar{a}$ and $\underline{a}$ to represent the upper and lower threshold values of $\bar{Y}^r_{cj}$. Using the *global heuristics*, we will adjust the value of ψ_{cj} as follow:

$$\psi^r_{cj} = \begin{cases} \kappa \psi^{r-1}_{cj} & if \quad \bar{Y}^{r-1}_{cj} < \bar{a} \\ \frac{1}{\kappa} \psi^{r-1}_{cj} & if \quad \bar{Y}^{r-1}_{cj} > \underline{a} \\ \psi^{r-1}_{cj} & Otherwise \end{cases}$$

In the aforementioned adjusting equations, the ψ^r_{cj} represents the modified investment cost of opening depots at the $r\text{-}th$ iteration of PHA. Further, the values of $\bar{a}$ and $\underline{a}$ are selected from ranges $0.7 \leq \bar{a} \leq 1$ and $0 \leq \underline{a} \leq 0.3$, respectively. The constant parameter κ is set to any value greater than 1.

Using the globally adjusted investment cost, ψ_{cj}, we adopt *local heuristics* to update the scenario-dependent investment costs, ψ_{cjn}. Given large difference between the design variables Y^r_{cjn} and the corresponding consensus parameters $\bar{Y}^r_{cj}$, a scenario-level adjustment of the investment costs are made. The local adjustment strategy is presented below:

$$\psi^r_{cjn} = \begin{cases} \kappa\psi^r_{cj} & if \quad |Y^{r-1}_{cjn} - \bar{Y}^r_{cj}| \geq a^{far} \quad and \quad Y^{r-1}_{cjn} = 0 \\ \frac{1}{\kappa}\psi^r_{cj} & if \quad |Y^{r-1}_{cjn} - \bar{Y}^r_{cj}| \geq a^{far} \quad and \quad Y^{r-1}_{cjn} = 1 \\ \psi^r_{cjn} & Otherwise \end{cases}$$

where ψ^r_{cjn} is the modified investment cost of opening a depot in scenario $n \in \mathcal{N}$ at the $r\text{-}th$ iteration of PHA. Further, κ is a constant parameter and its value is set to a number greater than 1. Finally, a^{far}, $0.5 < a^{far} < 1$, represents the threshold value for the gap between the binary variables and the corresponding consensus parameters beyond which the respective investment cost is updated.

A.4 Scenario Bundling

Using a *scenario grouping* method, commonly referred to as *scenario bundling* technique [4], we can further improve the computational performance in solving the N scenario-dependent subproblems **[BQP(PHA)]**. In this method, rather than solving for individual scenarios $n \in \mathcal{N}$,

the **[BQP(PHA)]** subproblems are solved for a bundle of scenarios, denoted by $g \in \mathcal{G}$. Different strategies could be employed to group $|\mathcal{G}|$ scenarios from the available N scenarios. For instance, in this study, one of the main sources of uncertainty is the availability of feedstock in the supply sites, $\overline{S}_{bit\omega}; \forall b \in \mathcal{B}, i \in \mathcal{I}, t \in \mathcal{T}, \omega \in \Omega$. One can select this parameter as a scenario grouping parameter and aim at grouping the scenarios into the following *three* major categories: low, medium, and high feedstock supply availabilities. The probability for each bundle can be calculated as follows: $\rho_g = \sum_{n \in g} \rho_n$. The following subproblem, referred to as **[BQP(PHA(g))]**, is now solved for each bundle $g \in \mathcal{G}$.

$$\textbf{[BQP(PHA(g))]} \underset{\mathbf{Y,S,X,H,P,Z,Q,L,R,D,U}}{Minimize} \sum_{c \in \mathcal{C}} \sum_{j \in \mathcal{J}} (\psi_{cj} + \zeta_{cjg} + \frac{\lambda}{2} - \lambda \bar{Y}_{cj}) Y_{cjg} + \sum_{n \in g} \frac{\rho_n}{\rho_g} \Big(\mathbb{Q}(\mathbf{Y}, \Theta_g) \Big) \tag{A.2}$$

subject to (1.5)-(1.10), (1.12)-(1.17), (1.19)-(1.21), (1.23)-(1.25), and (1.27). Note that the definition for $\{Y_{cjg}\}$ will remain same as **[BQP(PHA)]** but for each scenario bundle $g \in \mathcal{G}$.